Electronic Supplementary Information *Biomaterials Science*

for

Metal (M = Cr, Mo, W, Re) carbonyl complexes with porphyrin and carborane isocyanide ligands: light-induced oxidation and carbon oxide release for antitumor efficacy

Victoria M. Alpatova[a], Minh Tuan Nguyen[b], Evgeny G. Rys[a], Georgy K. Liklikadze[c], Elena G. Kononova[a], Alexander F. Smol'yakov[a,d], Yuri A. Borisov[a], Anton E. Egorov[b], Alexey A. Kostyukov[b], Anna V. Shibaeva[b], Ivan D. Burtsev[b], Alexander S. Peregudov[a], Vladimir A. Kuzmin[b], Alexander A. Shtil[e,f], Alina A. Markova[b,e] and Valentina A. Ol'shevskaya[a]*

[a.] *A.N.Nesmeyanov Institute of Organoelement Compounds, Russian Academy of Sciences, 28 Bld. 1 Vavilov Street, 119334 Moscow, Russian Federation. E-mail: olshevsk@ineos.ac.ru*

[b.] *Emanuel Institute of Biochemical Physics, Russian Academy of Sciences, 4 Kosygin Street, Moscow 119334, Russian Federation*

[c.] *Higher Chemical College of the Russian Academy of Sciences, D.I.Mendeleev Russian University of Chemical Technology, 9 Miusskaya Square, Moscow, 125047, Moscow, Russian Federation*

[d.] *Plekhanov Russian University of Economics, 36 Stremyanny Lane, 117997 Moscow, Russian Federation*

[e.] *Institute of Cyber Intelligence Systems, National Research Nuclear University MEPhI,115409 Moscow, Russian Federation*

[f.] *Blokhin National Medical Research Center of Oncology, 24 Kashirskoyeshosse, Moscow 115522, Russian Federation*

Table of Contents

1. X-ray crystallography

Table S1. Crystal data and structure refinement for compounds **3**, **6**

	3	**6**
Empirical formula	$C_{45}H_{29}N_5$	$C_{54}H_{29.5}N_5O_9Re_2$
Formula weight	639.73	1264.72
Temperature/K	120	120
Crystal system	monoclinic	triclinic
Space group	C2	P-1
a/Å	20.4485(13)	9.2059(6)
b/Å	15.3439(9)	12.6546(10)
c/Å	13.7172(16)	40.362(3)
α/°	90	96.231(5)
β/°	131.020(3)	93.349(4)
γ/°	90	90.525(4)
Volume/Å^3	3247.2(5)	4665.7(6)
Z	4	4
ρ_{calc}g/cm^3	1.309	1.800
μ/mm^{-1}	0.078	5.249
F(000)	1336.0	2442.0
Crystal size/mm^3	0.24 × 0.17 × 0.12	0.24 × 0.11 × 0.04
Radiation	MoKα (λ = 0.71073)	MoKα (λ = 0.71073)
2Θ range for data collection/°	3.936 to 59.574	4.008 to 59.432
Index ranges	-23 ≤ h ≤ 28, -21 ≤ k ≤ 20, -19 ≤ l ≤ 18	-12 ≤ h ≤ 12, -17 ≤ k ≤ 13, -56 ≤ l ≤ 53
Reflections collected	16071	99241
Independent reflections	8254 [R_{int} = 0.0482, R_{sigma} = 0.0746]	26136 [R_{int} = 0.1134, R_{sigma} = 0.0969]
Data/restraints/parameters	8254/13/452	26136/246/1208
Goodness-of-fit on F^2	1.031	1.117
Final R indexes [I>=2σ (I)]	R_1 = 0.0914, wR_2 = 0.2540	R_1 = 0.1646, wR_2 = 0.4063
Final R indexes [all data]	R_1 = 0.1346, wR_2 = 0.2982	R_1 = 0.1822, wR_2 = 0.4161
Largest diff. peak/hole / e Å^{-3}	1.25/-0.51	12.00/-12.26
Flack parameter	-4(7)	

Our repeated attempts to prepare the crystal form of porphyrin **6** were not successful. The obtained single crystal X-ray diffraction data for **6** are presented in Fig.S1.

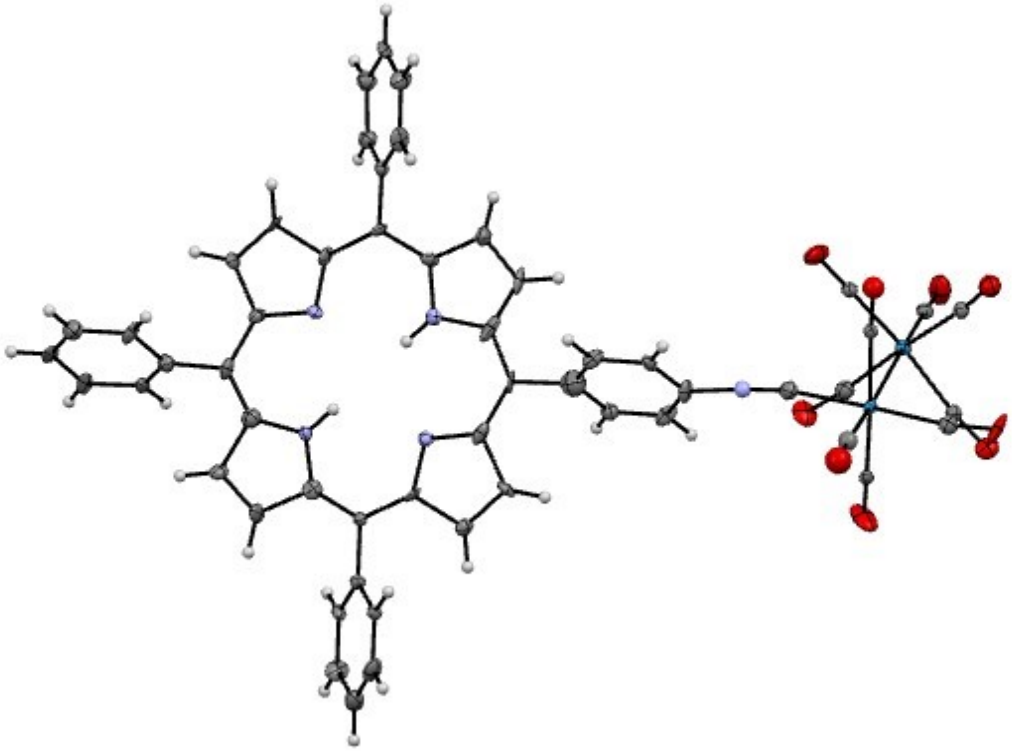

***Figure S1*.** Molecular structure of rhenium porphyrinisocyano complexes **6**.Other moleculesare omitted for clarity.

2. NMR spectra for compounds 2–13, 15–21

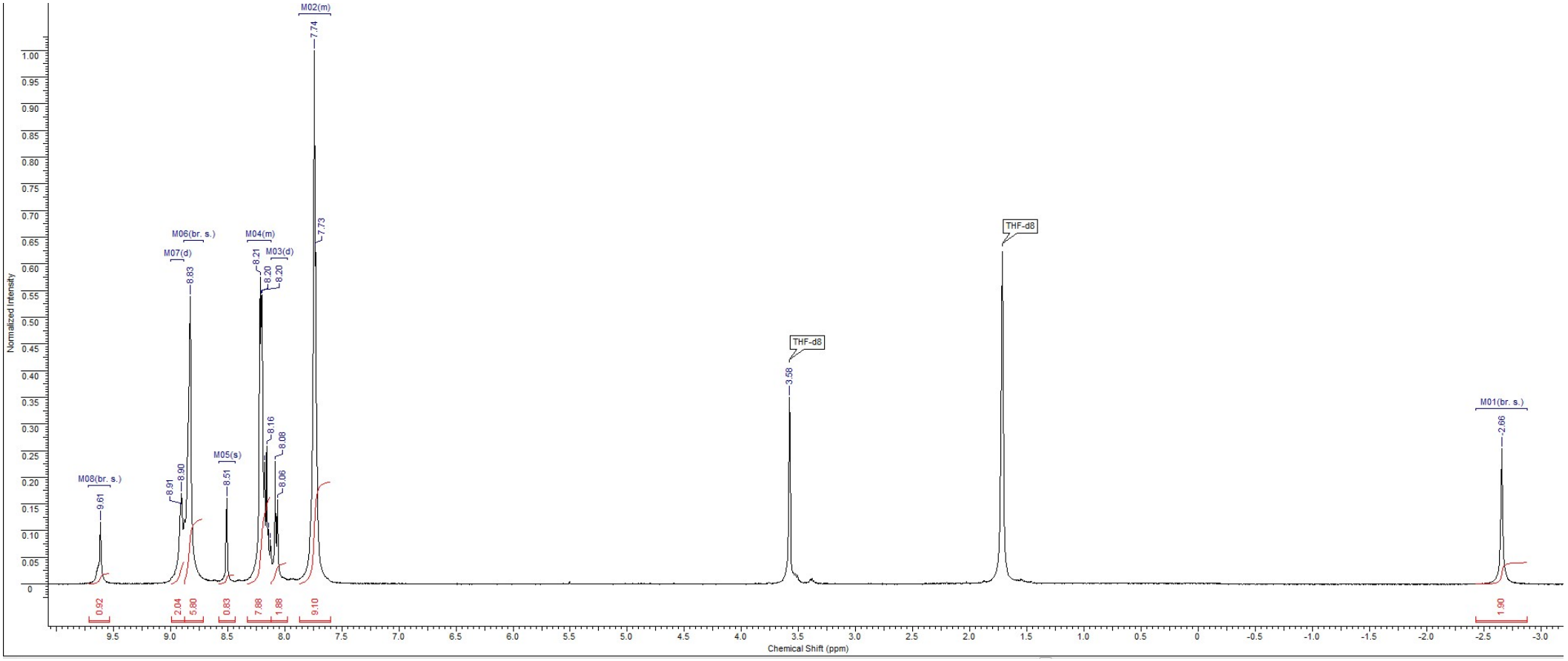

Figure S2. The ^{1}H spectrum of5-(*p*-*N*-formamidophenyl)-10,15,20-triphenylporphyrin(**2**) in THF-d_8.

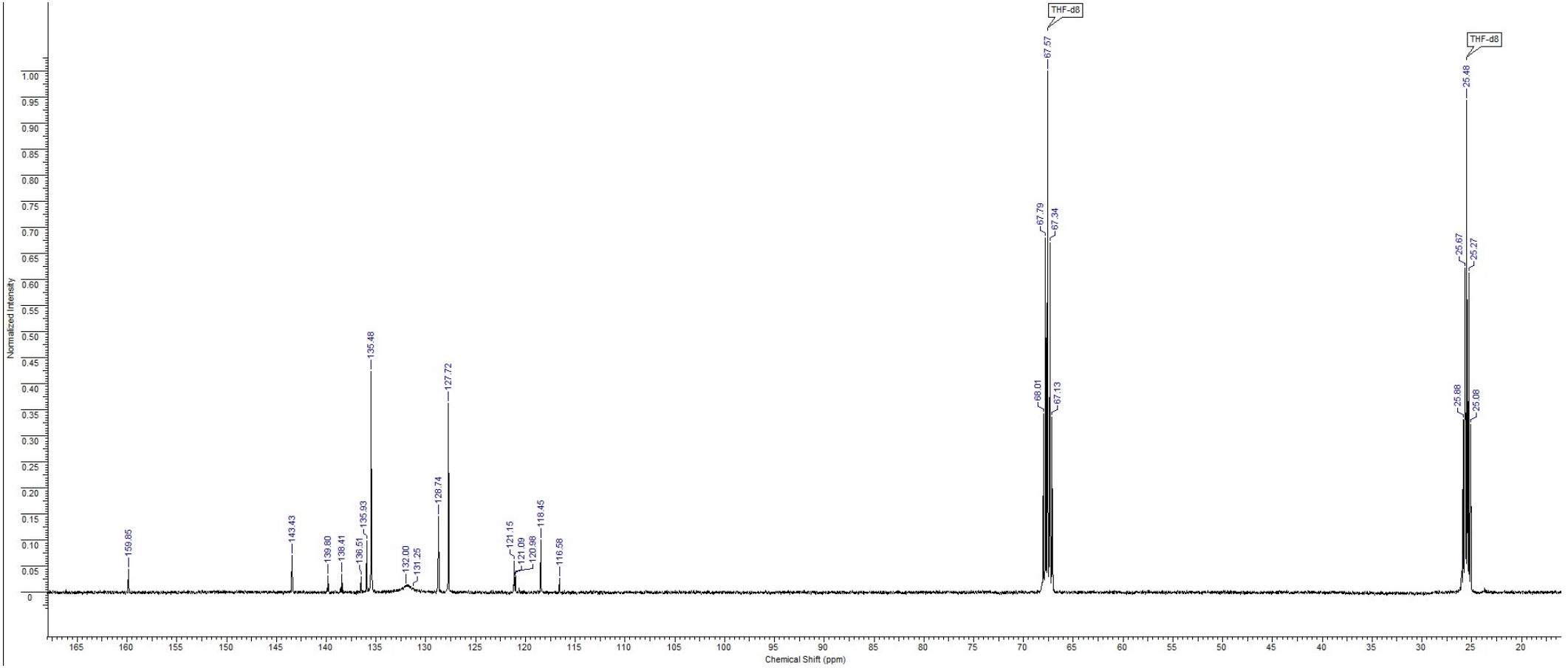

Figure S3. The ^{13}C spectrum of5-(*p*-*N*-formamidophenyl)-10,15,20-triphenylporphyrin(**2**) in THF-d_8.

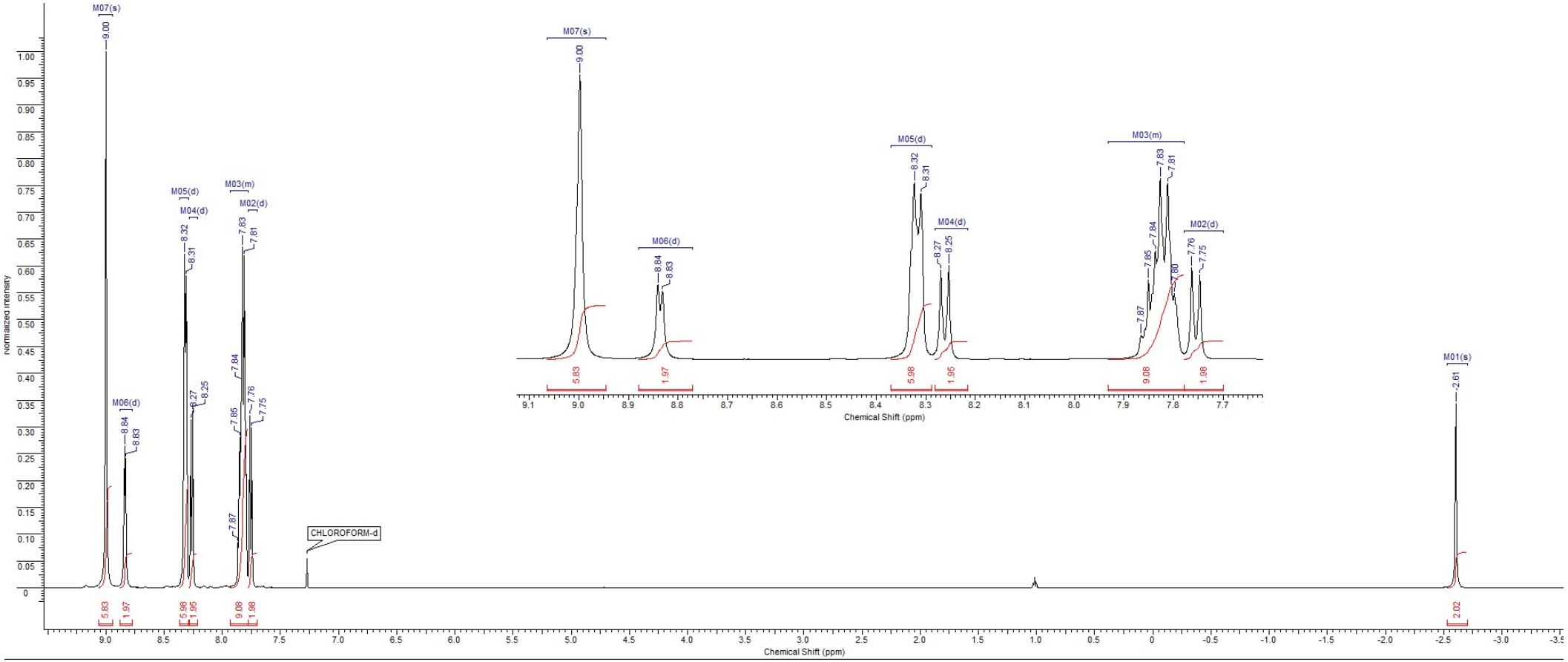

***Figure S4*.** The ^{1}H spectrum of5-(*p*-isocyanophenyl)-10,15,20-triphenylporphyrin (**3**) in $CDCl_3$.

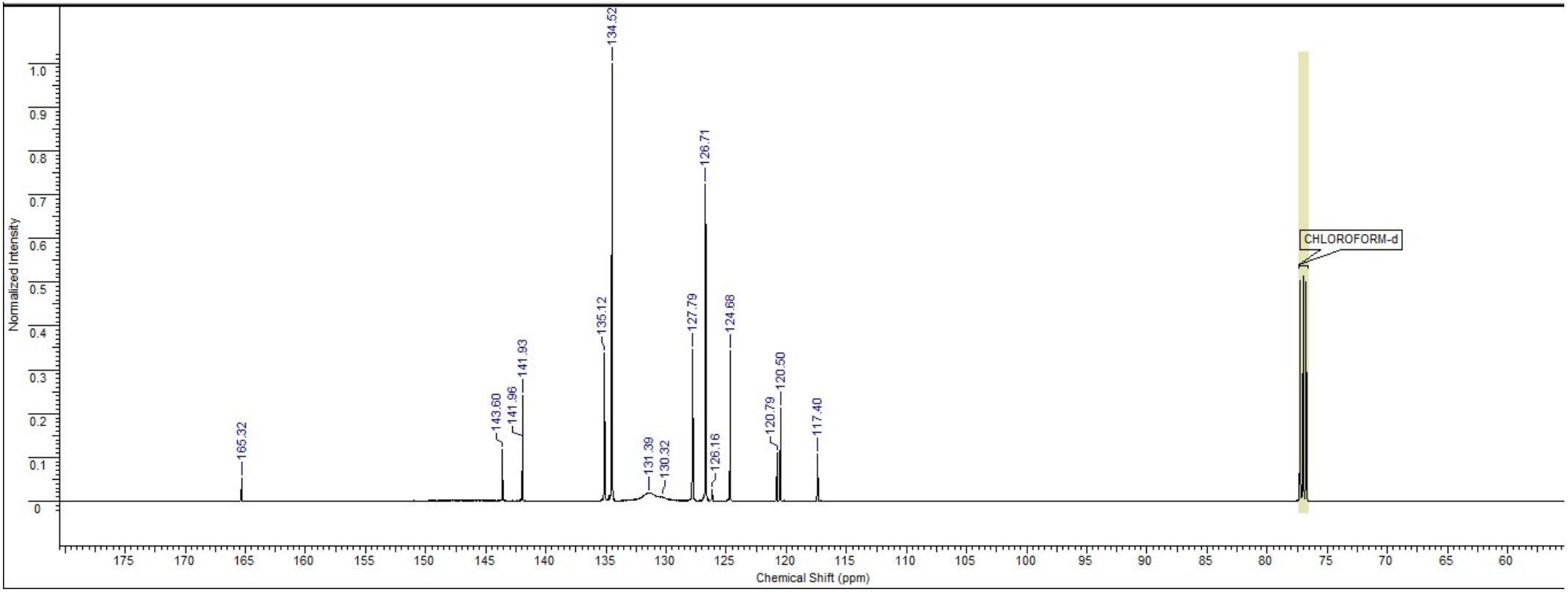

***Figure S5*.** The ^{13}C spectrum of5-(*p*-isocyanophenyl)-10,15,20-triphenylporphyrin (**3**) in $CDCl_3$.

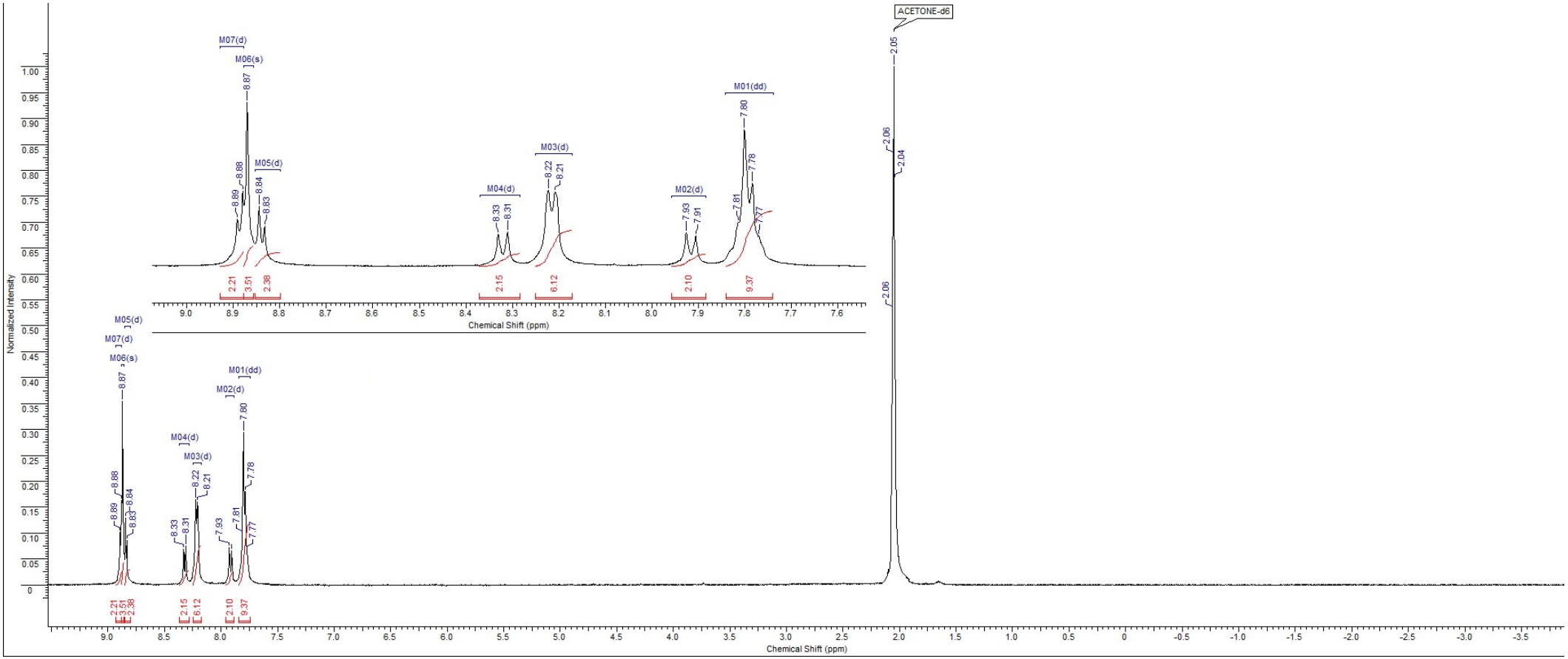

Figure S6. The ^{1}H spectrum of[5-(*p*-isocyanophenyl)-10,15,20-triphenylporphyrinato]zinc (**4**) in $(CD_3)_2CO$.

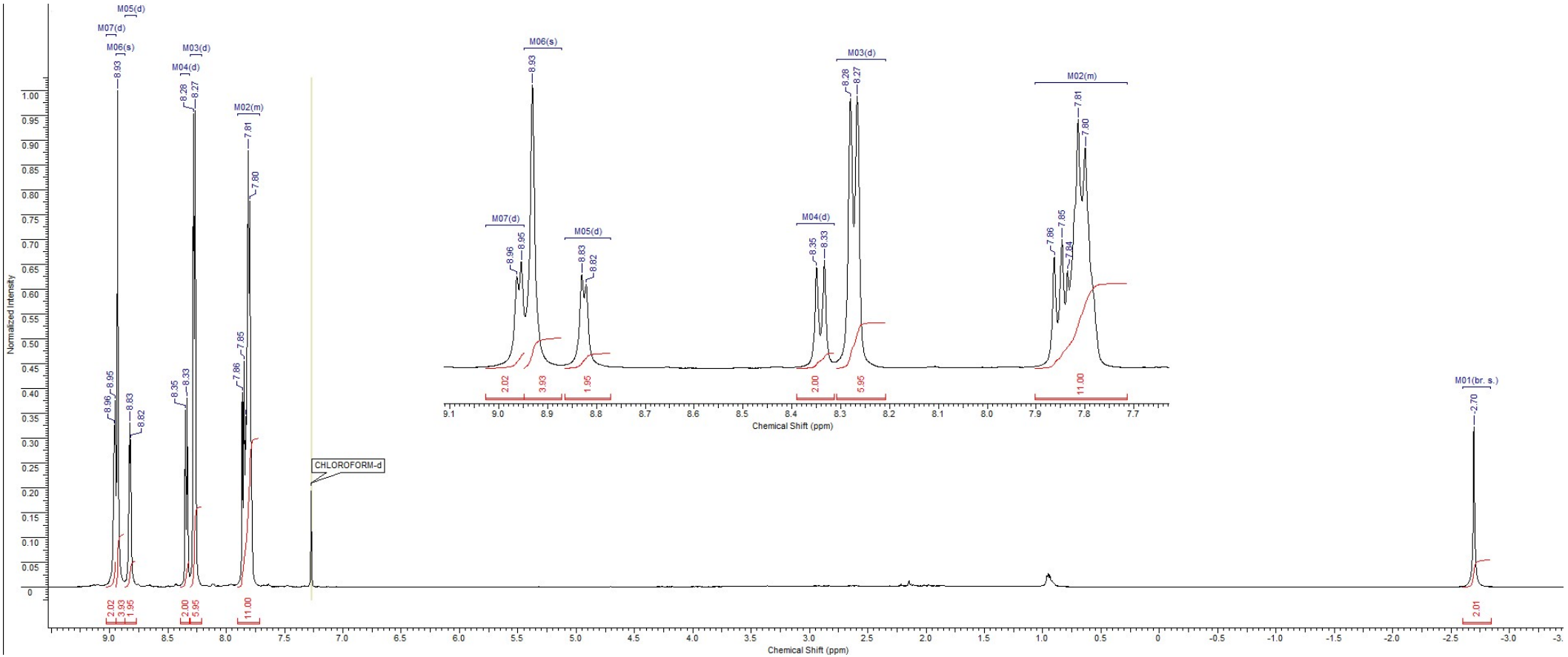

Figure S7. The ^{1}H spectrum of[5-(*p*-isocyanophenyl)-10,15,20-tetraphenylporphyrin](pentacarbonyl)molybdenum (**5**) in $CDCl_3$.

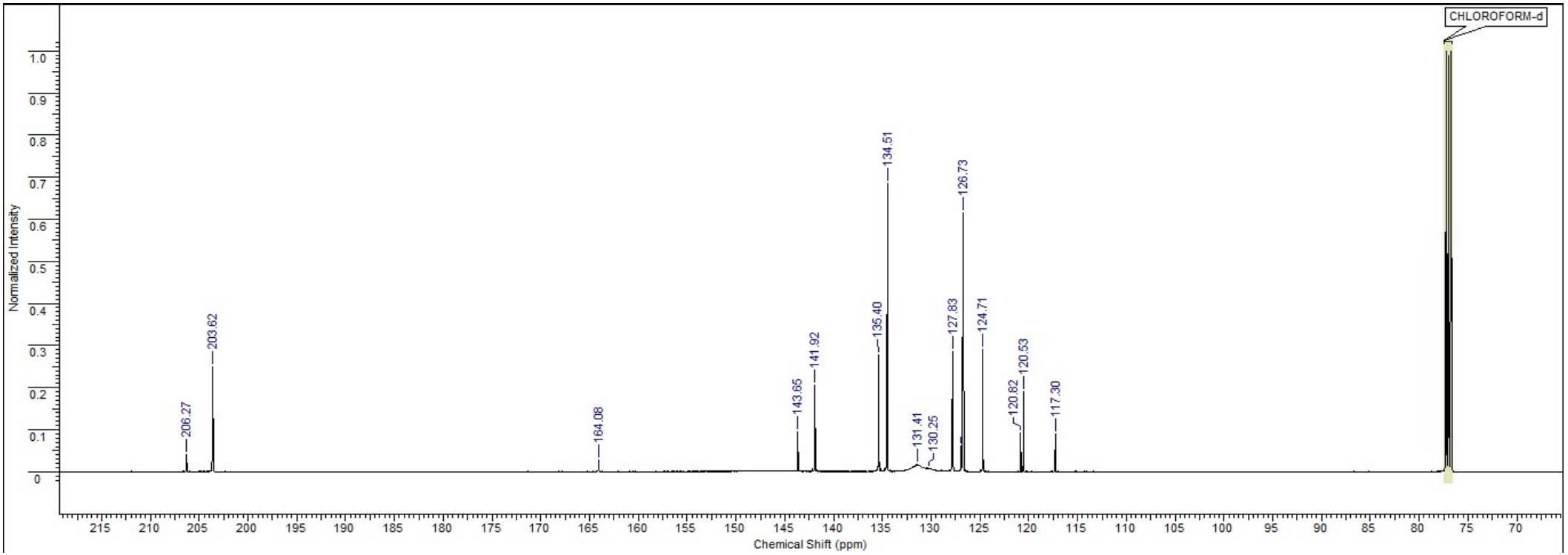

Figure S8. The ^{13}C spectrum of[5-(*p*-isocyanophenyl)-10,15,20-tetraphenylporphyrin](pentacarbonyl)molybdenum (**5**) in $CDCl_3$.

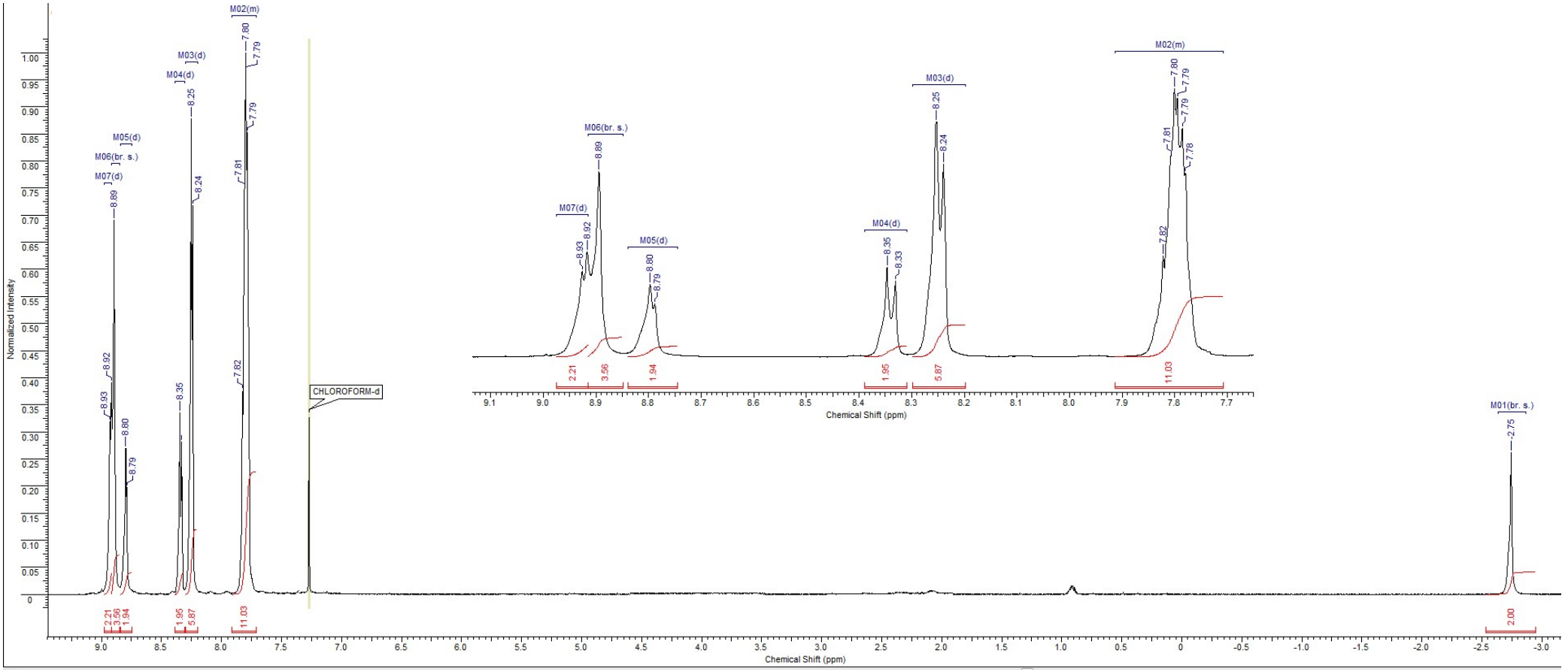

***Figure S9*.** The ^{1}H spectrum of[5-(*p*-isocyanophenyl)-10,15,20-tetraphenylporphyrin](nonacarbonyl)dirhenium (**6**) in $CDCl_3$.

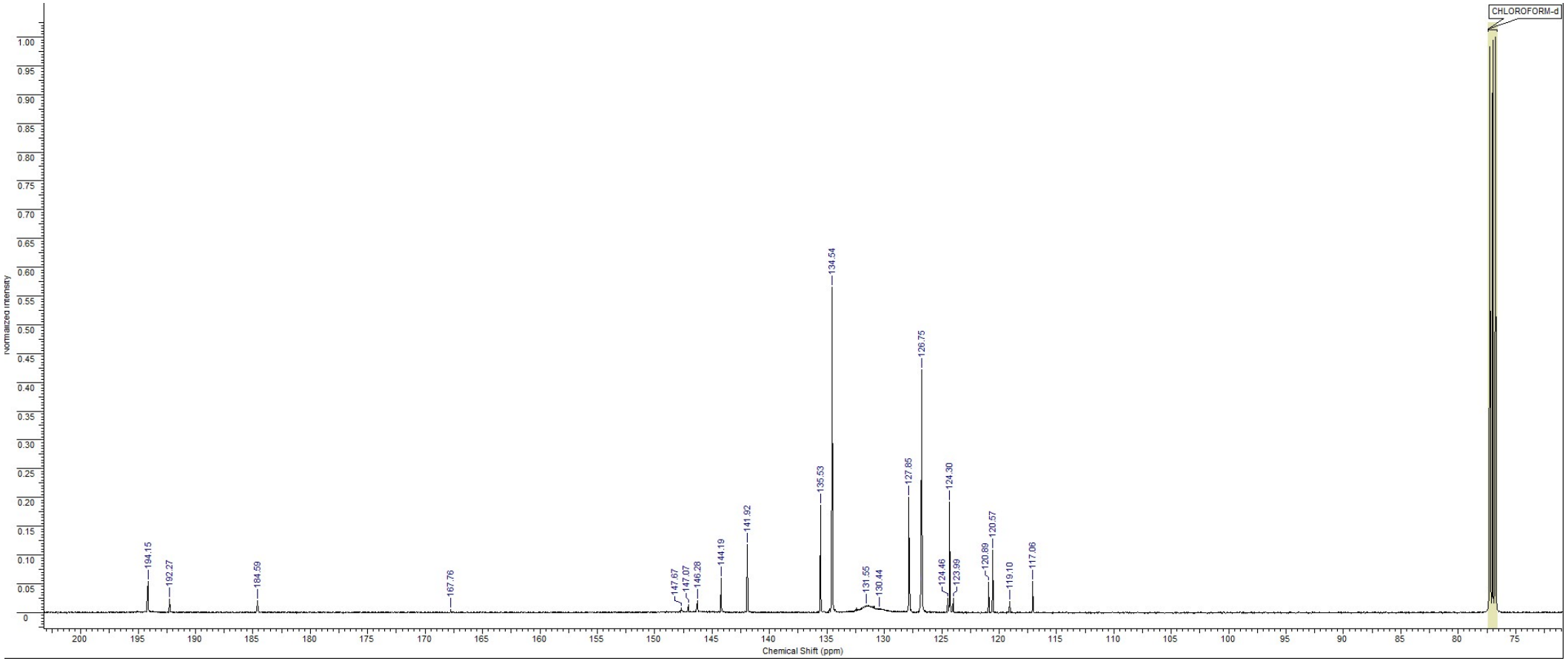

Figure S10. The ^{13}C spectrum of[5-(*p*-isocyanophenyl)-10,15,20-tetraphenylporphyrin](nonacarbonyl)dirhenium (**6**) in $CDCl_3$.

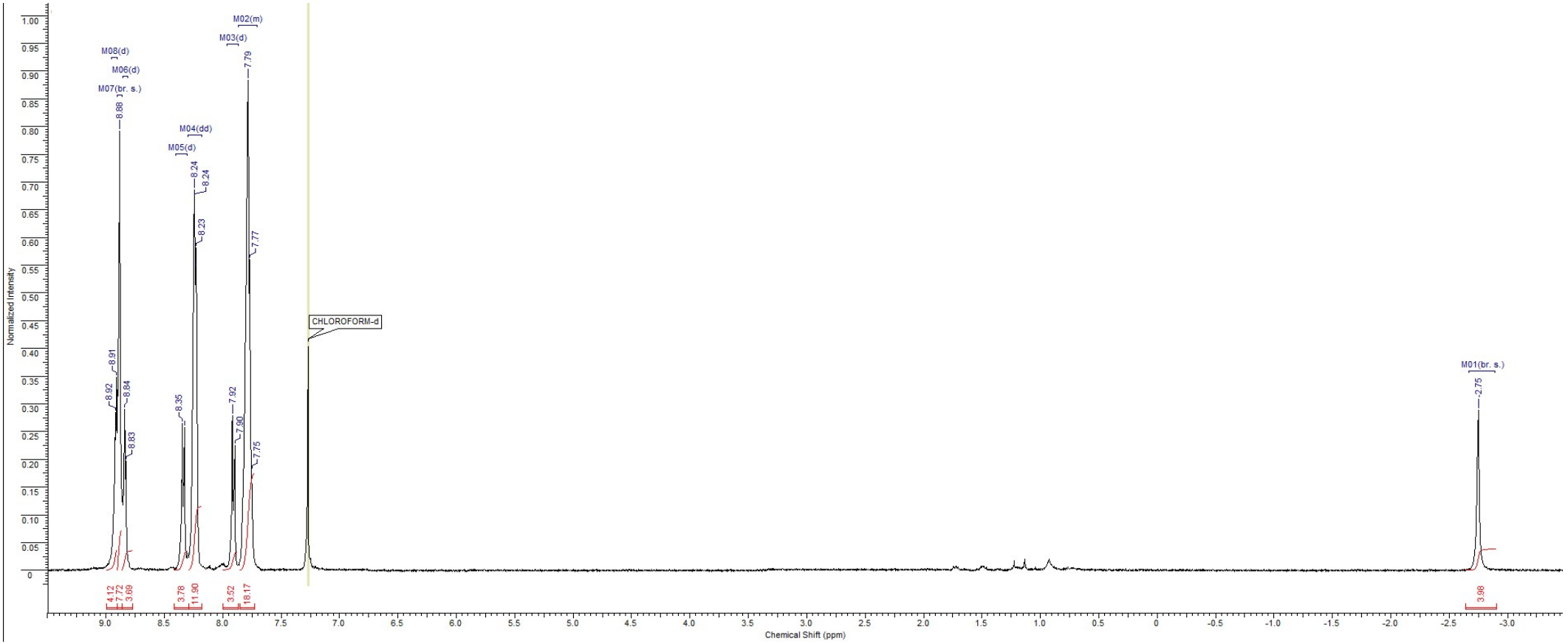

Figure S11. The ^{1}H spectrum ofbis-[(5-(*p*-isocyanophenyl)-10,15,20-triphenylporphyrin](tetracarbonyl)molybdenum (**7**)in $CDCl_3$.

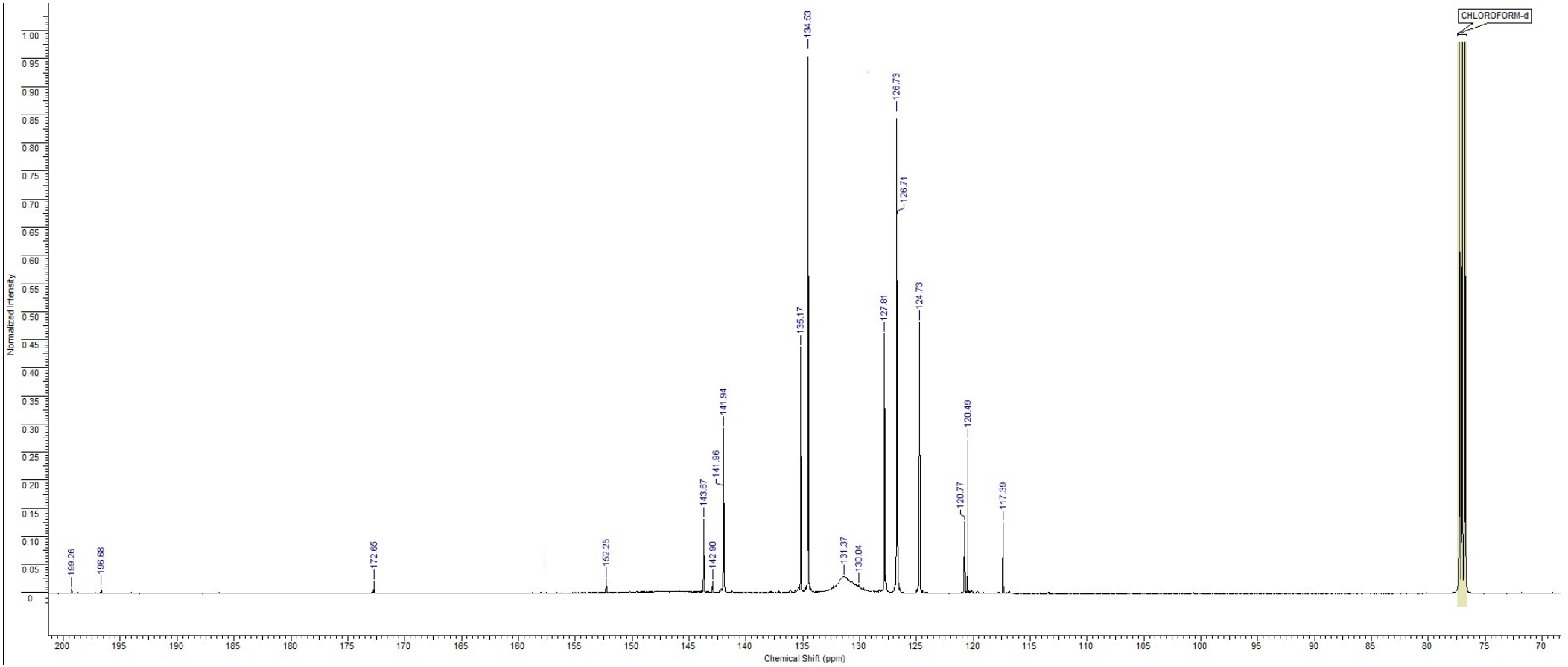

***Figure S12*.** The ^{13}C spectrum ofbis-[(5-(*p*-isocyanophenyl)-10,15,20-triphenylporphyrin](tetracarbonyl)molybdenum (**7**)in $CDCl_3$.

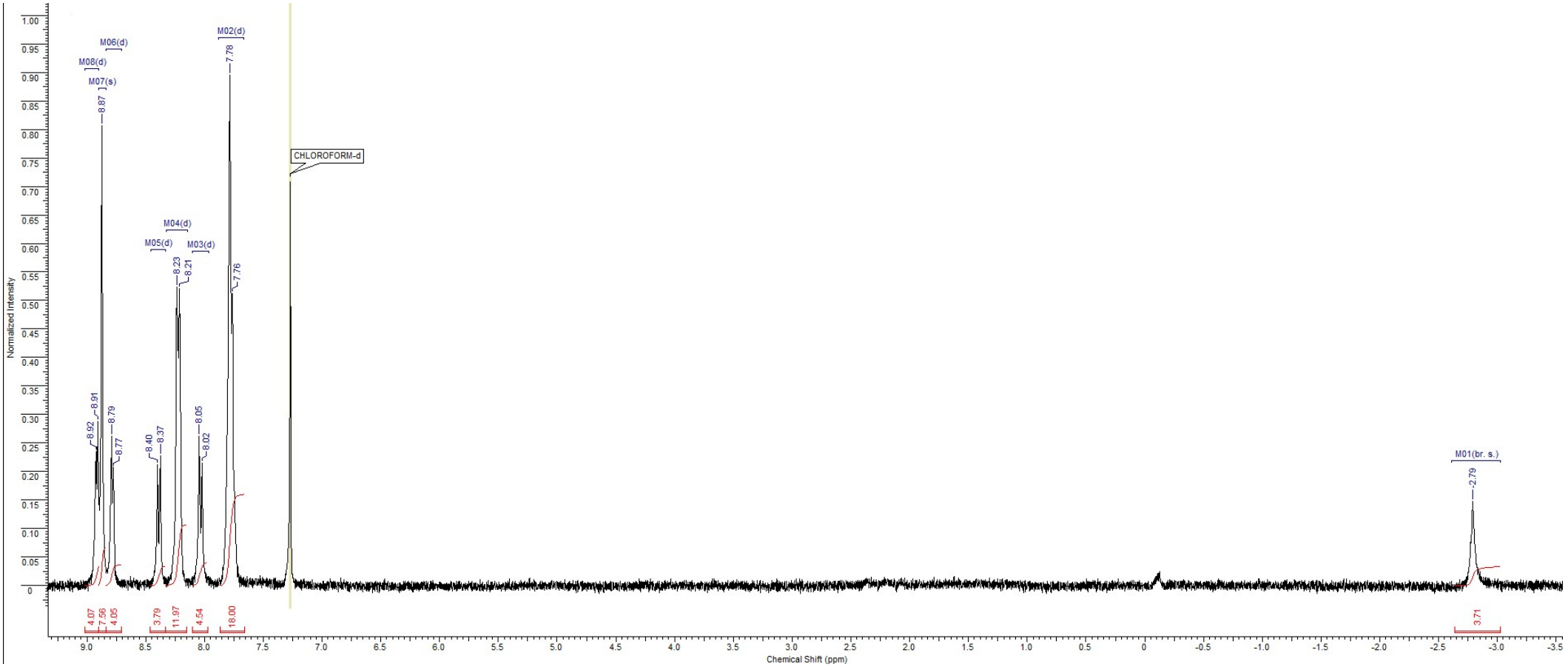

Figure S13. The ^{1}H spectrum of bis-[(5-(*p*-Isocyanophenyl)-10,15,20-triphenylporphyrin](octacarbonyl)dirhenium(**8**)in $CDCl_3$.

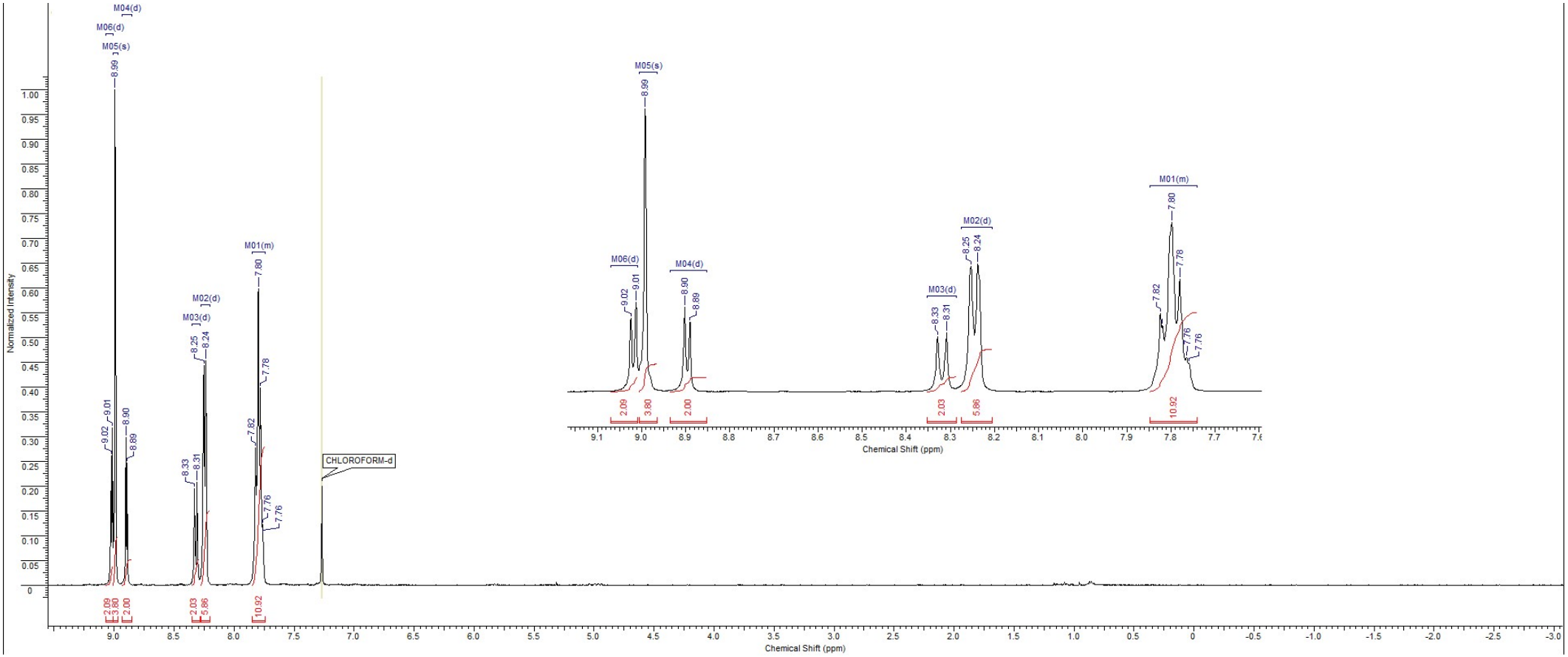

Figure S14. The ^{1}H spectrum of{[5-(*p*-isocyanophenyl)-10,15,20-triphenylporphyrinato]zinc}(pentacarbonyl)chromium (**9**) in $CDCl_3$.

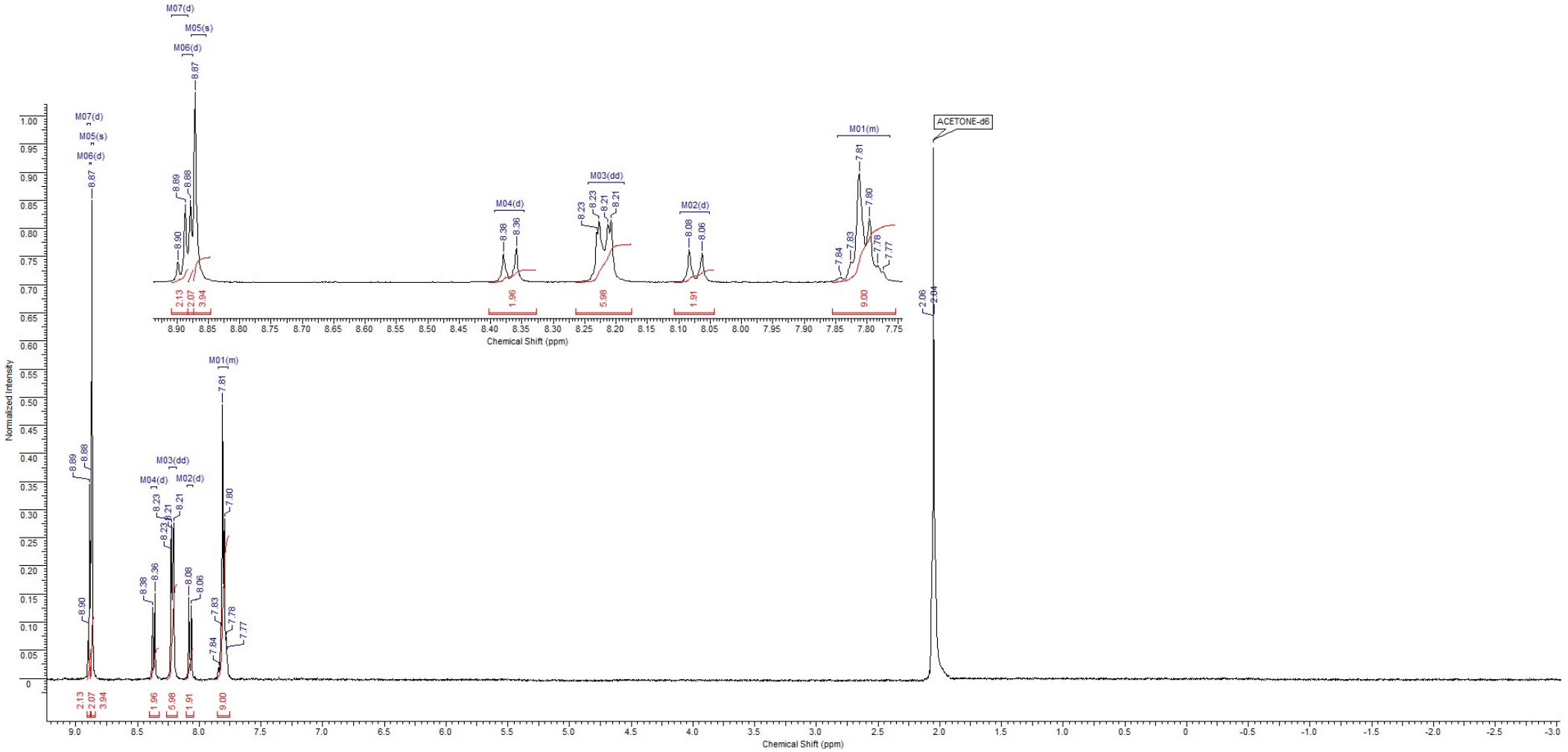

Figure S15. The ^{1}H spectrum of{[5-(*p*-isocyanophenyl)-10,15,20-triphenylporphyrinato]zinc}(pentacarbonyl)molybdenum (**10**) in $(CD_3)_2CO$.

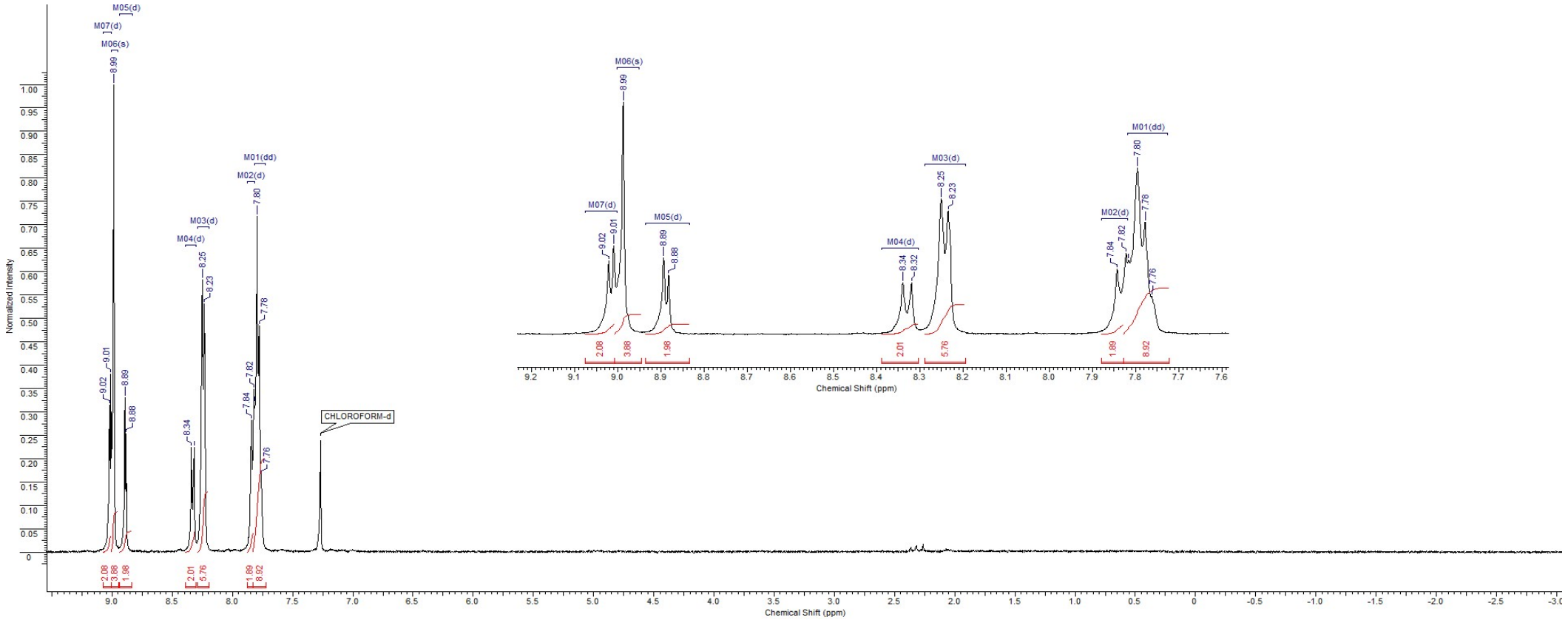

Figure S16. The ^{1}H spectrum of{[5-(*p*-isocyanophenyl)-10,15,20-triphenylporphyrinato]zinc}(pentacarbonyl)tungsten (**11**) in $CDCl_3$.

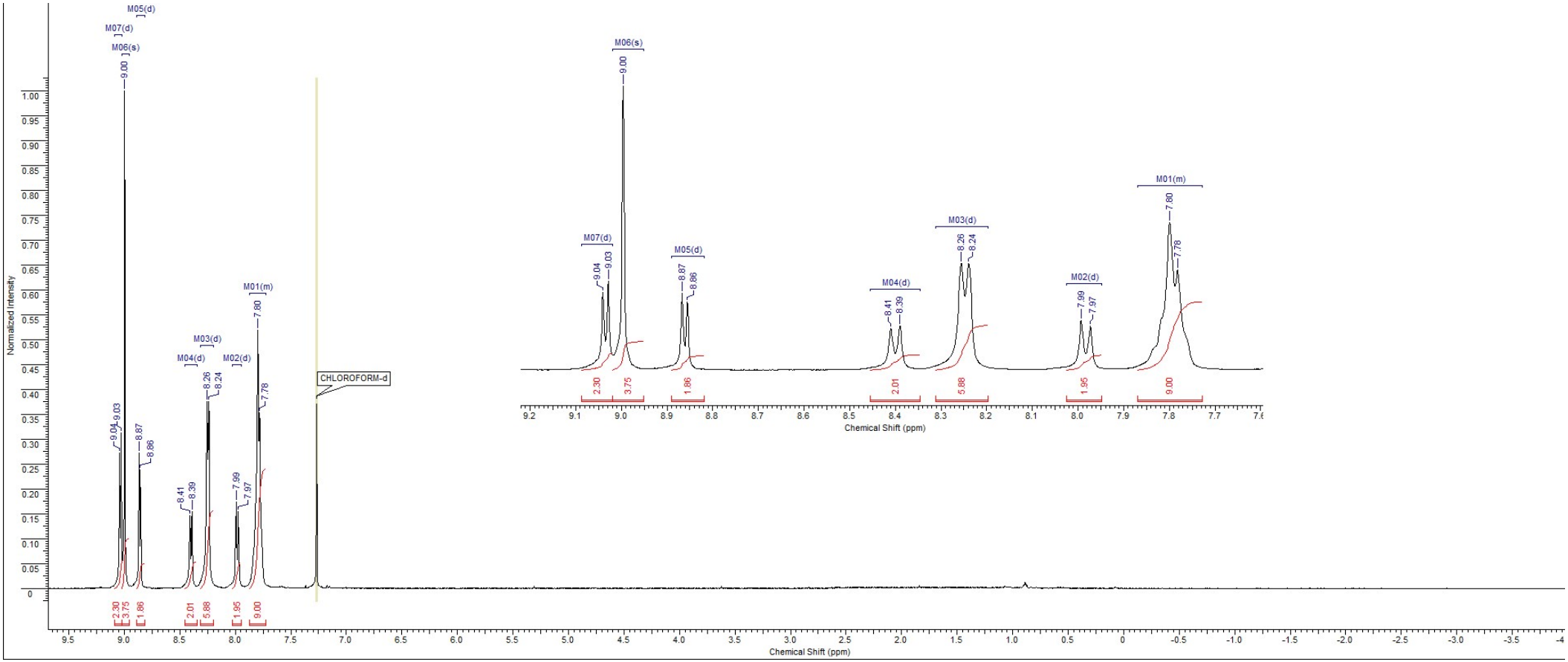

Figure S17. The ^{1}H spectrum of{[5-(*p*-isocyanophenyl)-10,15,20-triphenylporphyrinato]zinc}(tetracarbonyl)rhenium chloride (**12**) in $CDCl_3$.

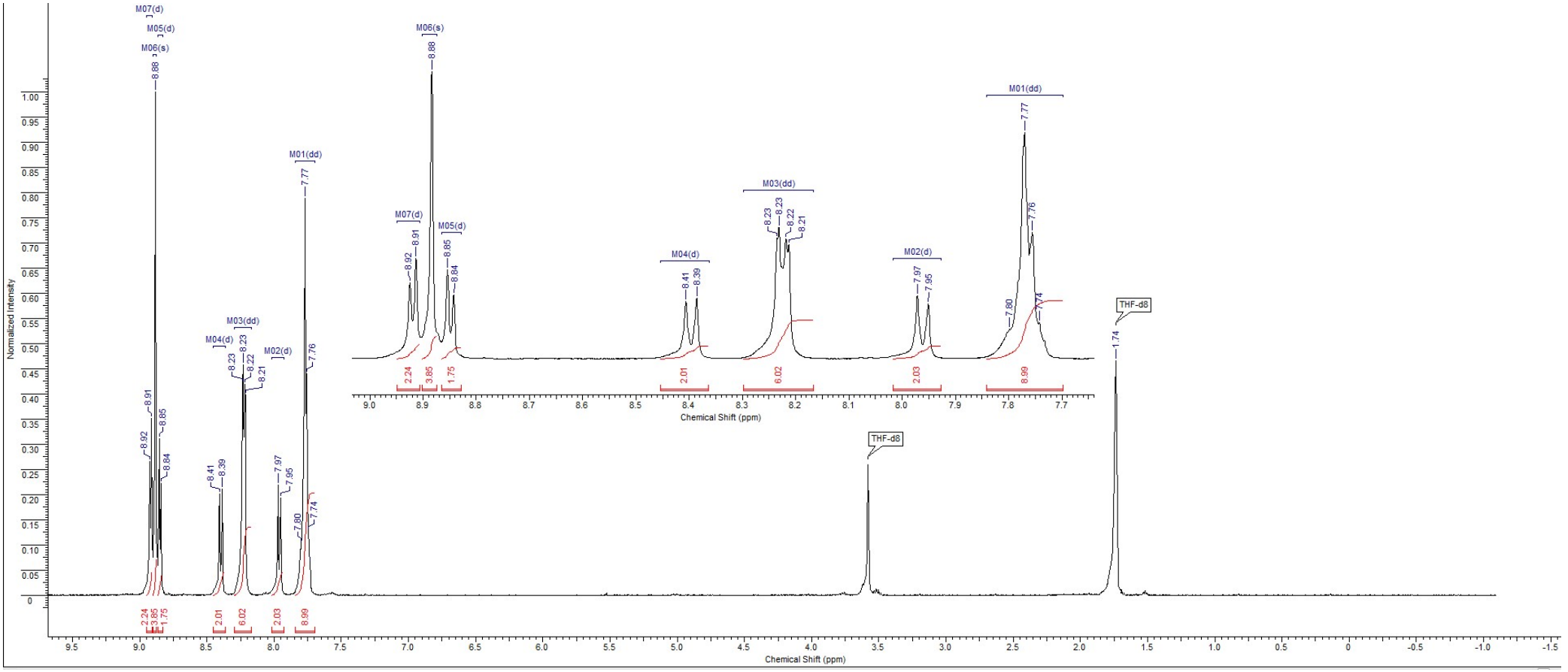

Figure S18. The ^{1}H spectrum of{[5-(*p*-isocyanophenyl)-10,15,20-triphenylporphyrinato]zinc}(nonacarbonyl)dirhenium (**13**) in $CDCl_3$.

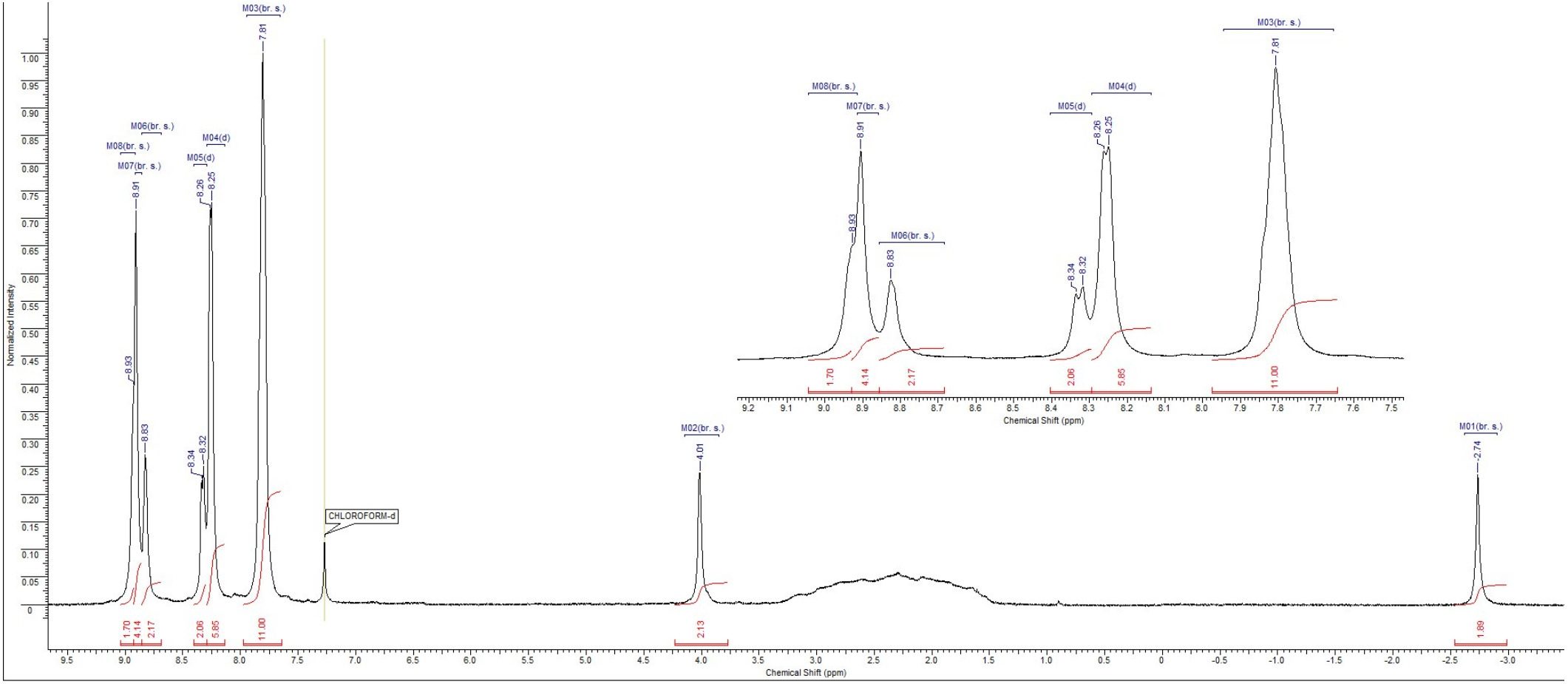

Figure S19. The ^{1}H spectrum of(3-isocyano-*o*-carborane)-[(5-(*p*-isocyanophenyl)-10,15,20-tetraphenylporphyrin](tetracarbonyl)molybdenum (**15**) in $CDCl_3$.

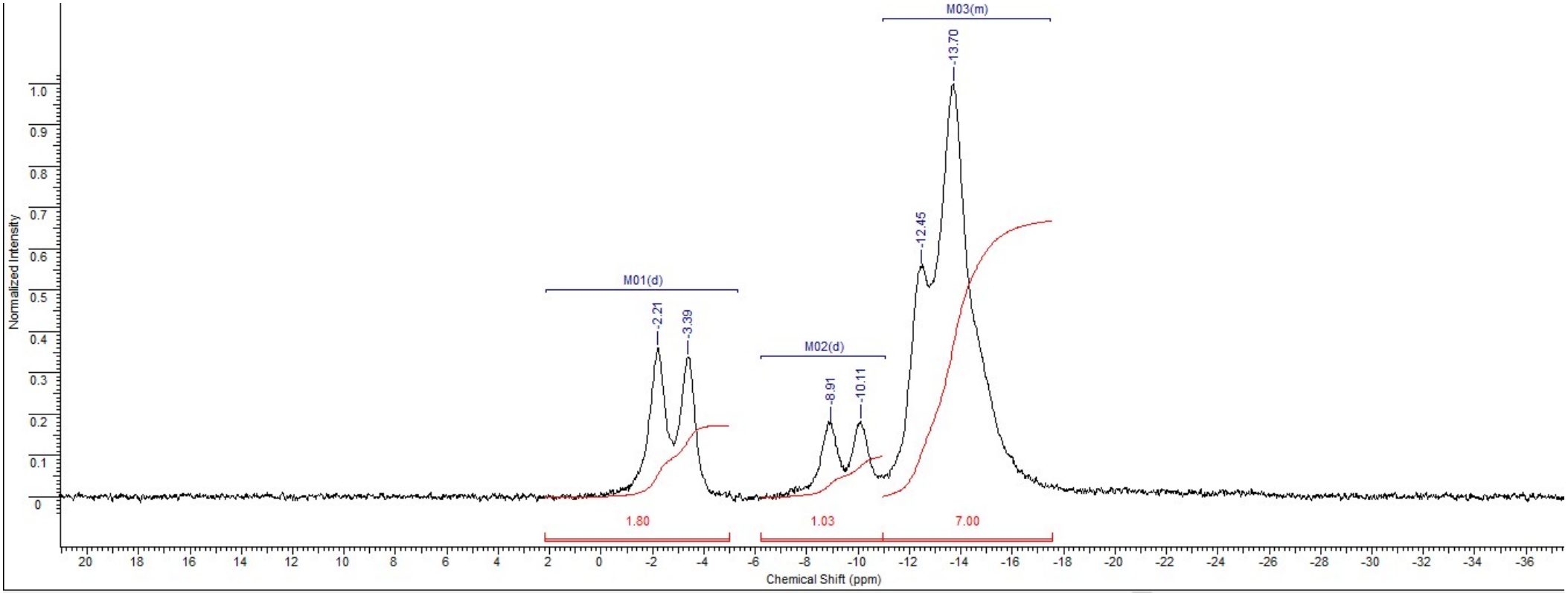

***Figure S20*.** The ^{11}B spectrum of(3-isocyano-*o*-carborane)-[(5-(*p*-isocyanophenyl)-10,15,20-tetraphenylporphyrin](tetracarbonyl)molybdenum (**15**) in $CDCl_3$.

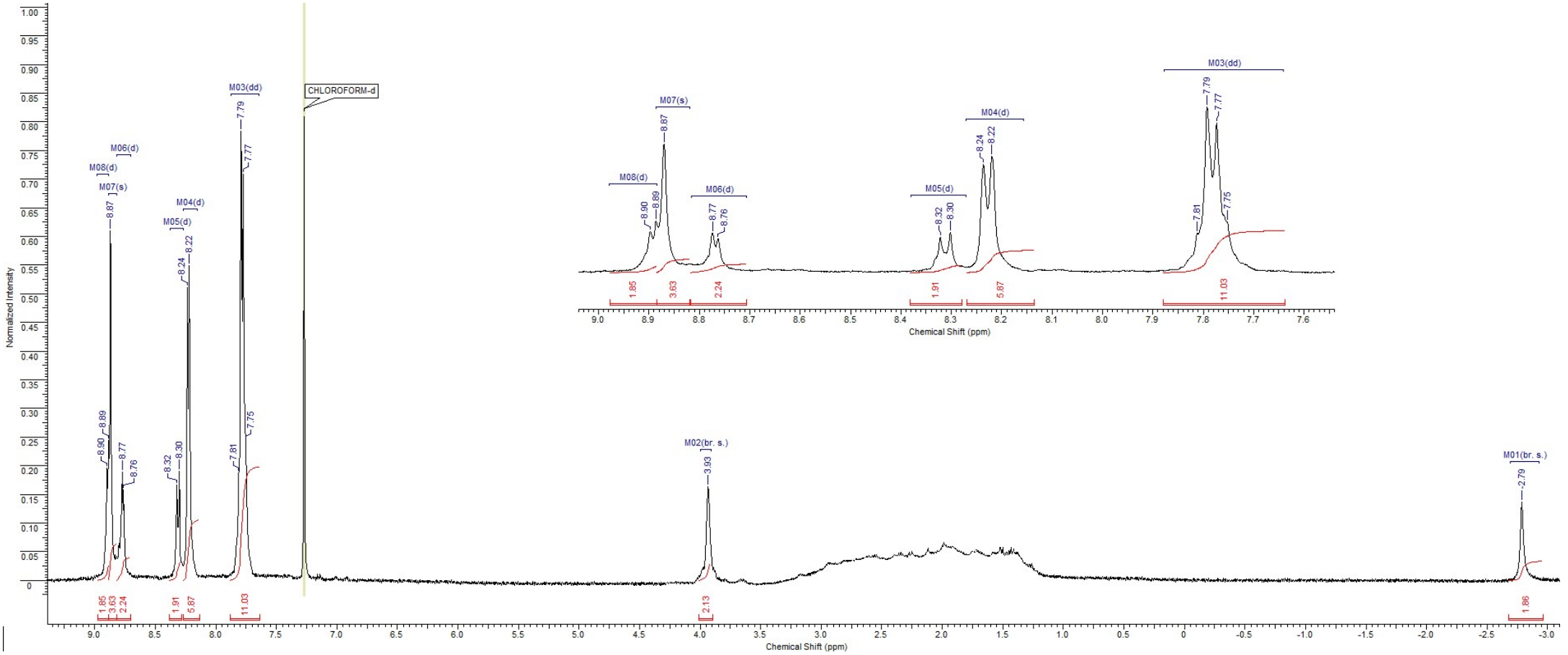

Figure S21. The ^{1}H spectrum of(3-isocyano-*o*-carborane)-[(5-(*p*-isocyanophenyl)-10,15,20-tetraphenylporphyrin](octacarbonyl)dirhenium (**16**) in $CDCl_3$.

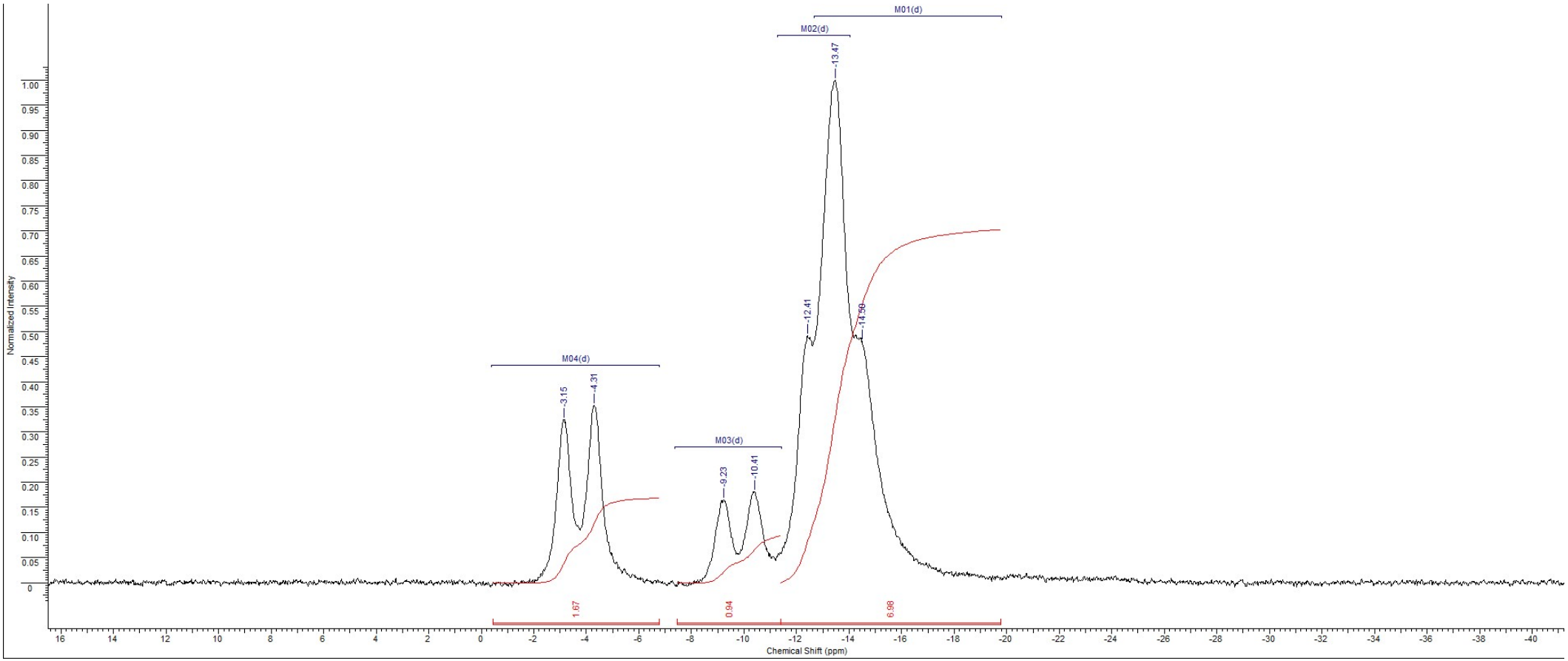

Figure S22. The ^{11}B spectrum of(3-isocyano-*o*-carborane)-[(5-(*p*-isocyanophenyl)-10,15,20-tetraphenylporphyrin](octacarbonyl)dirhenium (**16**) in $CDCl_3$.

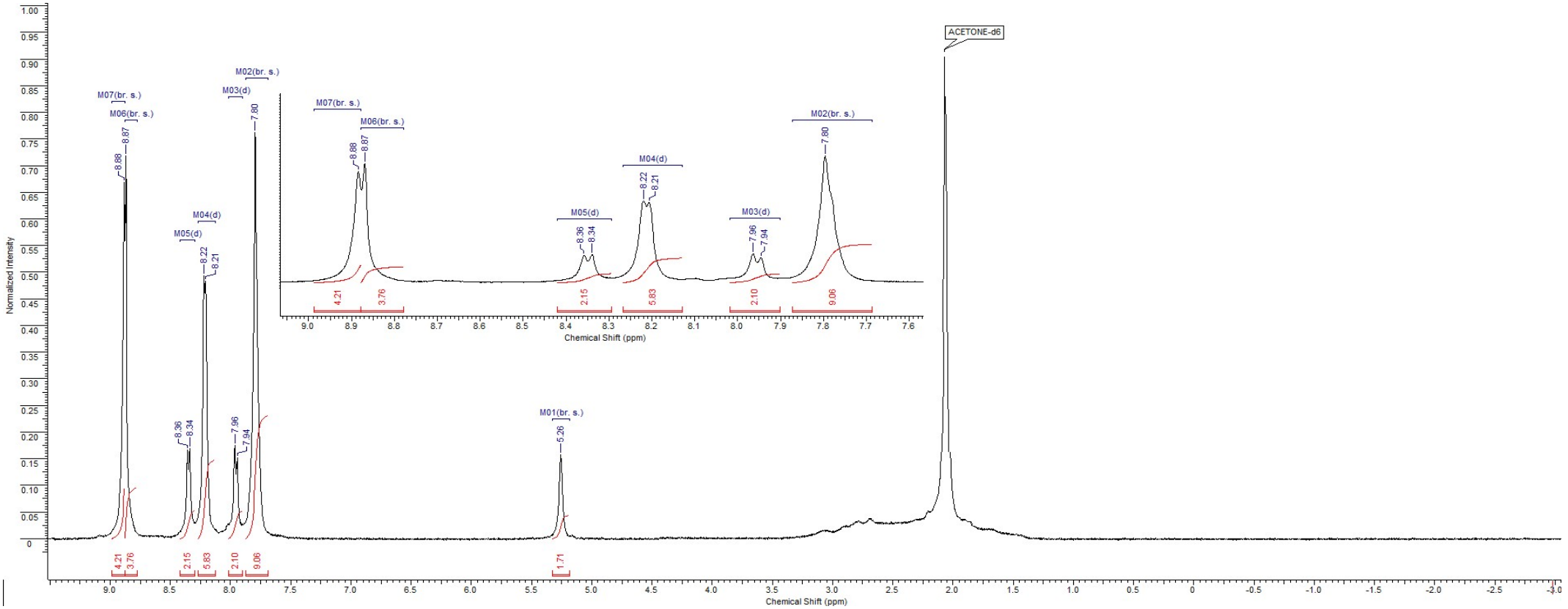

Figure S23. The ^{1}H spectrum of(3-isocyano-*o*-carborane)-{[5-(*p*-isocyanophenyl)-10,15,20-triphenylporphyrinato]zinc}(tetracarbonyl)chromium (**17**) in $(CD_3)_2CO$.

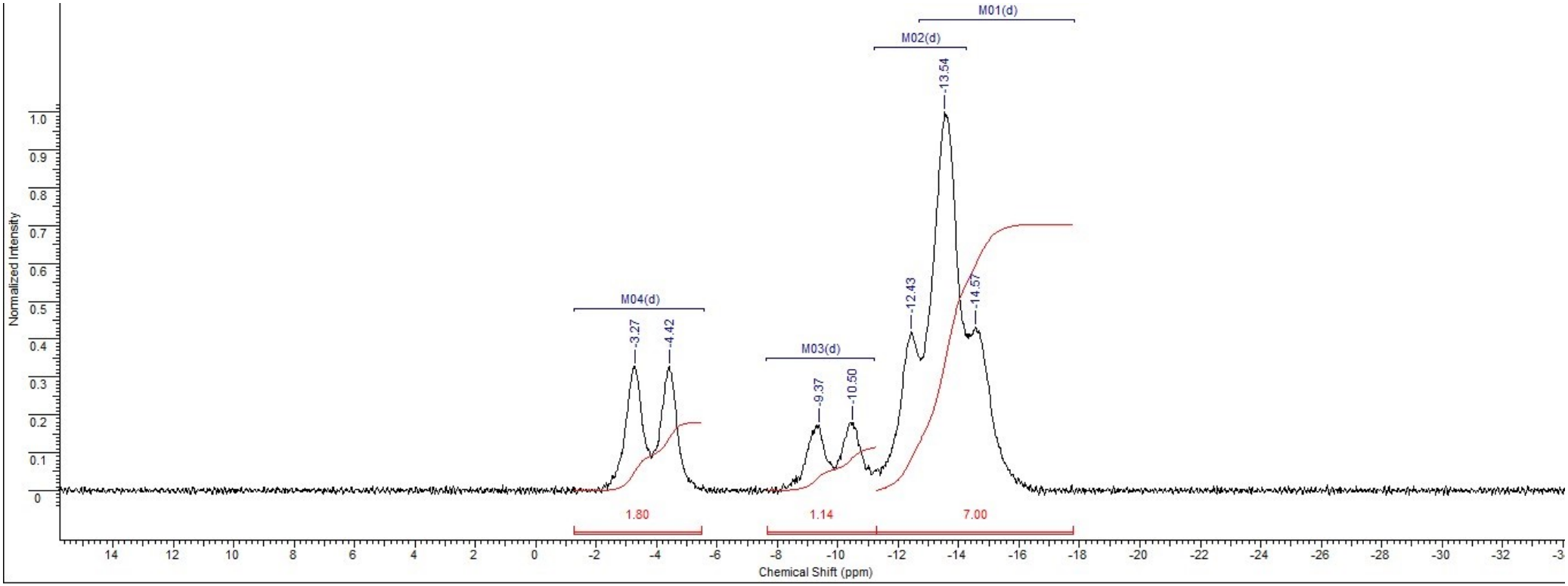

***Figure S24*.** The ^{11}B spectrum of(3-isocyano-*o*-carborane)-[(5-(*p*-isocyanophenyl)-10,15,20-tetraphenylporphyrin](tetracarbonyl)chromium (**17**) in $(CD_3)_2CO$.

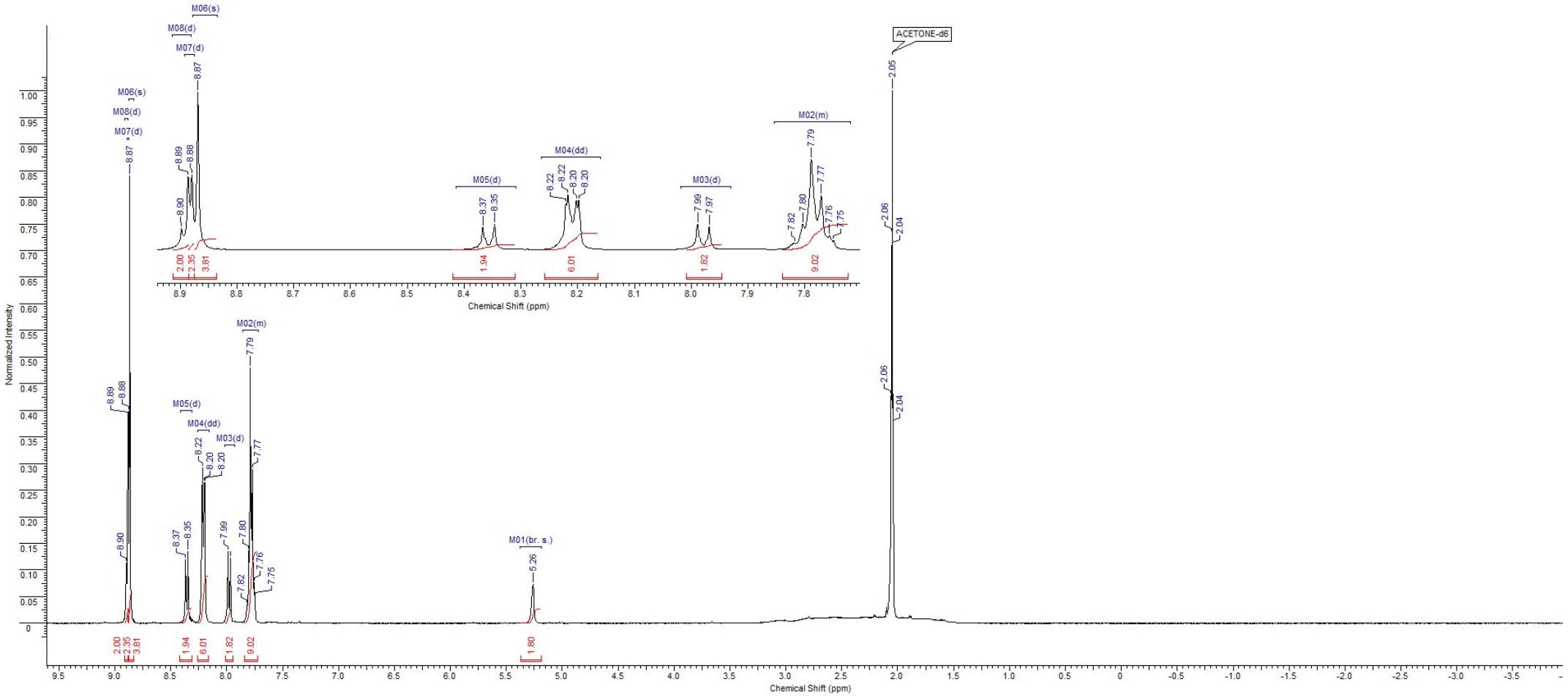

Figure S25. The ^{1}H spectrum of(3-isocyano-*o*-carborane)-{[5-(*p*-isocyanophenyl)-10,15,20-triphenylporphyrinato]zinc}(tetracarbonyl)molybdenum (**18**) in $(CD_3)_2CO$.

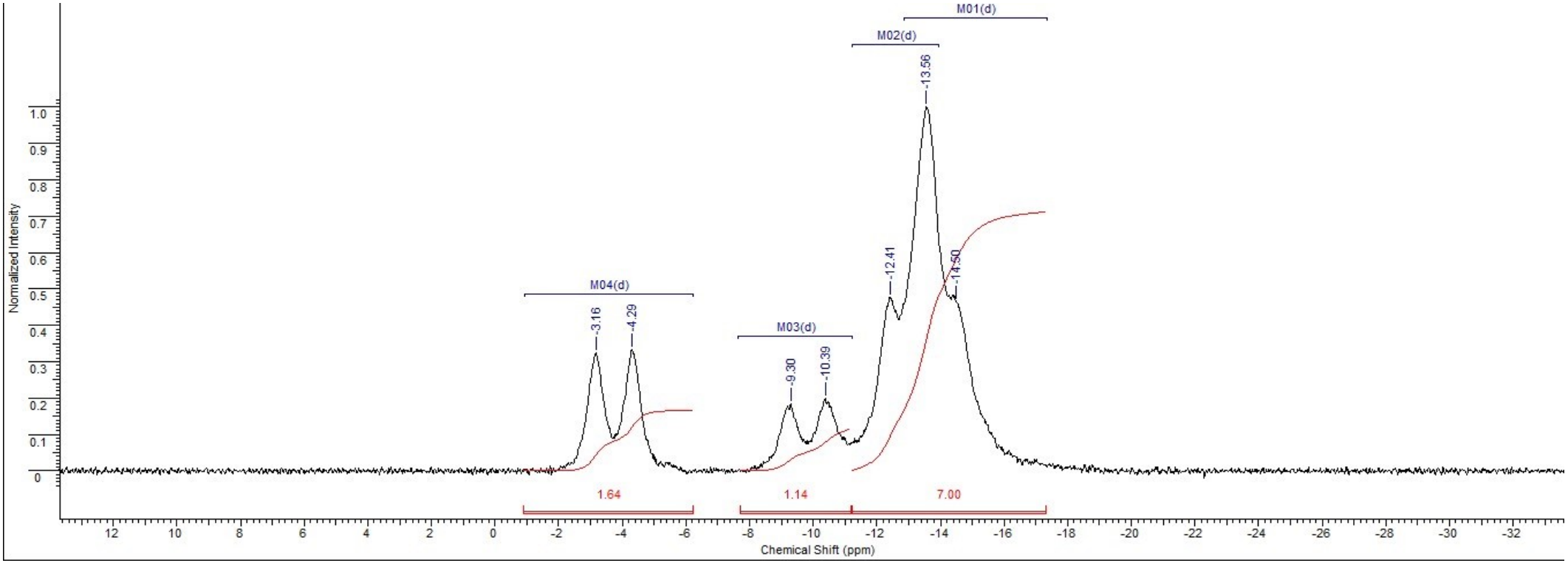

Figure S26. The ^{11}B spectrum of(3-isocyano-*o*-carborane)-{[5-(*p*-isocyanophenyl)-10,15,20-triphenylporphyrinato]zinc}(tetracarbonyl)molybdenum (**18**) in $(CD_3)_2CO$.

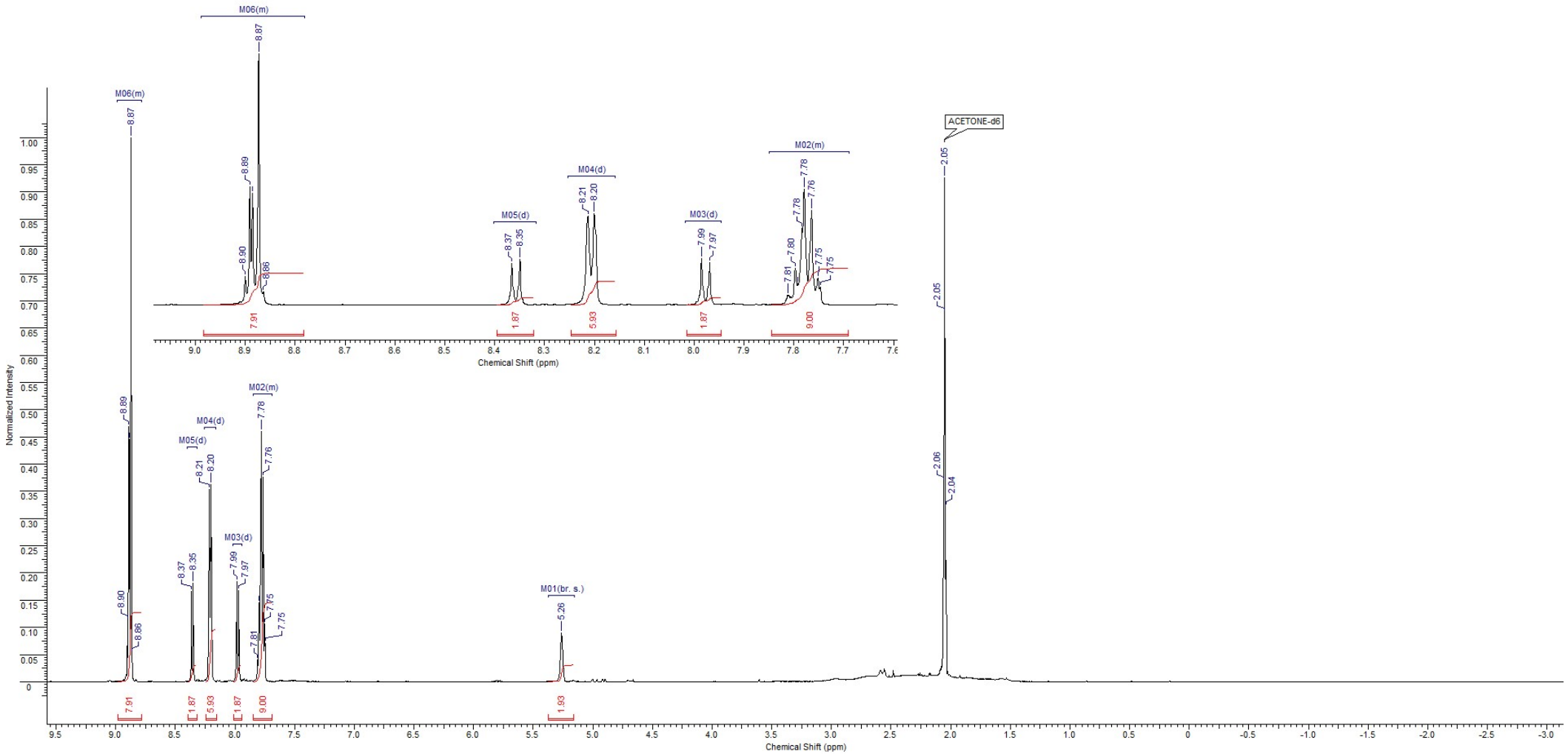

Figure S27. The ^{1}H spectrum of(3-isocyano-*o*-carborane)-{[5-(*p*-isocyanophenyl)-10,15,20-triphenylporphyrinato]zinc}(tetracarbonyl)tungsten (**19**) in $(CD_3)_2CO$.

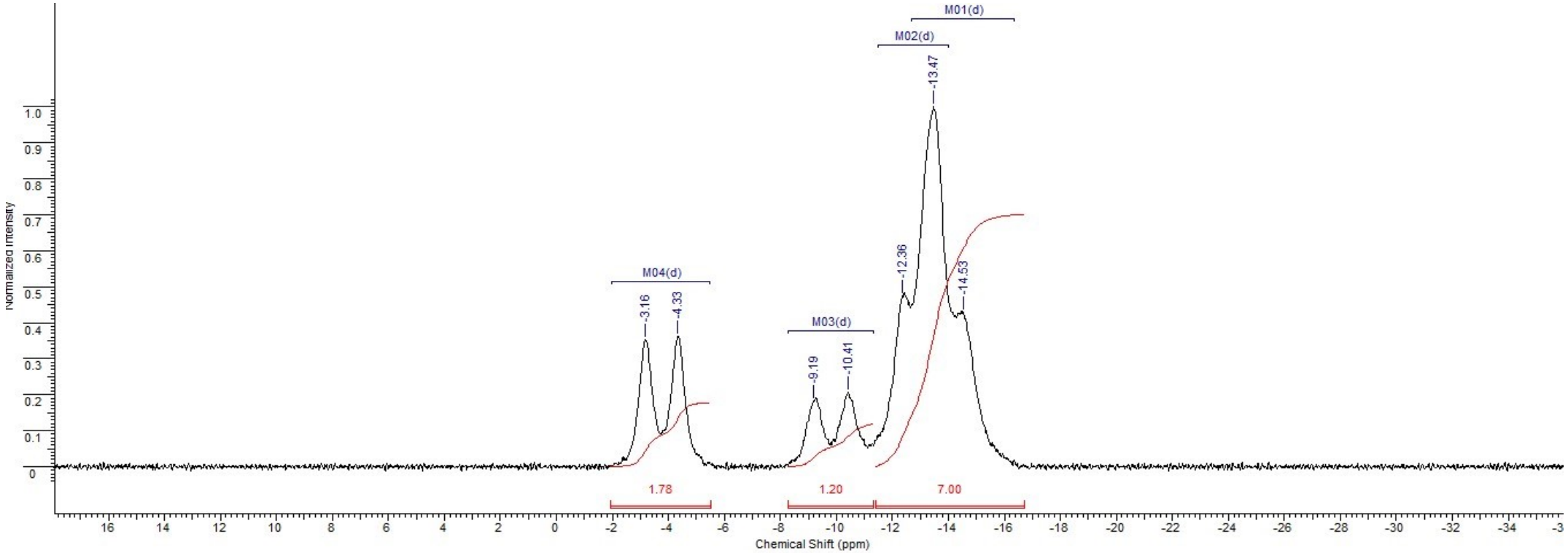

***Figure S28*.** The ^{11}B spectrum of(3-isocyano-*o*-carborane)-{[5-(*p*-isocyanophenyl)-10,15,20-triphenylporphyrinato]zinc}(tetracarbonyl)tungsten (**19**) in $(CD_3)_2CO$.

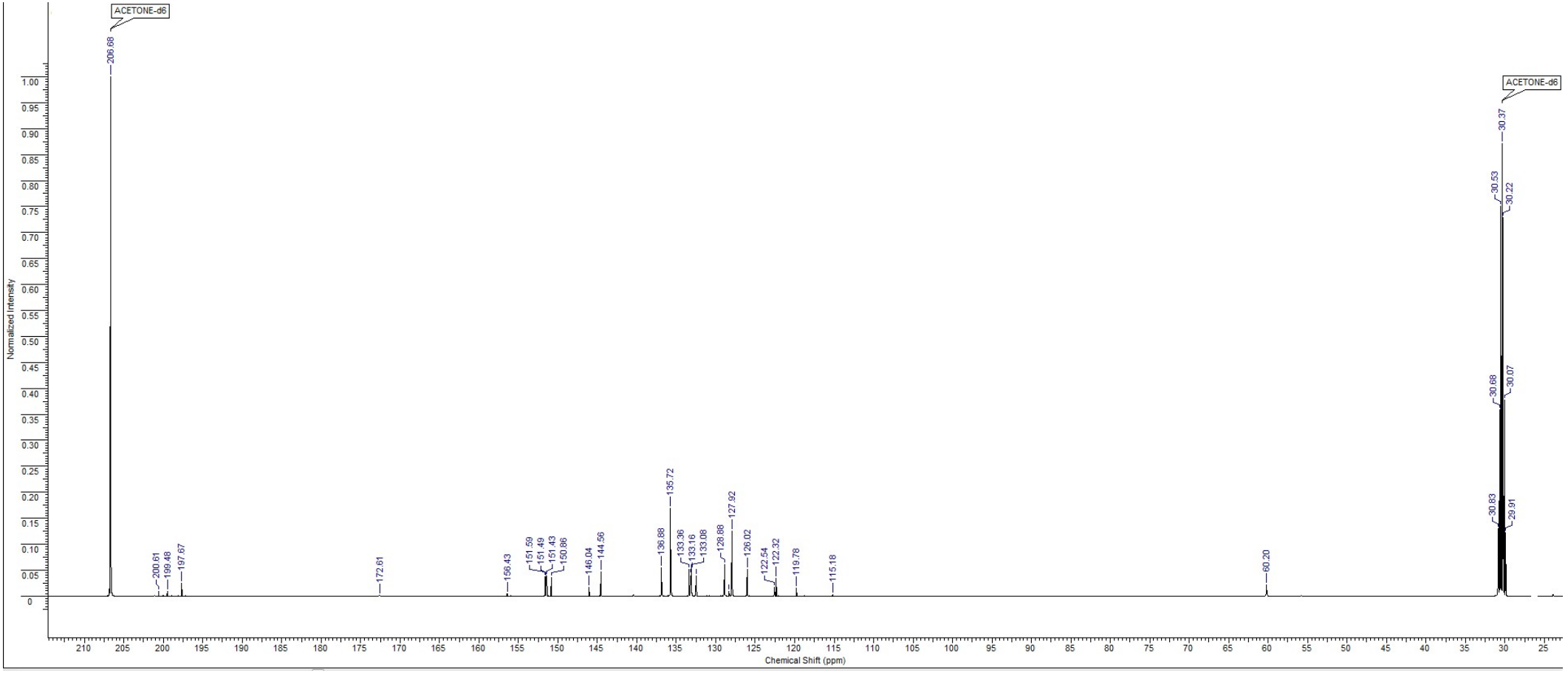

***Figure S29*.** The ^{13}C spectrum of(3-isocyano-*o*-carborane)-{[5-(*p*-isocyanophenyl)-10,15,20-triphenylporphyrinato]zinc}(tetracarbonyl)tungsten (**19**) in $(CD_3)_2CO$.

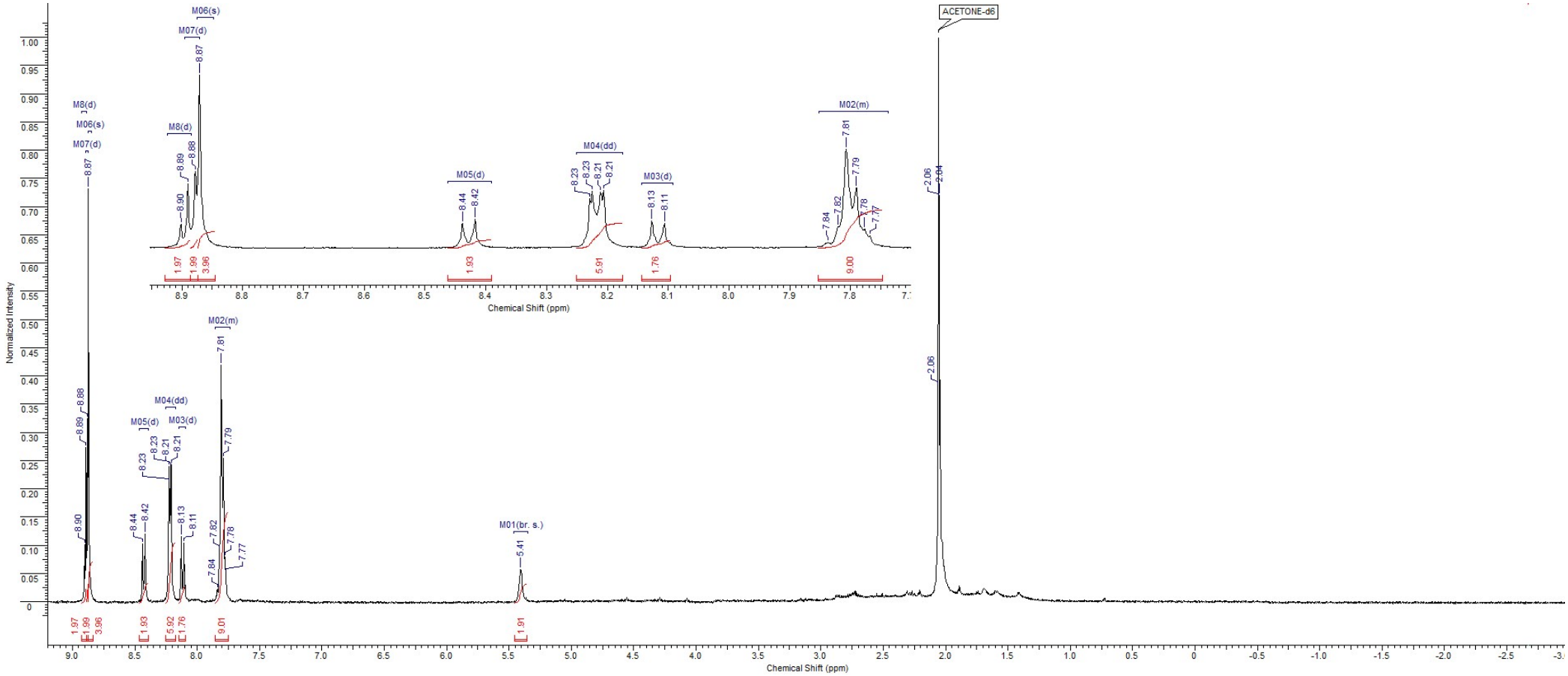

Figure S30. The ^{1}H spectrum of(3-isocyano-*o*-carborane)-{[5-(*p*-isocyanophenyl)-10,15,20-triphenylporphyrinato]zinc}(tricarbonyl)rhenium chloride (**20**) in $(CD_3)_2CO$.

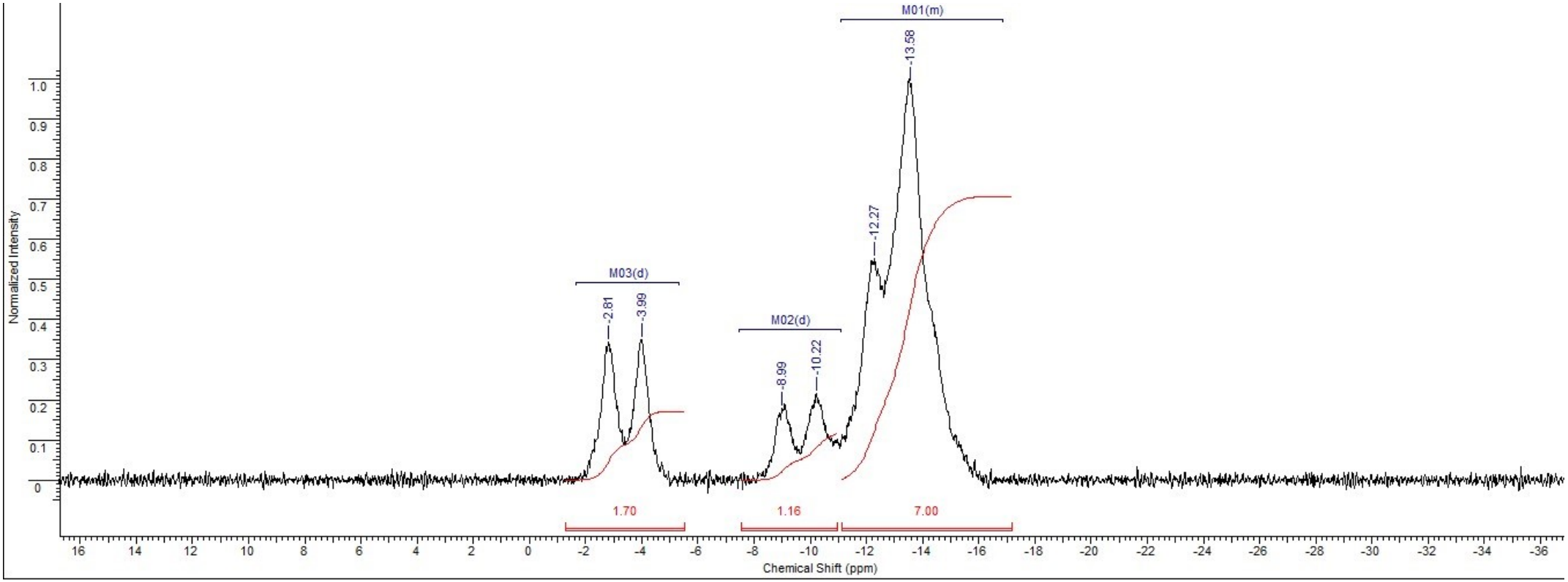

Figure S31. The ^{11}B spectrum of(3-isocyano-*o*-carborane)-{[5-(*p*-isocyanophenyl)-10,15,20-triphenylporphyrinato]zinc}(tricarbonyl)rhenium chloride (**20**) in $(CD_3)_2CO$.

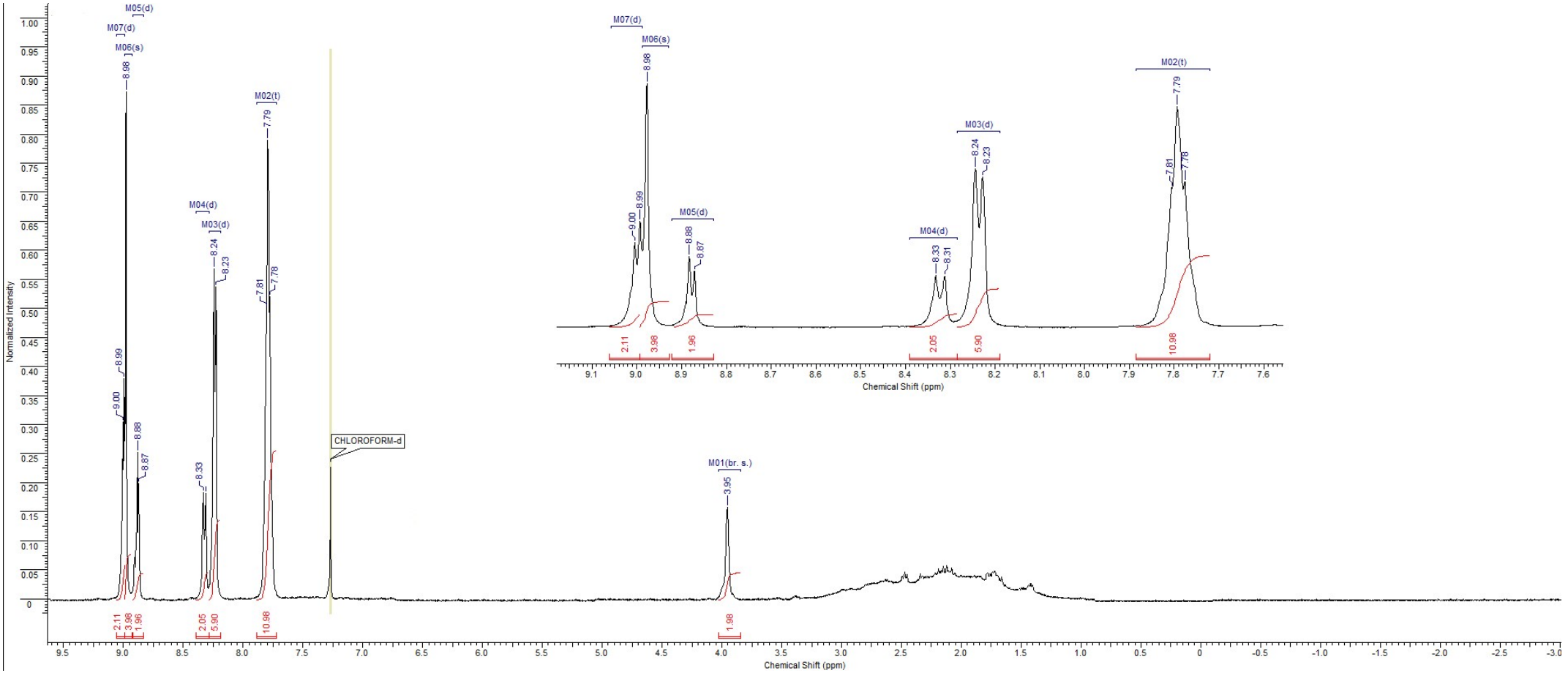

Figure S32. The ^{1}H spectrum of((3-isocyano-*o*-carborane)-{[5-(*p*-isocyanophenyl)-10,15,20-triphenylporphyrinato]zinc}(octacarbonyl)dirhenium (**21**) in $CDCl_3$.

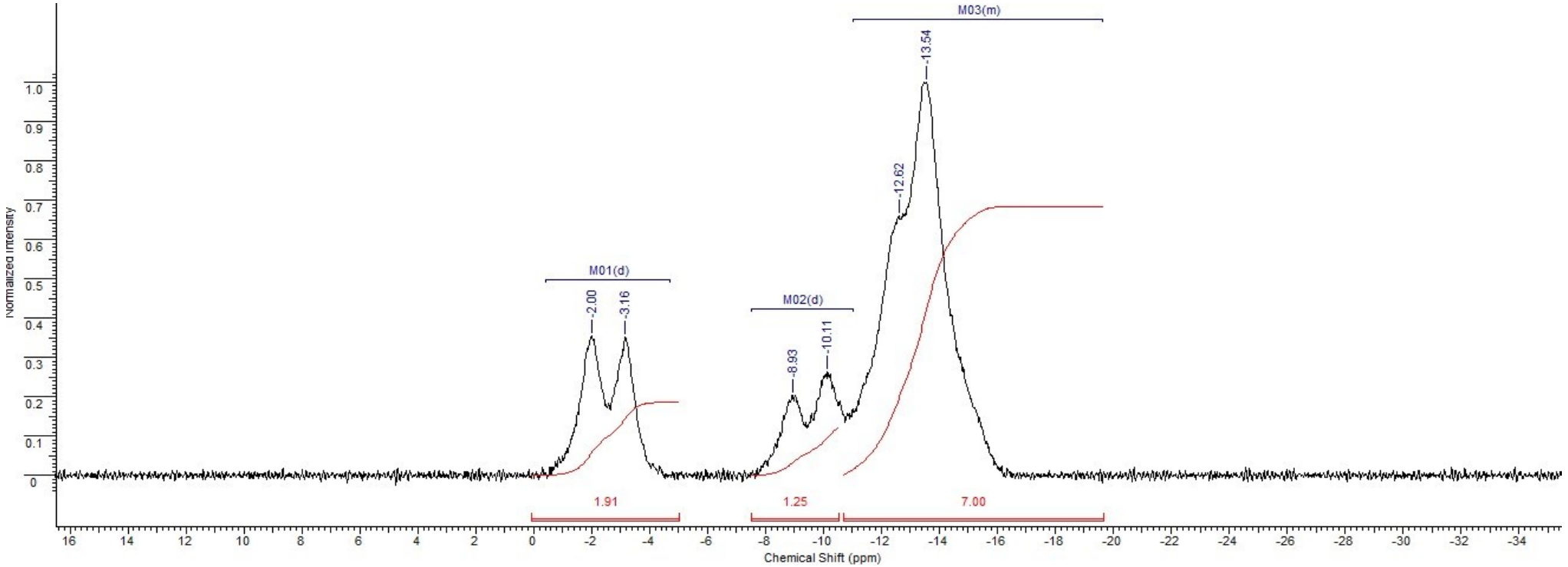

Figure S33. The ^{11}B spectrum of(3-isocyano-*o*-carborane)-{[5-(*p*-isocyanophenyl)-10,15,20-triphenylporphyrinato]zinc}(octacarbonyl)dirhenium (**21**) in $(CD_3)_2CO$.

3. Geometry and Electronic Structure for compound 3, 5, 10–12, 15, 18–20

The geometry of porphyrin conjugates **3**, **5**, **10**–**12**, **15**, **18**–**20** are presented below (Figures S34-S42).

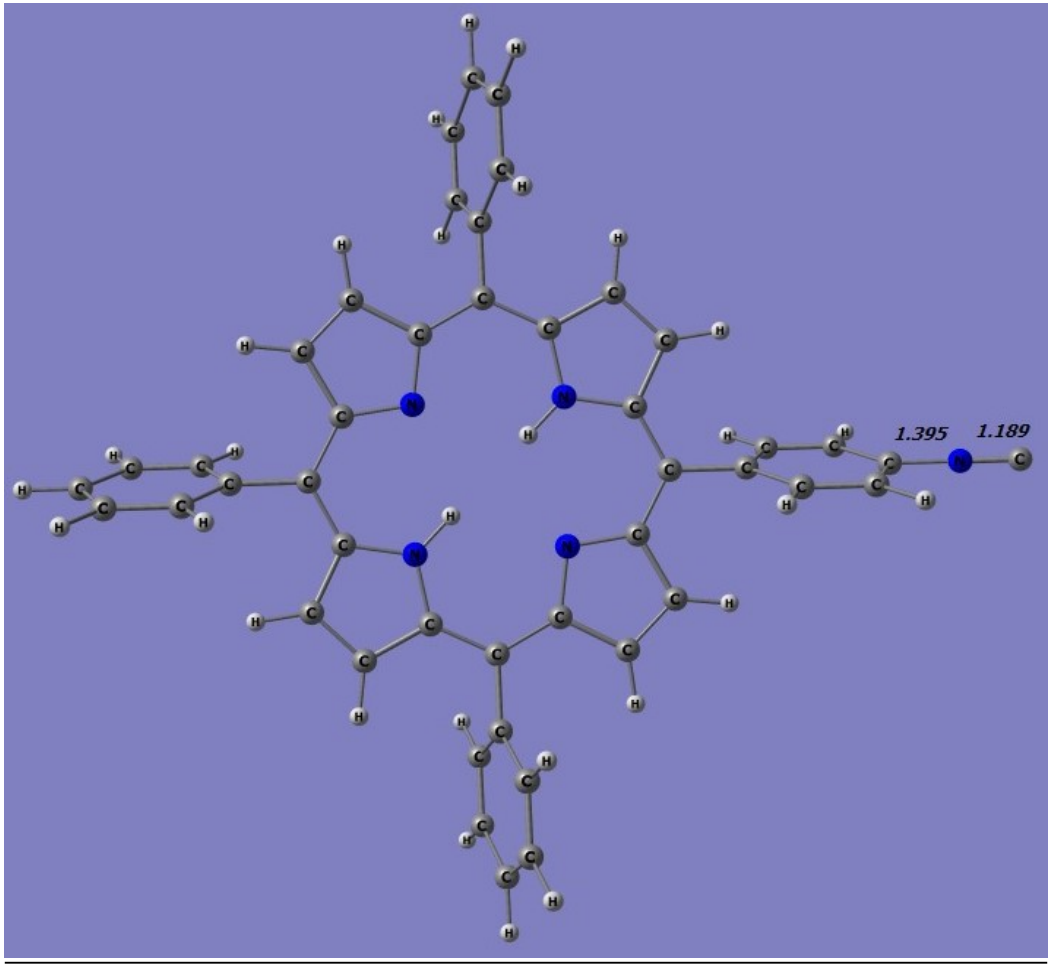

Figure S34. The optimized geometry structure of compound **3** using DFT wb97dt/ LanL2DZ.

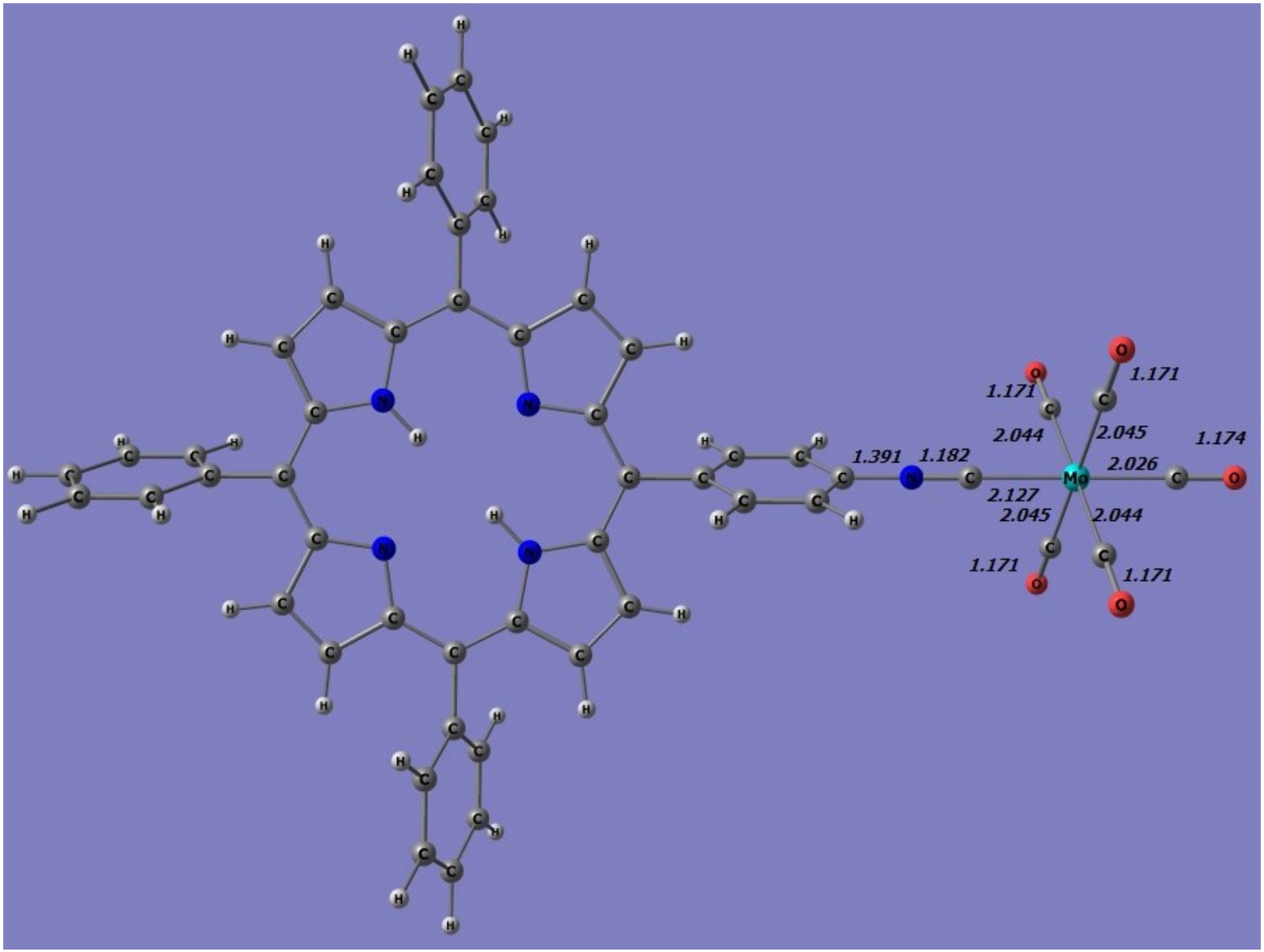

Figure S35. The optimized geometry structure of compound **5** using DFT wb97dt/ LanL2DZ.

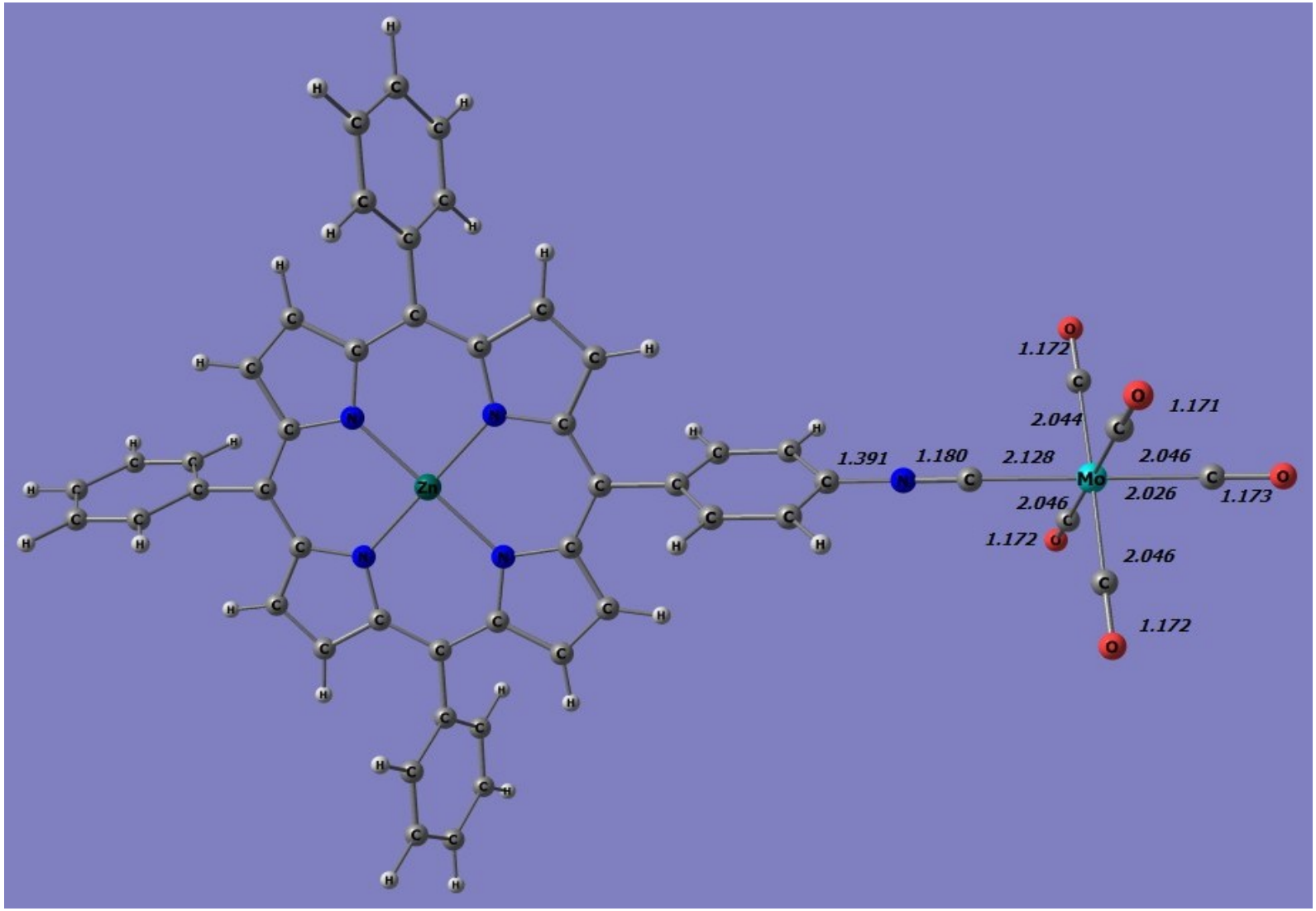

Figure S36. The optimized geometry structure of compound **10** using DFT wb97dt/ LanL2DZ.

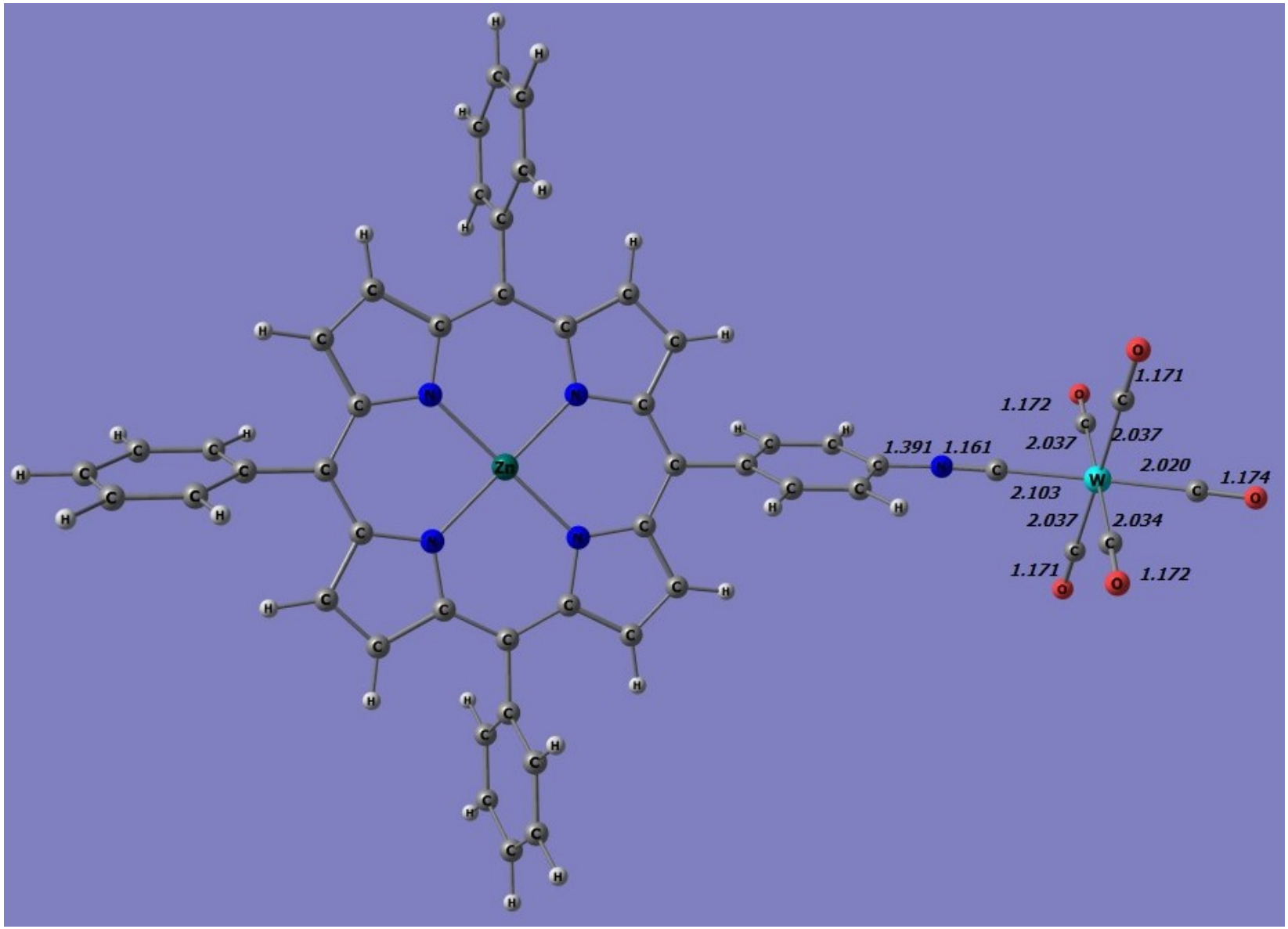

Figure S37. The optimized geometry structure of compound **11** using DFT wb97dt/ LanL2DZ.

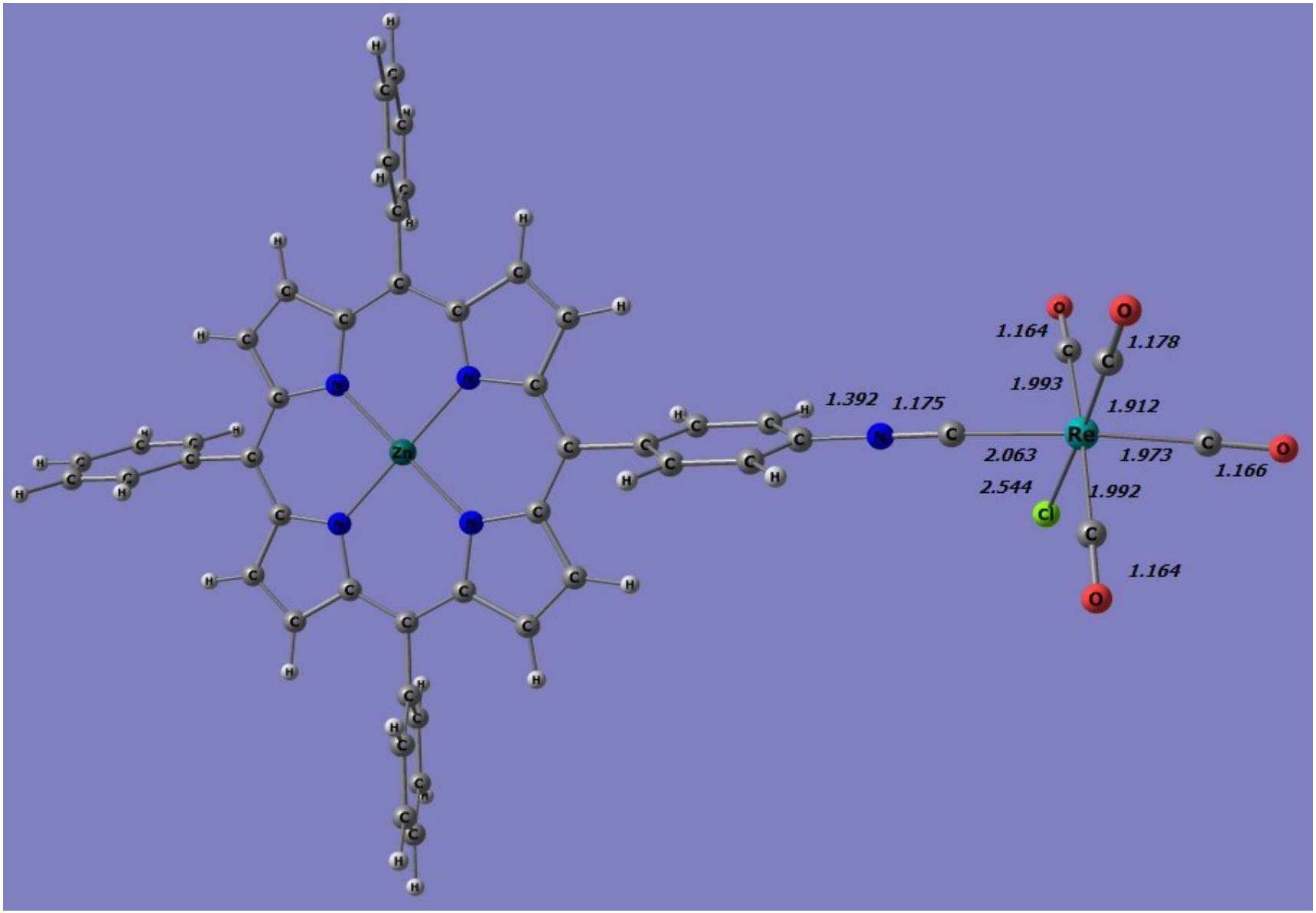

Figure S38. The optimized geometry structure of compound **12** using DFT wb97dt/ LanL2DZ.

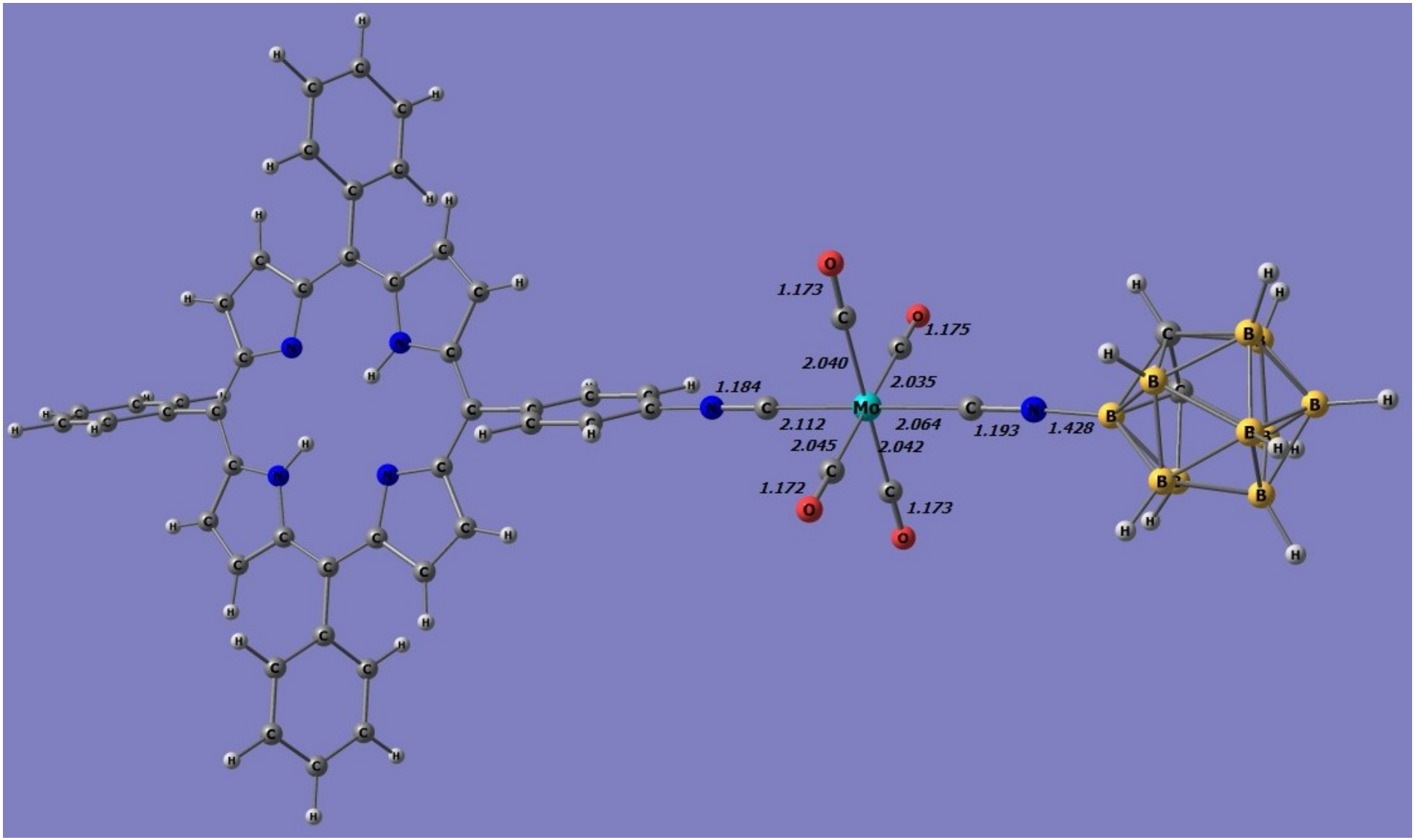

Figure S39. The optimized geometry structure of compound **15** using DFT wb97dt/ LanL2DZ.

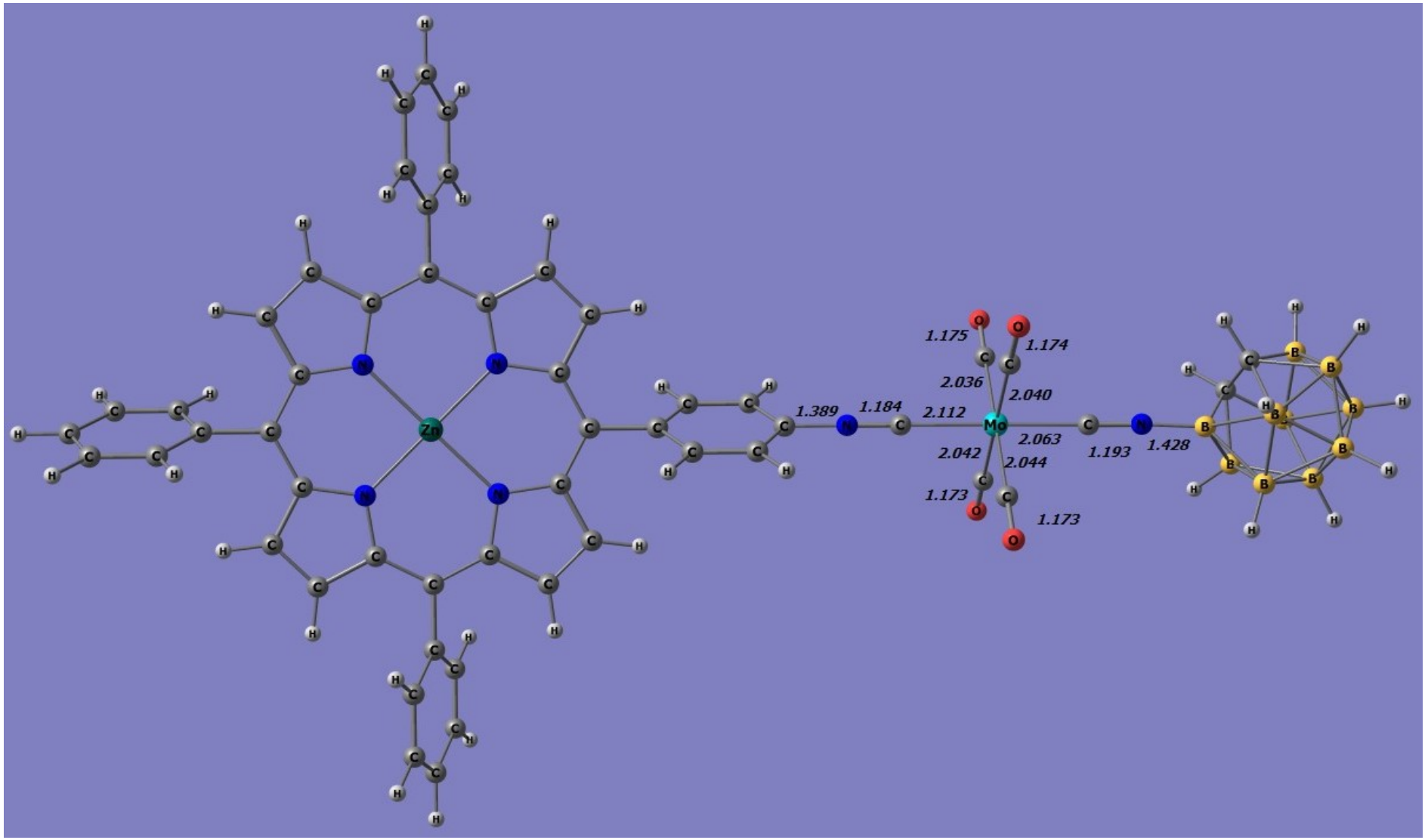

Figure S40. The optimized geometry structure of compound **18** using DFT wb97dt/ LanL2DZ.

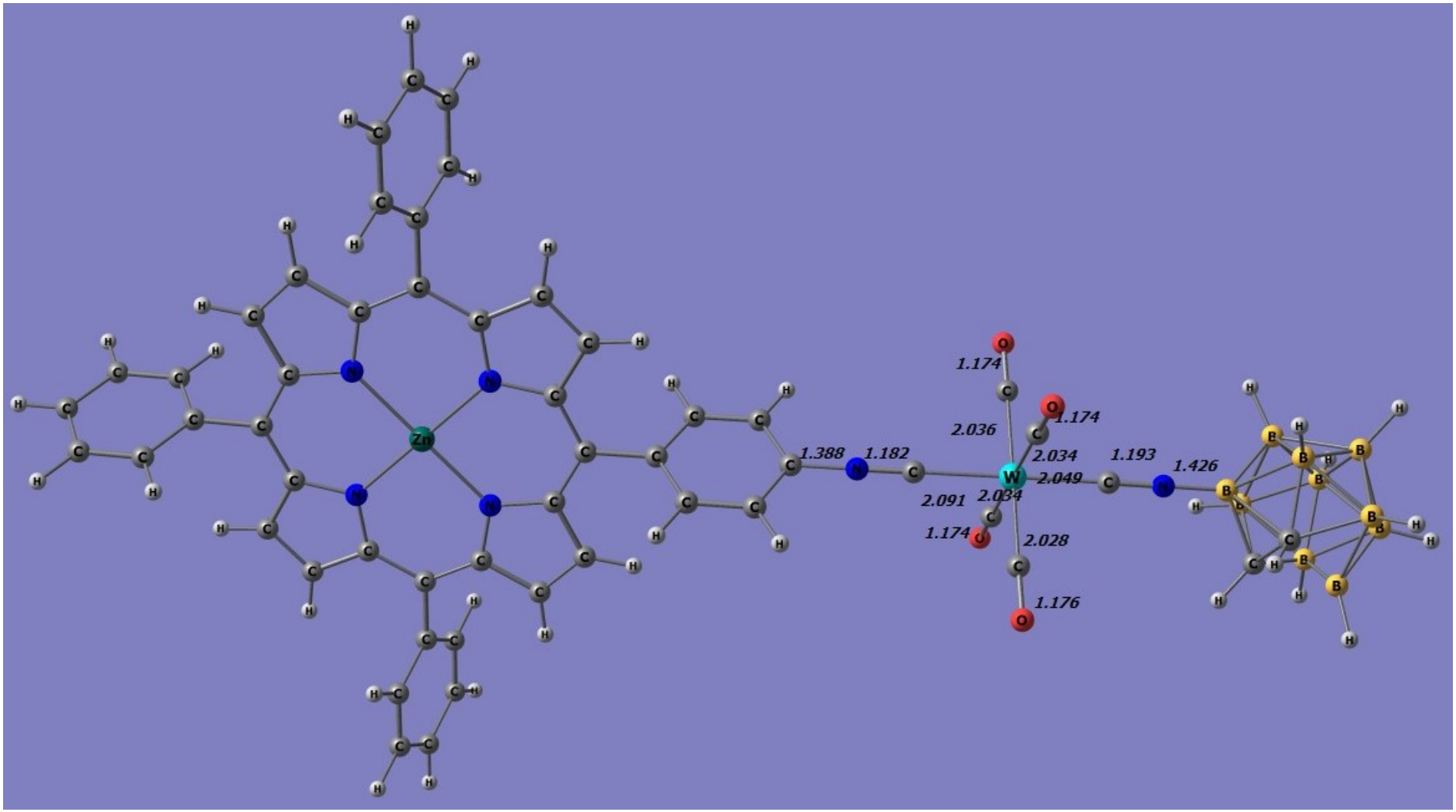

Figure S41. The optimized geometry structure of compound **19** using DFT wb97dt/ LanL2DZ.

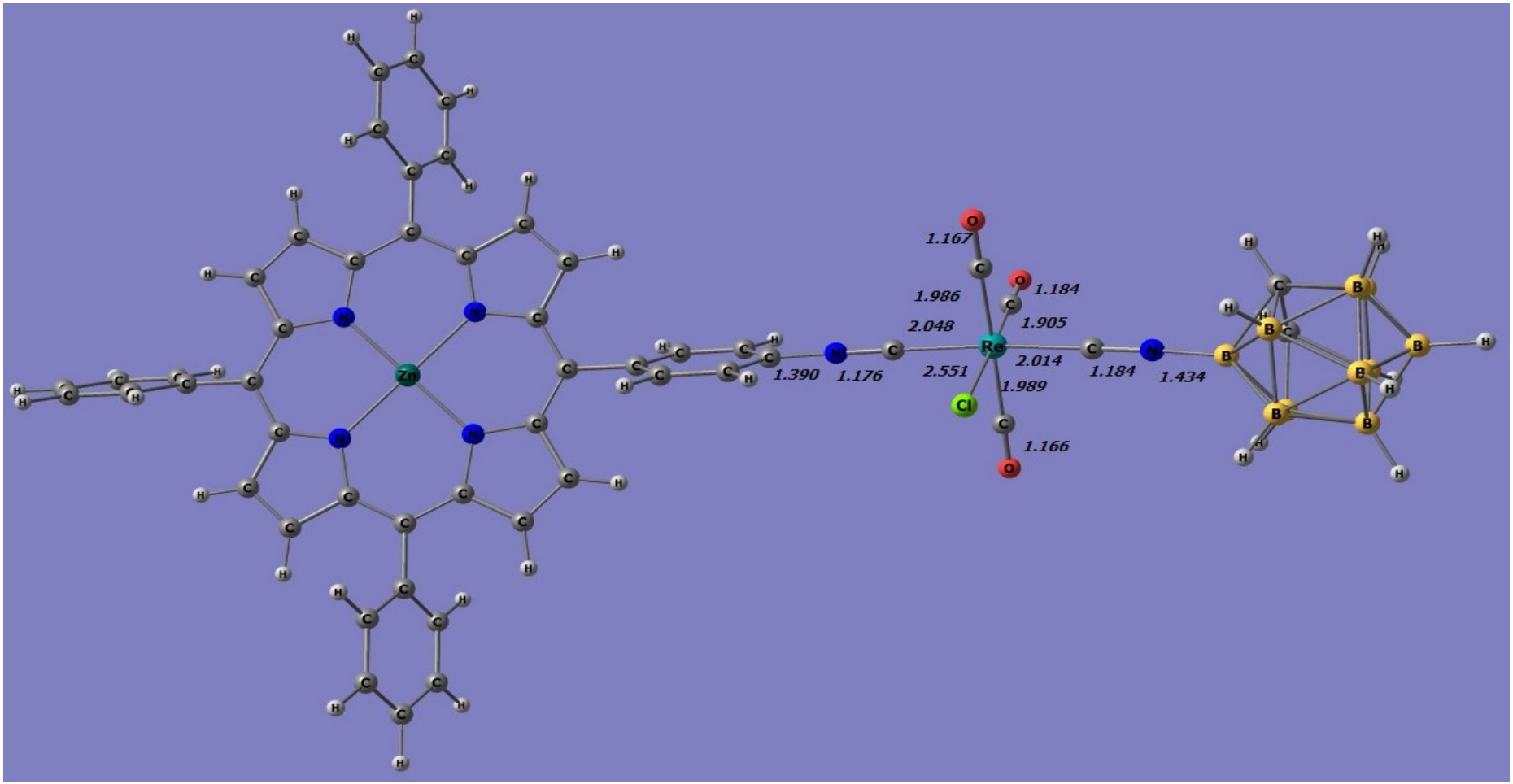

Figure S42. The optimized geometry structure of compound **20** using DFT wb97dt/ LanL2DZ.

4. The calculated ^{13}C NMR spectra for compound 5, 6, 10–12, 15, 18, 20

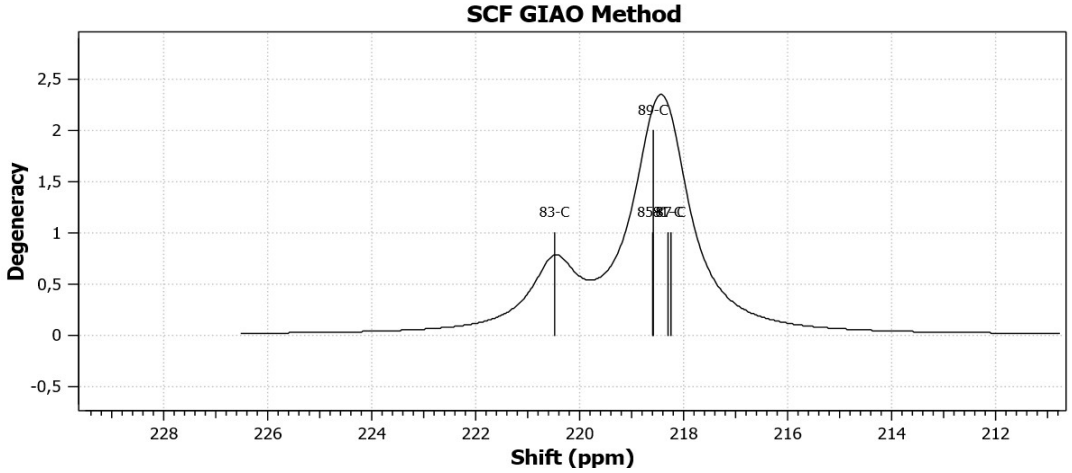

Figure S43. Fragment of the calculated ^{13}C NMR spectrum using the DFT wb97dt/ LanL2DZ method for compound **5**.

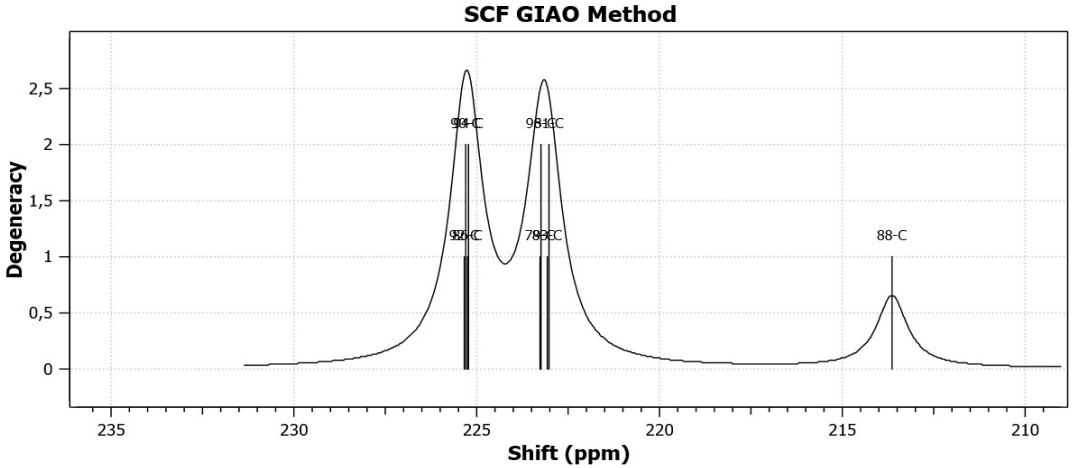

Figure S44. Fragment of the calculated ^{13}C NMR spectrum using the DFT wb97dt/ LanL2DZ method for compound **6**.

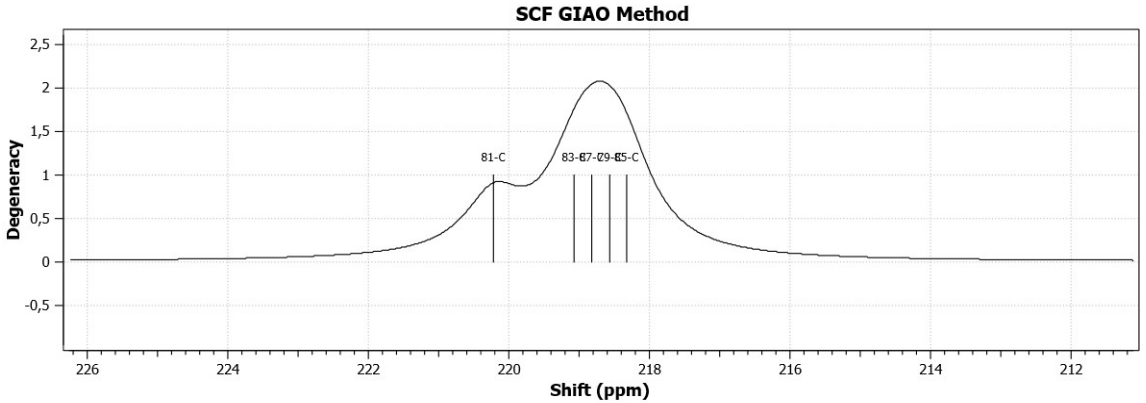

Figure S45. Fragment of the calculated ^{13}C NMR spectrum using the DFT wb97dt/ LanL2DZ method for compound **10**.

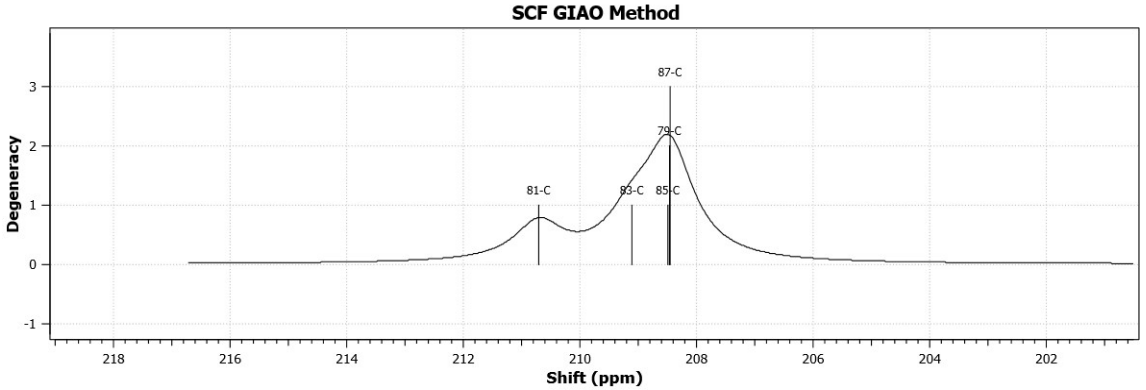

Figure S46. Fragment of the calculated ^{13}C NMR spectrum using the DFT wb97dt/ LanL2DZ method for compound **11**.

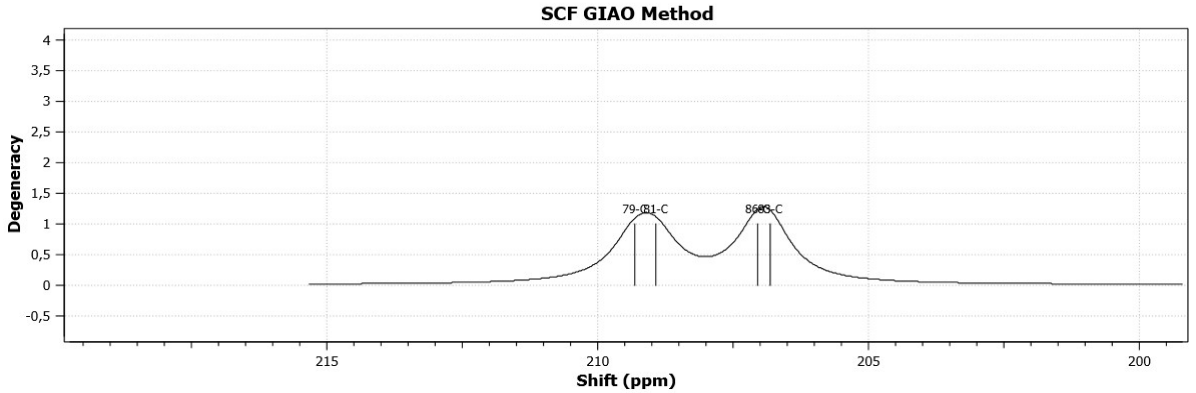

Figure S47. Fragment of the calculated ^{13}C NMR spectrum using the DFT wb97dt/ LanL2DZ method for compound **12**.

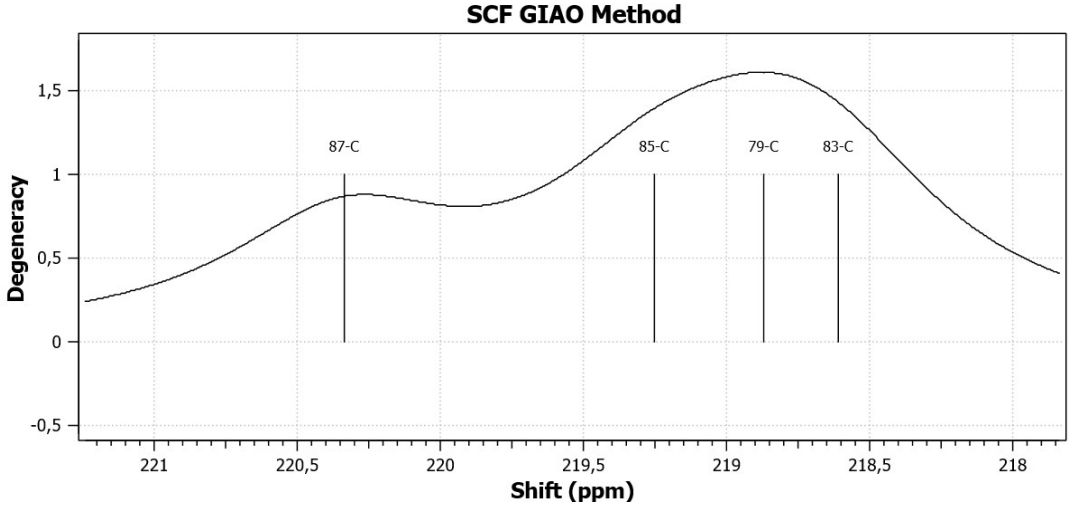

Figure S48. Fragment of the calculated ^{13}C NMR spectrum using the DFT wb97dt/ LanL2DZ method for compound **15**.

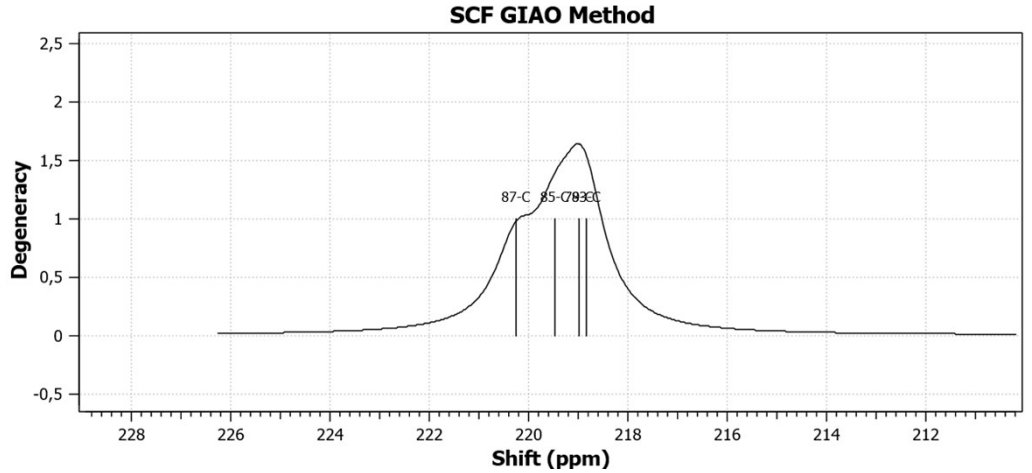

Figure S49. Fragment of the calculated ^{13}C NMR spectrum using the DFT wb97dt/ LanL2DZ method for compound **18**.

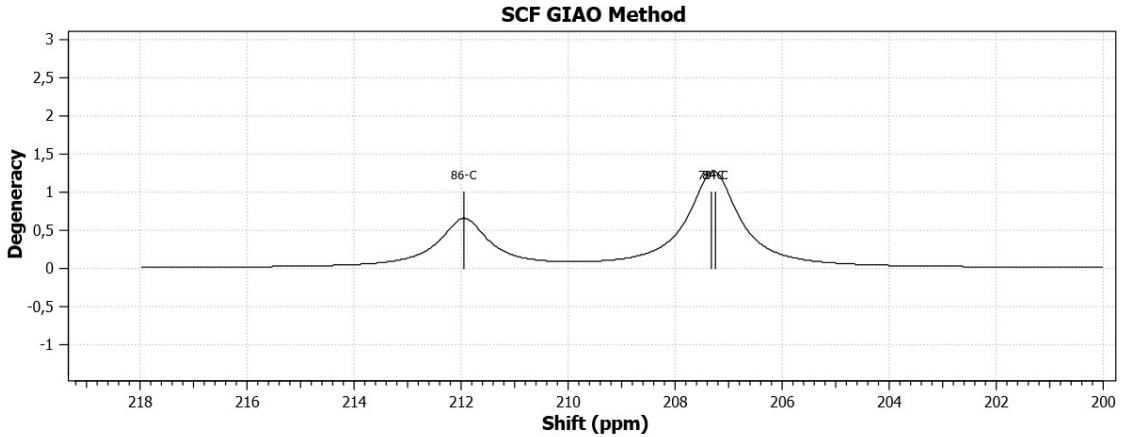

Figure S50. Fragment of the calculated ^{13}C NMR spectrum using the DFT wb97dt/ LanL2DZ method for compound **20**.

5. Spectral and photochemical properties

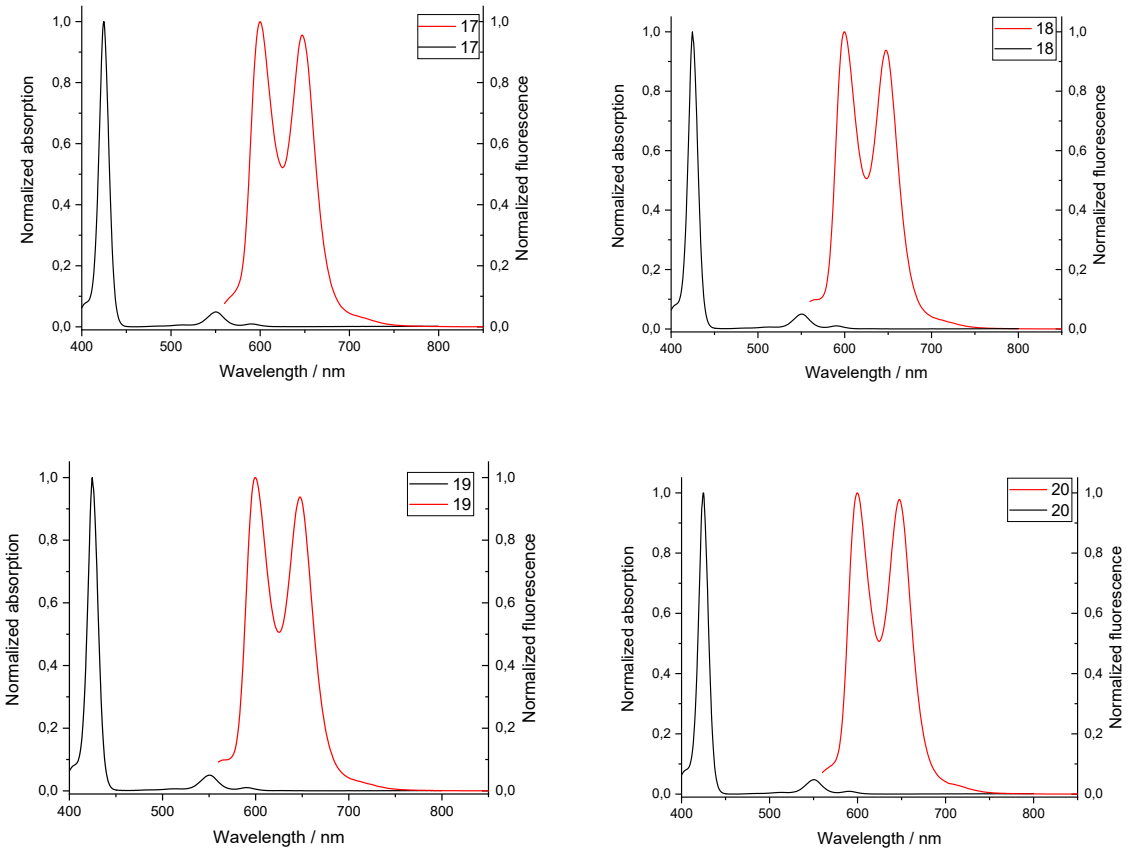

Figure S51. Normalized absorption (black line) and fluorescence (red line) spectra (λ_{ex} = 550 nm) of **17**, **18**, **19** and **20** in toluene.

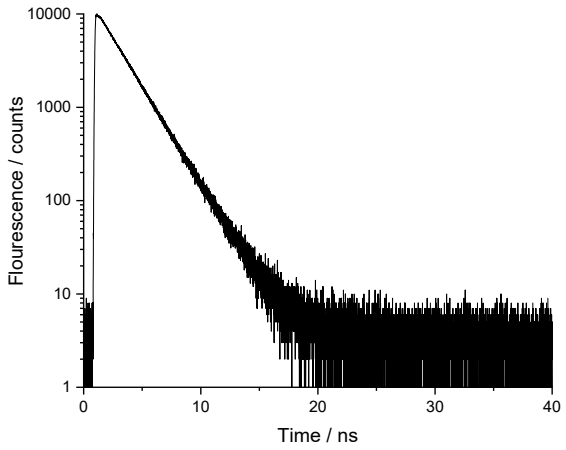

Figure S52.Compound **20** fluorescence decay in toluene (λ_{ex} = 550 nm)

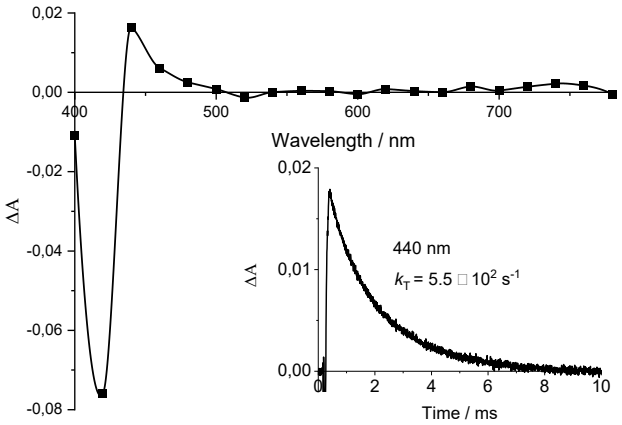

Figure S53. Triplet-triplet absorption spectra of **15** (1×10^{-6} M) in toluene. 400 μs after flash. Inset depicts triplet state decay kinetics. $k_T = 5.5 \times 10^2$ s^{-1}

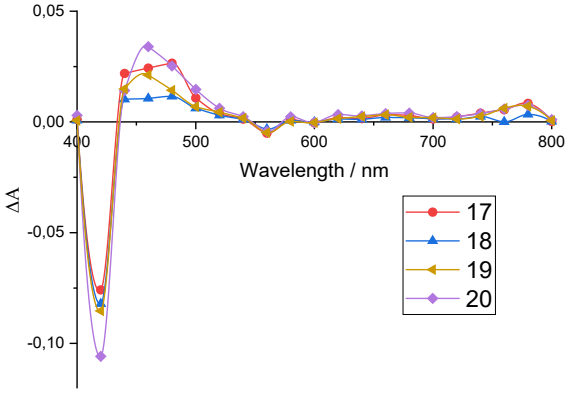

Figure S54. Triplet-triplet spectra of compounds **18**, **19**, **17**, **20** in toluene 50 ns after flash, λ_{ex} = 550 nm.

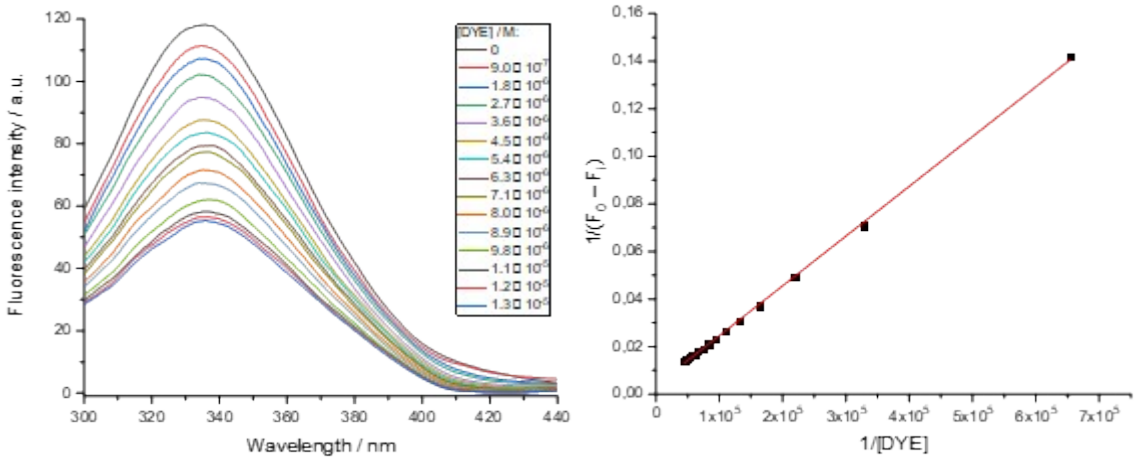

Figure S55. Fluorescence spectra of HSA (1×10^{-6} M) (left) in presence of different **15** concentration, Lineweaver–Burk plot (right). $K_b = 2.0 \times 10^4$ M^{-1}.

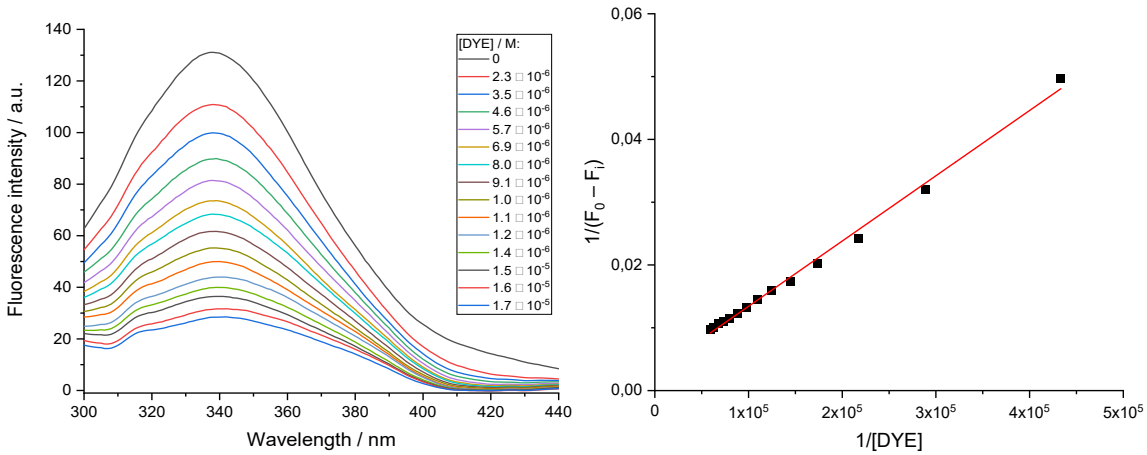

Figure S56. Fluorescence spectra of HSA (1 × 10^{-6} M) (left) in presence of different **17** concentrations, Lineweaver–Burk plot (right). K_b = 2.9 × 10^4 M^{-1}.

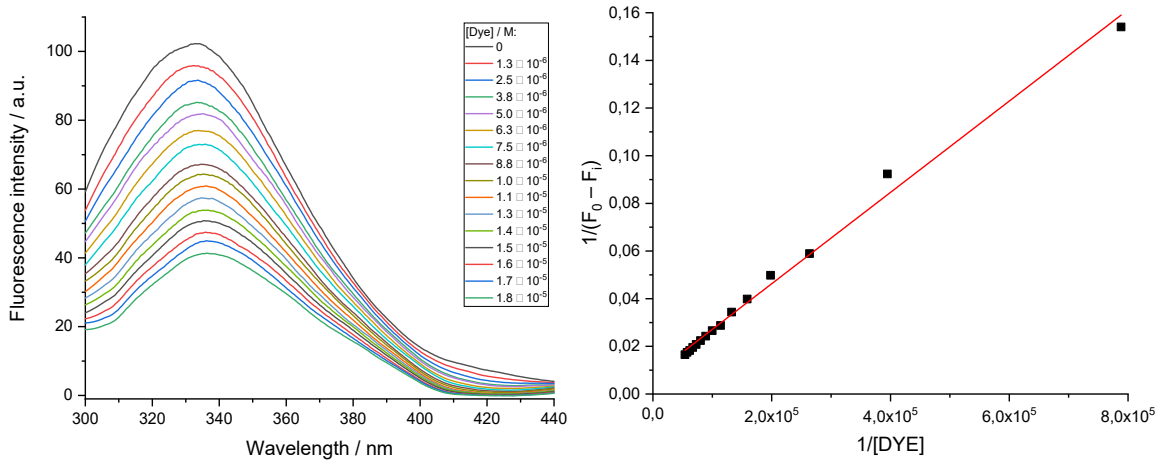

Figure S57. Fluorescence spectra of HSA (1 × 10^{-6} M) (left) in presence of different **18**concentrationsLineweaver–Burk plot (right). K_b = 4.2 × 10^4 M^{-1}.

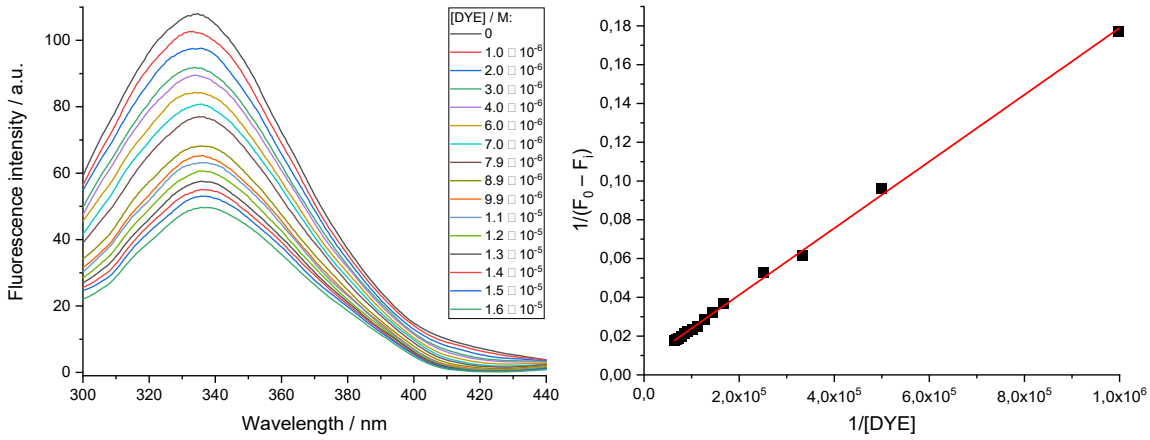

Figure S58. Fluorescence spectra of HSA (1 × 10^{-6} M) (left) in presence of different **19** concentrations, Lineweaver–Burk plot (right).

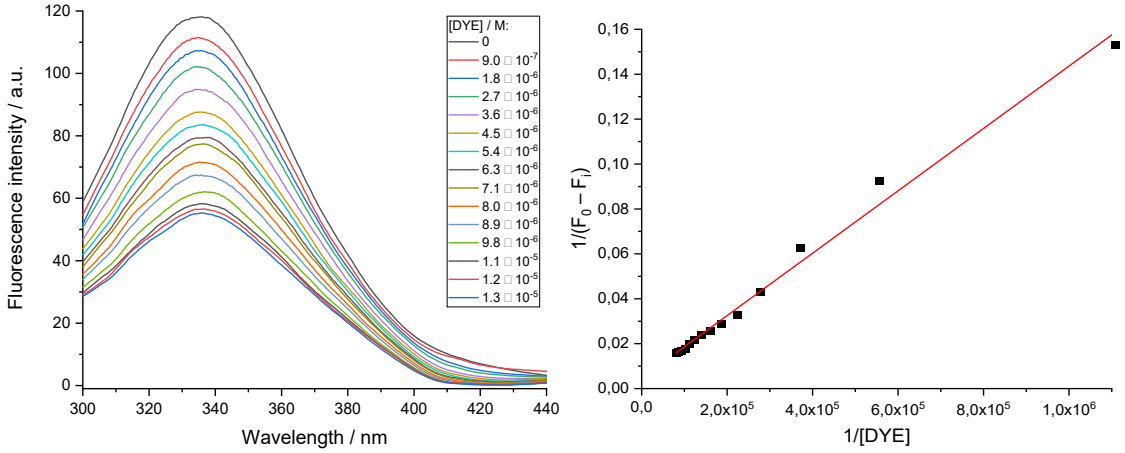

Figure S59. Fluorescence spectra of HSA (1×10^{-6} M) (left) in presence of different **20** concentrations, Lineweaver–Burk plot (right). $K_b = 3.4 \times 10^4$ M^{-1}.

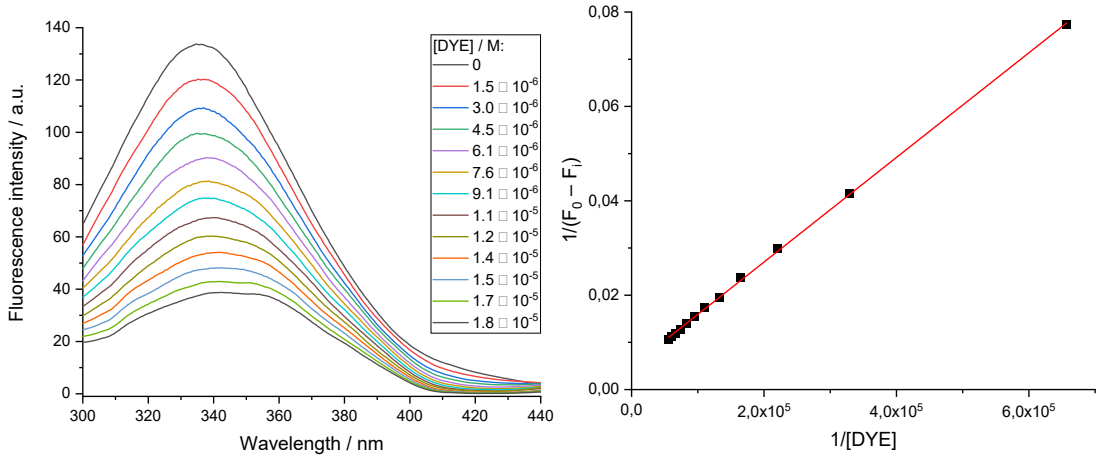

Figure S60. Fluorescence spectra of HSA (1×10^{-6} M) (left) in presence of different **21** concentrations, Lineweaver–Burk plot (right). $K_b = 4.4 \times 10^4$ M^{-1}.

6. Synthesis and spectral data of zinc complex of carboranylporphyrin 25

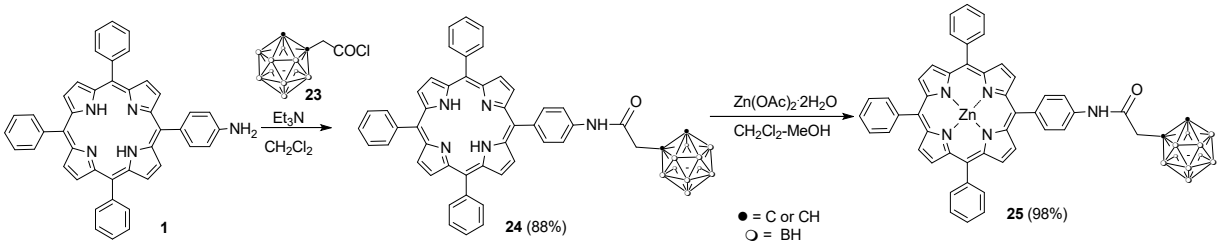

Scheme S1. Synthesis of zinc complex of carboranyl porphyrin **25**.

5-(*p*-(*o*-Carborane-1'-yl)-acetamidophenyl)-10,15,20-triphenylporphyrin (24)

A mixture of 1-carboxymethyl-*o*-carborane **22** (17 mg, 0.084 mmol) and $SOCl_2$ (0.5 mL) in C_6H_6 (2 mL) was stirred under reflux for 1h under argon. Then solvents were removed in vacuo to give corresponding acyl chloride **23**. To a solution of compound **23** in CH_2Cl_2 (2 mL) a mixture of aminoporphyrin**1** (50 mg, 0.08 mmol) and Et_3N (14 µl, 0.10 mmol) in CH_2Cl_2 (5 mL) was added dropwise at 5°C under argon for 30 min. Then the reaction mixture was treated with water (100 mL) and extracted with CH_2Cl_2 (3x10 mL). The combined organic solution was dried over Na_2SO_4. After the removing of the solvent the product was purified by column chromatography on silica gel using hexane – $CHCl_3$ (2:8) mixture as an eluent to give 57 mgof porphyrin **24** in 88% yield as purple solid. IR (KBr, cm^{-1}) ν_{max}: 3435 (NH), 3042 (carborane CH), 2591 (BH), 1684 (C=O). ^{1}H NMR (300.13 MHz, THF-d_8), δ (ppm): 10.14 (br s, 1H, NHCO), 8.89 (d, *J* = 4.6 Hz, 2H, β-H), 8.84 (d, *J* = 5.0 Hz, 2H, β-H), 8.83 (s, 4H, β-H), 8.20 (m, 8H, Ph), 8.07 (d, *J* = 8.2 Hz, 2H, Ph), 7.77 (d, *J* = 3.2 Hz, 9H, Ph), 5.18 (br s, 1H, carborane CH), 3.51 (br s, 2H, CH_2), –2.68 (br s, 2H, NH). ^{11}B NMR (128.38 MHz, THF-d_8), δ (ppm): – 4.3 (d, *J* = 147 Hz, 1B), –7.1 (d, *J* = 154 Hz, 1B), –11.4 (d, *J* = 142 Hz, 4B), –13.5 (d, *J* = 161 Hz, 4B).UV-vis ($(CH_3)_2CO$) λ_{max}, nm (log ε): 415 (5.56), 511(4.09), 547 (3.83), 591 (3.64), 647 (3.54). MALDI-MS, Found: *m/z* 814.00$[M]^+$(DCTBmatrix); '$C_{48}H_{43}B_{10}N_5O$' requires $[M]^+$ 813.45.

[5-(*p*-(*o*-Carborane-1'-yl)-acetamidophenyl)-10,15,20-triphenylporphyrinato]zinc (25)

To a solution of carboranylporphyrin **24** (50 mg, 0.061 mmol) in CH_2Cl_2 (5 mL) a solution of $Zn(OAc)_2{\cdot}2H_2O$ (50 mg, 0.228 mmol) in MeOH (5 mL) was added and the mixture was stirred for 1h at room temperature. Then the reaction mixture was treated with water and extracted with CH_2Cl_2 (3x40mL). The organic extract was dried over Na_2SO_4, and the solvent was removed under reduced pressure to give 52 mg (98%) of porphyrin 25. IR (KBr, cm^{-1}) ν_{max}: 3430 (NH),3047 (carborane CH),

2591 (BH), 1649 (C=O). ^{1}H NMR (300 MHz, THF-d_8), δ (ppm): 10.00 (s, 1H, N*H*-C=O), 8.92 (d, *J* = 4.7 Hz, 2H, β-H), 8.88 (d, *J* = 6.6 Hz, 2H, β-H), 8.87 (s, 4H, β-H), 8.21 (m, 8H, Ph), 8.04 (d, *J* = 8.2 Hz, 2H, Ph), 7.76 (d, *J* = 3.6 Hz, 9H, Ph), 5.22 (br s, 1H, carborane CH), 3.53 (s, 2H, CH_2). ^{11}B NMR (128.38 MHz, THF-d_8), δ (ppm): –2.4 (d, *J* = 142 Hz, 1B), –5.3 (d, *J* = 140 Hz, 1B), –9.6 (d, *J* = 144 Hz, 4B), –11.6 (d, *J* = 154 Hz, 4B). UV-vis ($(CH_3)_2CO$) λ_{max}, nm (ε): 422 (5.45), 555 (4.14), 595 (3.75). MALDI-MS, Found: *m/z* 876.92 $[M]^+$ (DCTB matrix); '$C_{48}H_{41}B_{10}N_5OZn$' requires $[M]^+$ 877.36.

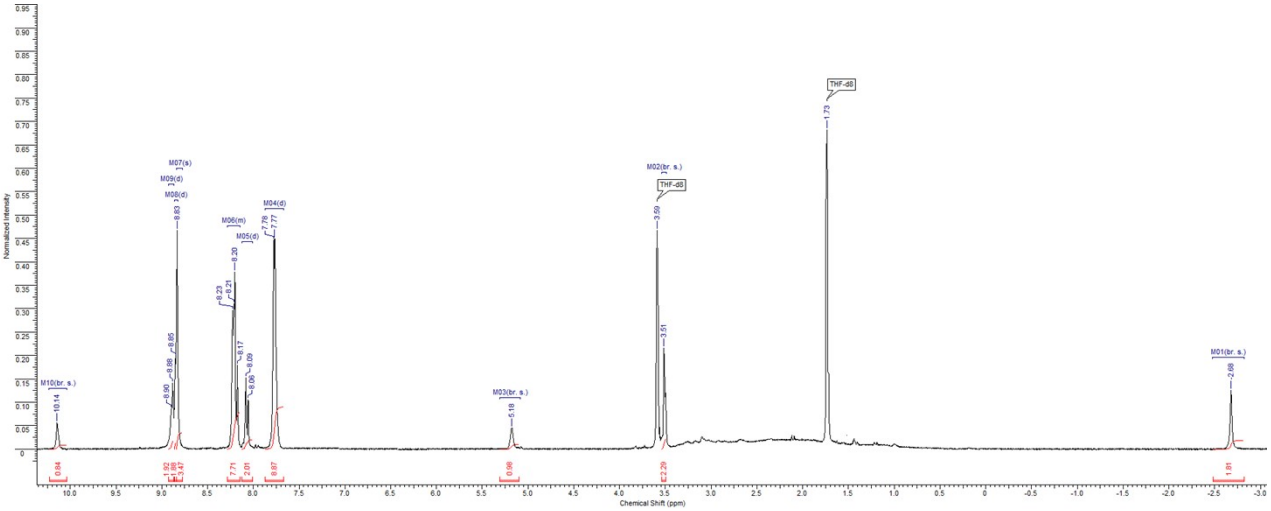

***Figure S61*.** The ^{1}H spectrum 5-(*p*-(*o*-carborane-1'-yl)-acetamidophenyl)-10,15,20-triphenylporphyrin(**24**) in THF-d_8.

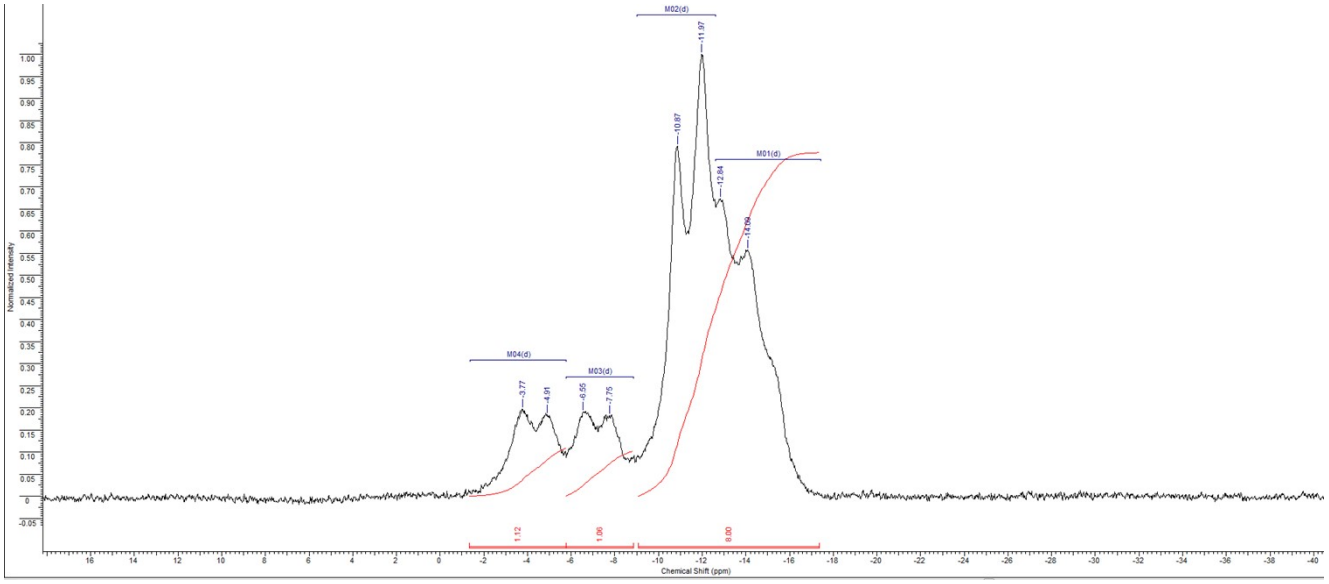

***Figure S62*.** The spectrum 5-(*p*-(*o*-carborane-1'-yl)-acetamidophenyl)-10,15,20-triphenylporphyrin(**24**) in THF-d_8.

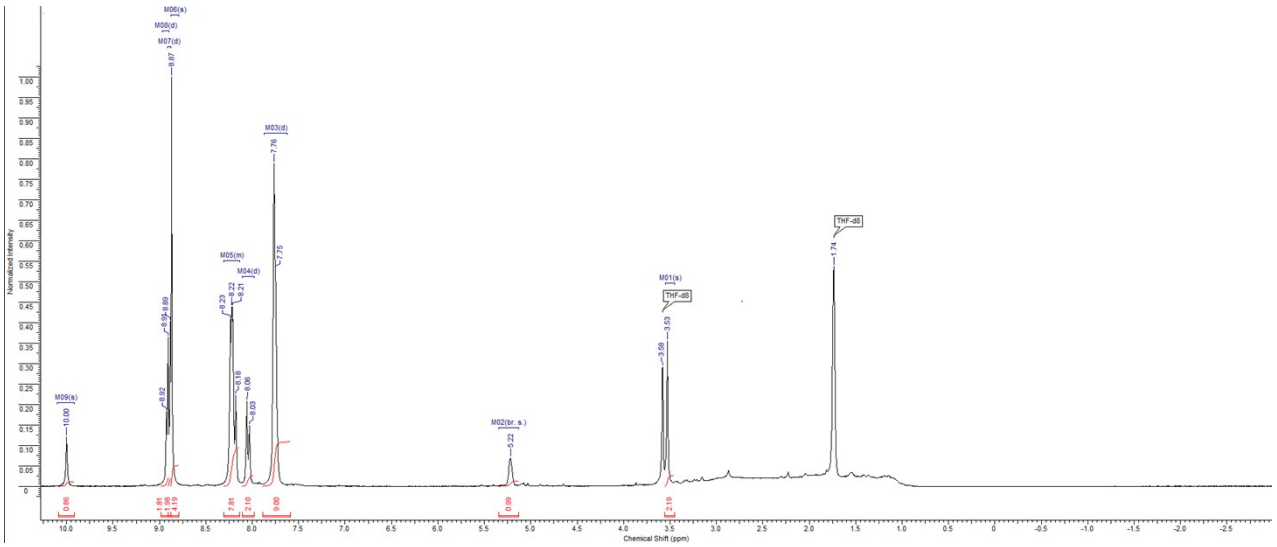

***Figure S63*.** The ^{1}H spectrum [5-(*p*-(*o*-carborane-1'-yl)-acetamidophenyl)-10,15,20-triphenylporphyrinato]zinc(**25**) in THF-d_8.

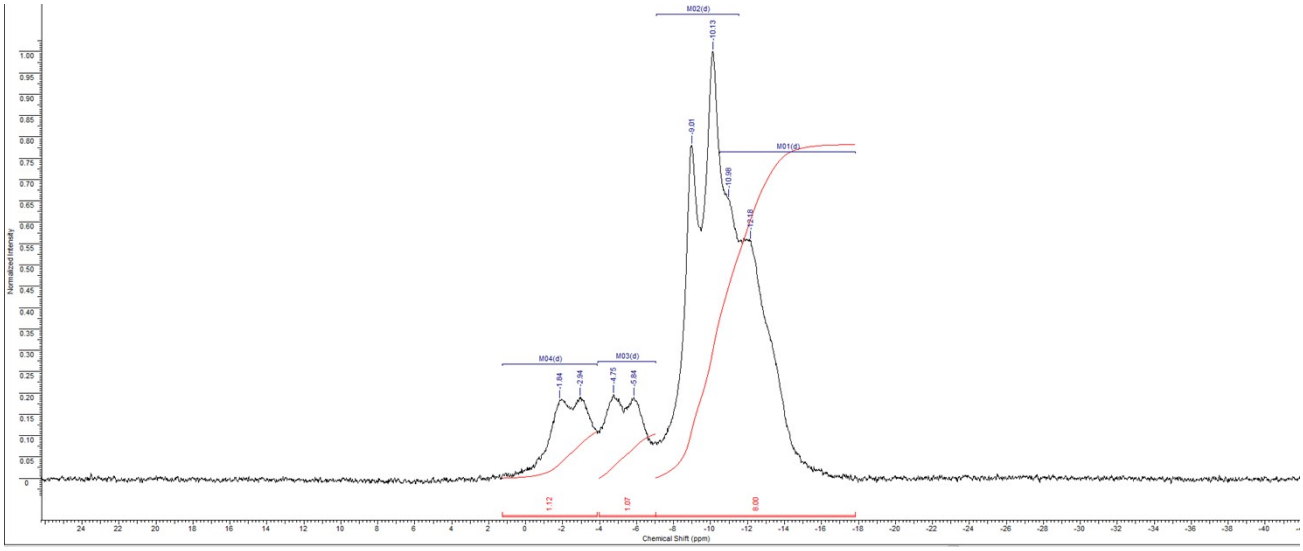

***Figure S64*.** The ^{11}B spectrum [5-(*p*-(*o*-carborane-1'-yl)-acetamidophenyl)-10,15,20-triphenylporphyrinato]zinc(**25**) in THF-d_8.

7. Biological properties

A

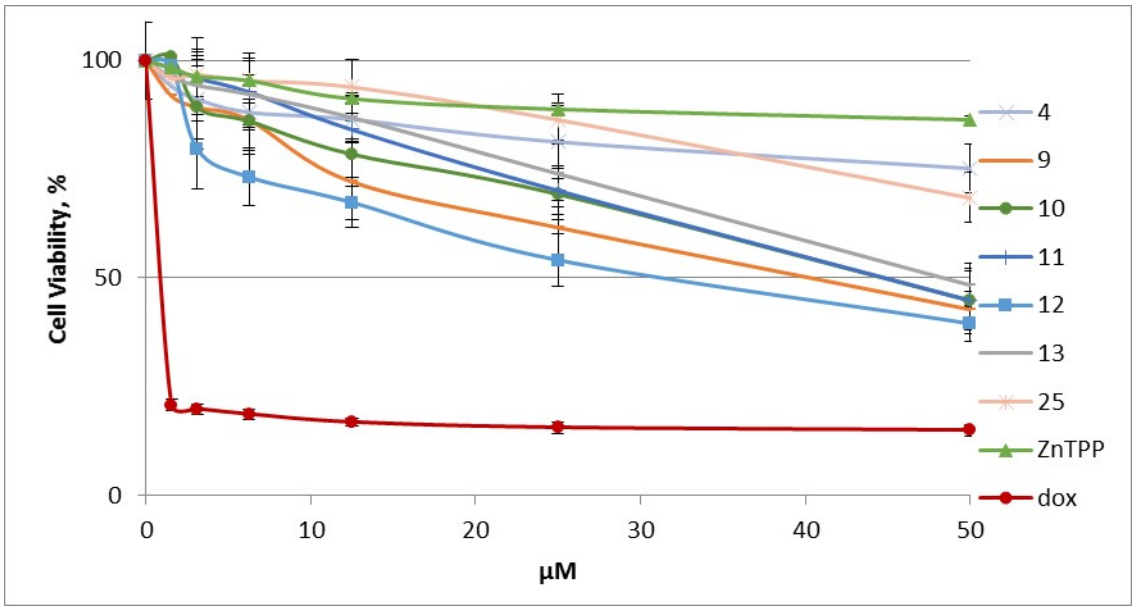

B

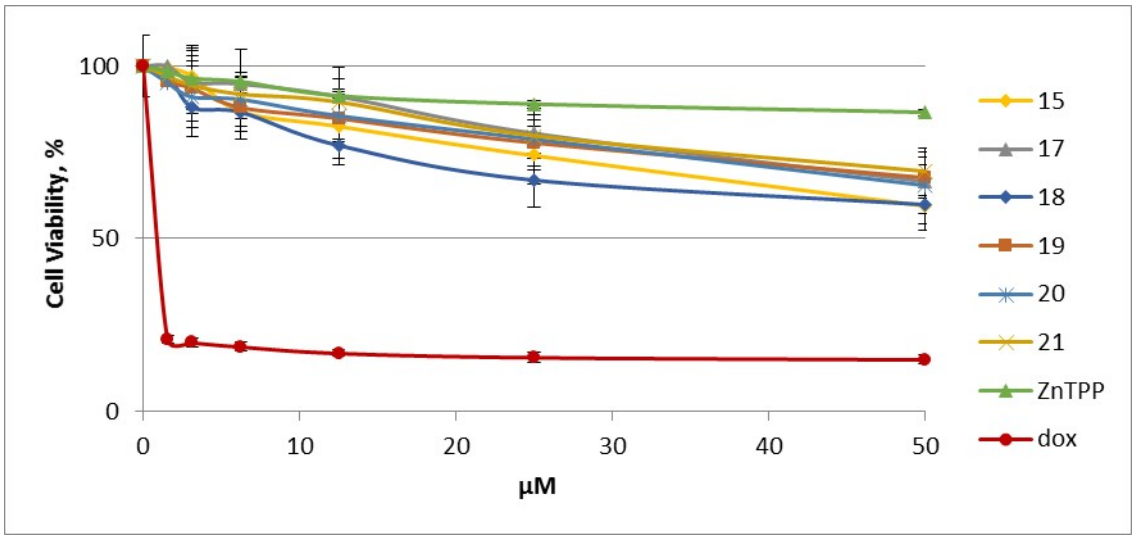

Figure S65. Dark cytotoxicity of compounds not containing (A) and containing (B) carboranyl substituents. Dox, positive control for cytotoxicity.

The HCT116 cells were treated with the indicated compounds for 72 h followed by viability tests (MTT assays; see Materials and Methods). Data are mean±SD of three measurements, each concentration in duplicate.

A

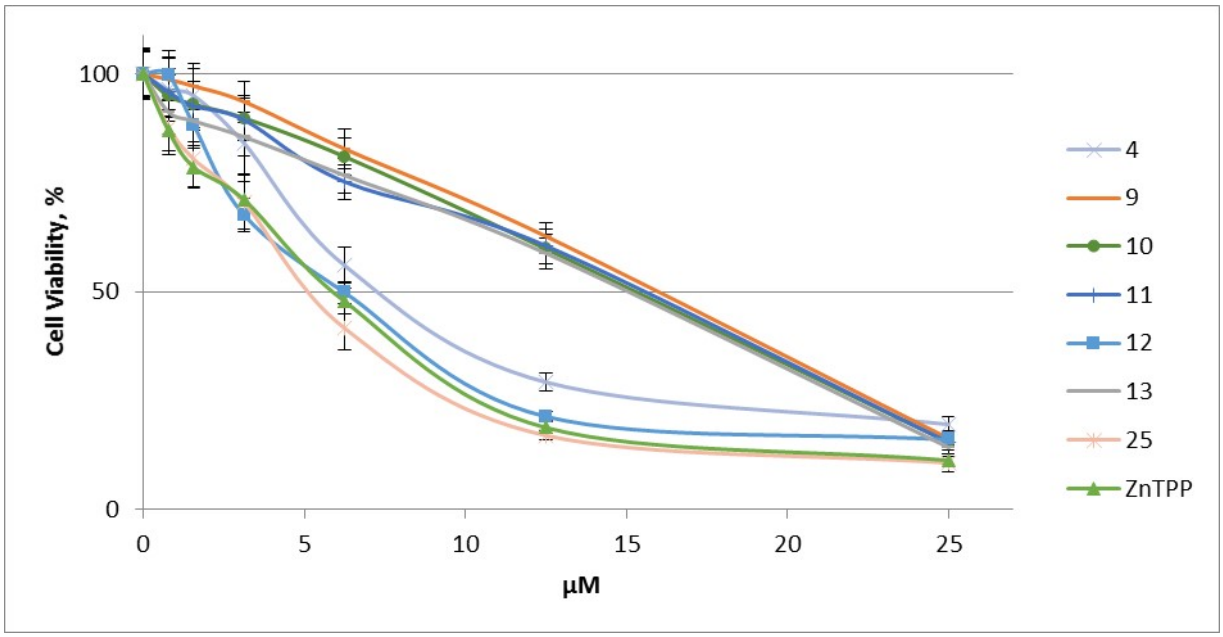
Cell Viability, %
100
50
0
0
5
10
15
20
25
µM
4
9
10
11
12
13
25
ZnTPP

B

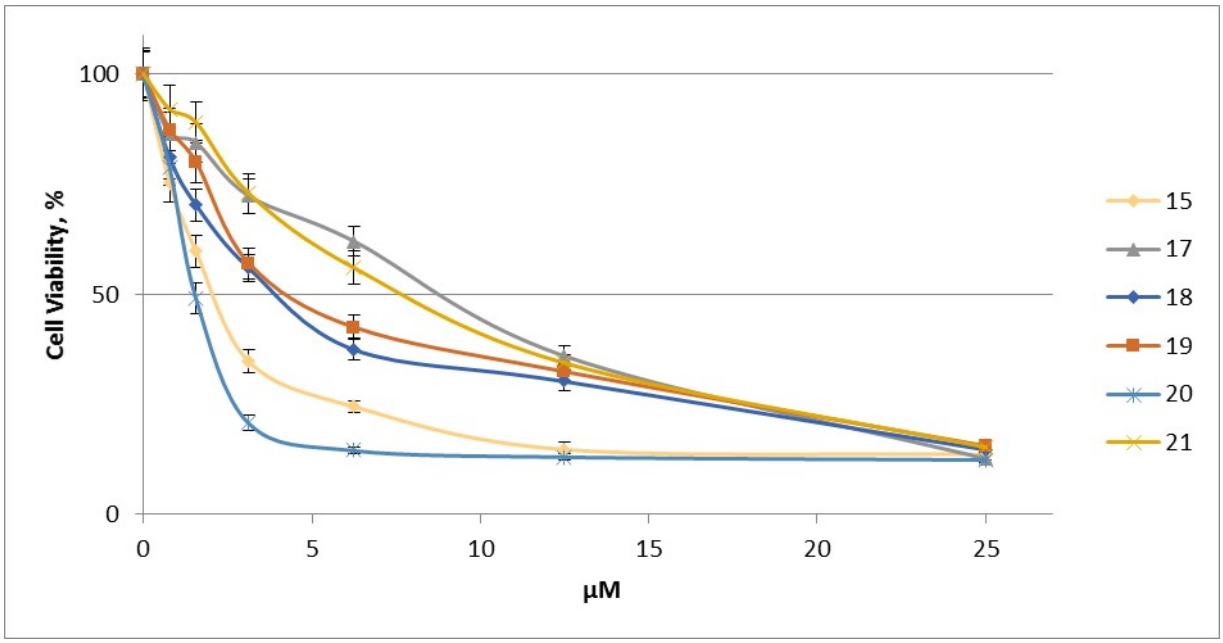
Cell Viability, %
100
50
0
0
5
10
15
20
25
µM
15
17
18
19
20
21

C

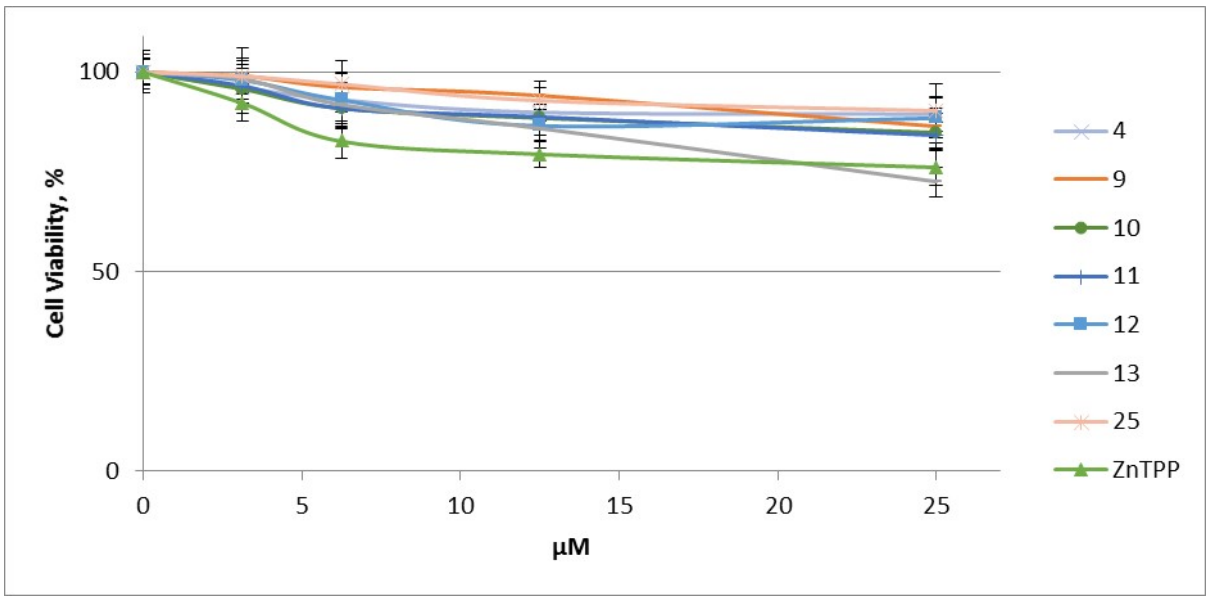

D

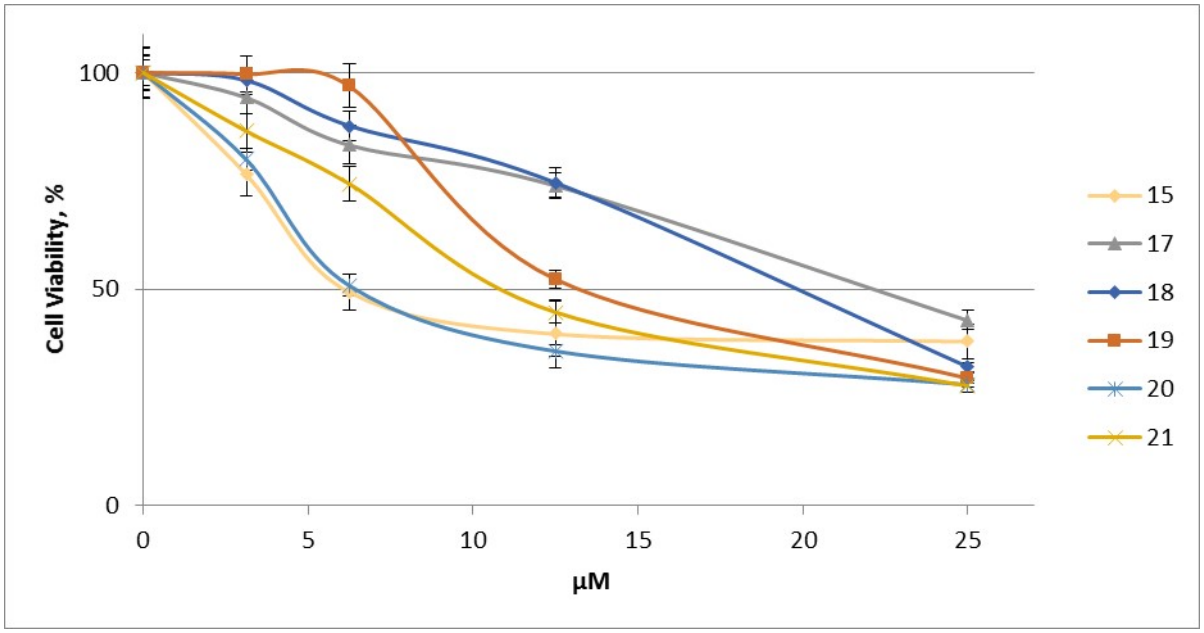

Figure S66. Photoinduced cytotoxicity of compounds not containing (A, C) and containing (B, D) carboranyl substituents.

The HCT116 cells were loaded with the indicated compounds (12.5 μM each) at 37°C, 5% CO_2 for 24 h, washed and illuminated with the laser source: 405 nm 2.5 J/cm^2(A, B); 530 nm, 20 J/cm^2(C, D). Cells were incubated under the same conditions for an additional 24 h. Cell viability was assessed by MTT assays. Data are mean±SD of three measurements, each concentration in duplicate.

Table S2. Criteria of CO formation after illumination with HbO_2 in one solution.

Compound	Minimum at 420 nm
4	no
9	no
10	no
11	no
12	no
13	no
15	yes
17	yes
18	yes
19	yes
20	no
21	no
25	no
ZnTPP	no

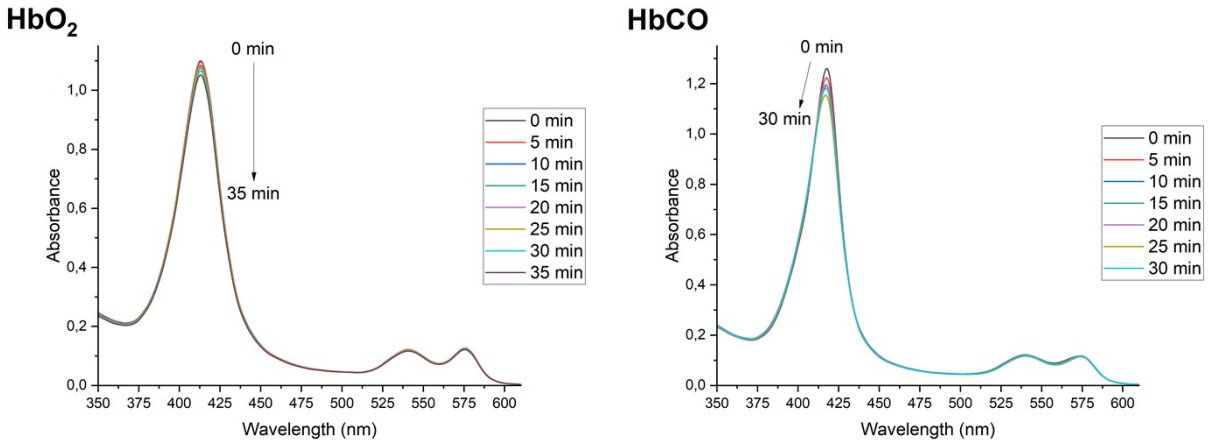

Figure S67. Changes of UV-Vis absorption spectra upon illumination (530 nm, fluence rate 9 mW/cm^2).

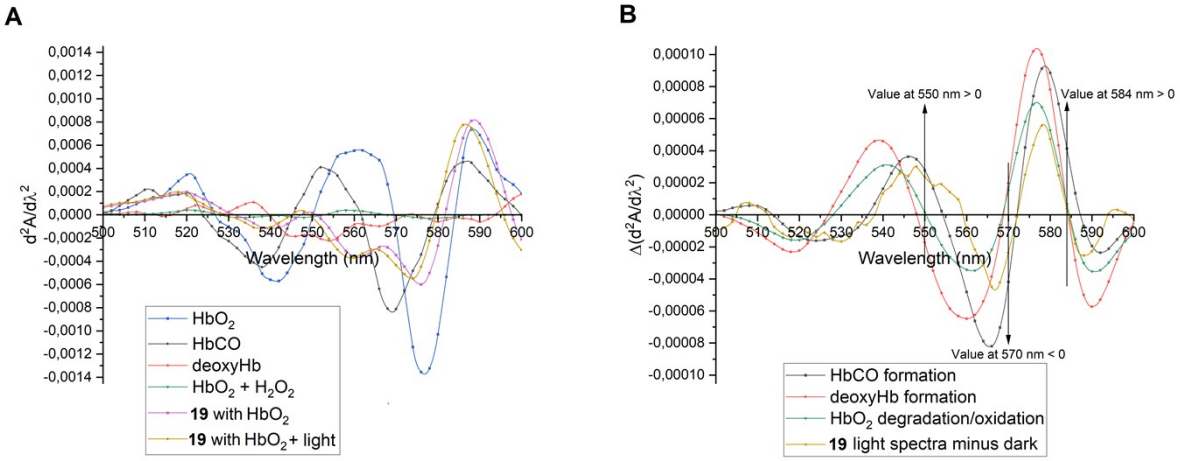

Figure S68. Additional criteria of HbCO formation based on zero-crossing points. Shown are 2nd derivative spectra of Hb-containing species before (A) and after (B) illumination.

Table S3. Criteria of HbCO formation after illumination (SNAPS method).

compound	420 nm	550 nm	570 nm	584 nm
4	yes	no	no	no
9	yes	yes	yes	yes
10	yes	no	no	no
11	yes	yes	no	no
12	yes	yes	no	no
13	yes	yes	no	yes
15	yes	yes	yes	yes
17	yes	yes	yes	yes
18	yes	yes	yes	no
19	yes	yes	yes	yes
20	yes	yes	yes	yes
20	yes	yes	yes	yes
25	no	no	yes	yes
ZnTPP	no	no	no	no

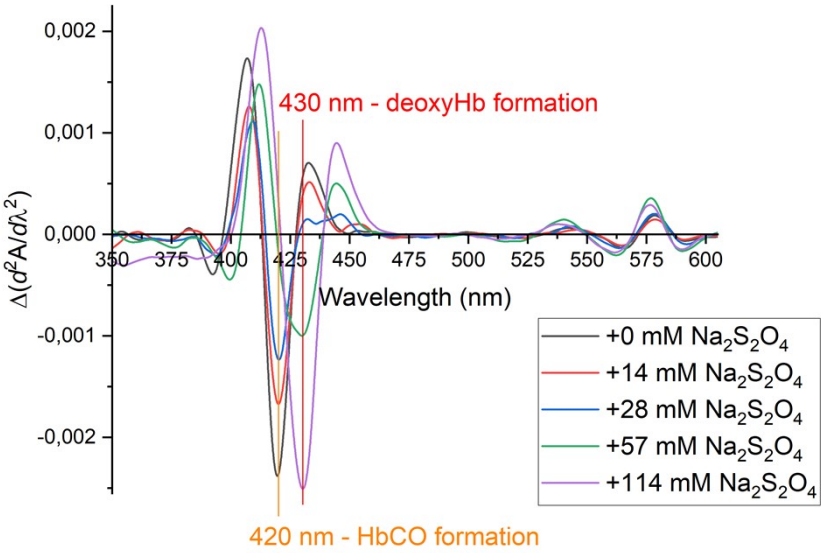

Figure S69. Second derivative difference spectra of compound **15** with Hb at different $Na_2S_2O_4$ concentrations after irradiation with a 530 nm laser, fluence rate 9 mW/cm^2, 2 min.

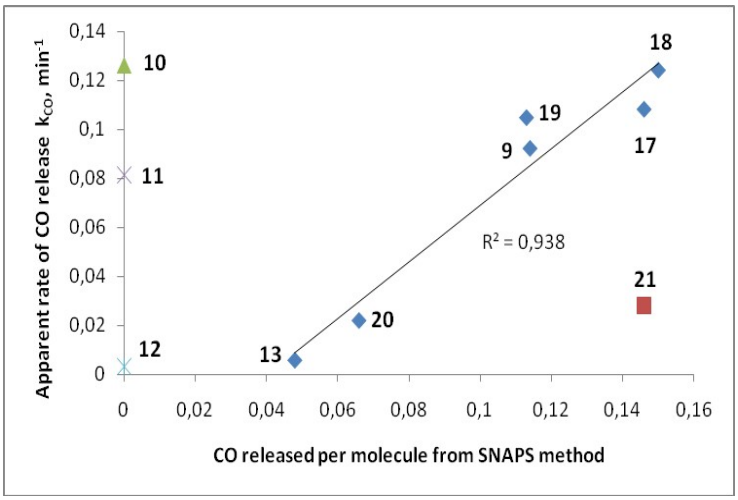

Figure S70. Correlation between CO release per molecule (SNAPS method) and apparent rate of CO release k_{CO}.

8. Synthesis and spectral data of 3-nitro-*N*-phenyl-1,8-naphthalimide (COFP)

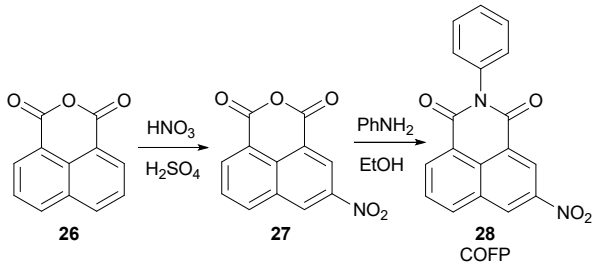

Scheme S2. Synthesis of 3-nitro-*N*-phenyl-1,8-naphthalimide COFP (**28**).

3-nitro-1,8-naphthalic anhydride (27) [1]

Naphthalic anhydride (**26**) (2.00 g, 10.10 mmol) was dissolved in 5 mL of sulfuric acid at 0 ^{o}C. Then a solution of nitric acid (0.5 mL, 11.0 mmol) in sulfuric acid (5 mL) was added dropwise. The reaction mixture was vigorously stirred at room temperature for 2 h and then poured into ice water to get the yellow crude product. The solid was recrystallized from glacial acetic acid to give pure 3-nitro-1,8-naphthalic anhydride (**27**) (1.69 g, 69 %. IR (KBr, cm^{-1}) ν_{max}: 1776 (C=O), 1745 (C=O), 1630 (NO_2), 1345 (NO_2).^{1}H NMR (300.13 MHz, DMSO-d_6) δ (ppm): 9.52 (d, *J* = 1.7 Hz, 1H), 8.92 (d, *J* = 1.9 Hz, 1H), 8.82 (d, *J* = 8.3 Hz, 1H), 8.70 (d, *J* = 7.3, Hz, 1H), 8.08 (t, *J* = 7.9 Hz, 1H).

3-nitro-*N*-phenyl-1,8-naphthalimide (COFP) (28) [2]

A solution of aniline (0.225 mL, 2.47 mmol) in EtOH (10 mL) was added dropwise to a solution of 3-nitro-1,8-naphthalic anhydride (**27**) (0.500 g, 2.06 mmol) in EtOH (10 mL) with stirring. The mixture was refluxed for 5 h and cooled to room temperature. The obtained solid was filtered and purified by column chromatography on a silica gel using $CHCl_3$ as an eluent to afford 3-nitro-*N*-phenyl-1,8-naphthalimide (**28**) as a white solid (523 mg, 80%). IR (KBr, cm^{-1}) ν_{max}: 1715 (C=O), 1674 (C=O), 1538 (NO_2), 1338 (NO_2).^{1}H NMR (300.13 MHz, $CDCl_3$) δ (ppm): 9.35 (d, *J* = 1.7 Hz, 1H), 9.21 (d, *J* = 1.9 Hz, 1H), 8.84 (d, *J* = 7.3 Hz, 1H), 8.50 (d, *J* = 8.4, Hz, 1H), 8.00 (t, *J* = 7.8 Hz, 1H), 7.56 (m, 3H, Ph), 7.33 (d, *J* = 7.4 Hz, 2H, Ph).

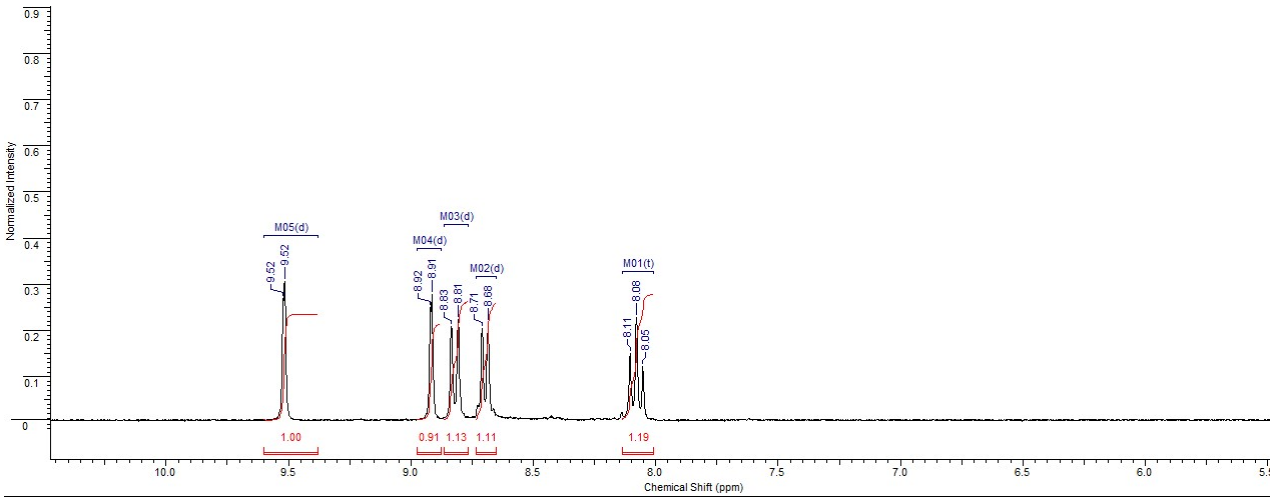

Figure S71. The ^{1}H spectrum 3-nitro-1,8-naphthalic anhydride (**27**) in DMSO-d_6.

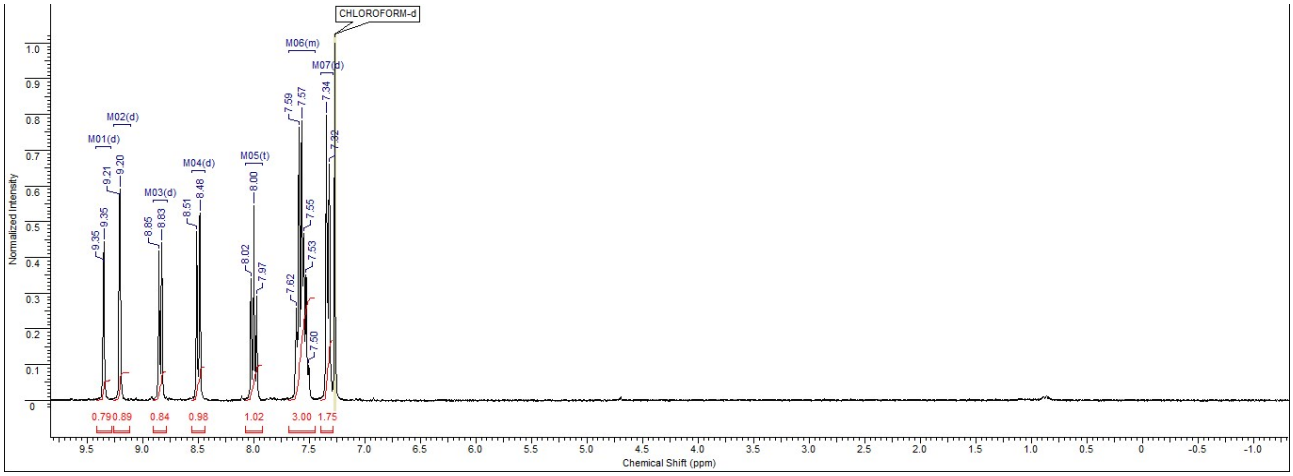

Figure S72. The ^{1}H spectrum 3-nitro-*N*-phenyl-1,8-naphthalimide (**28**) in $CDCl_3$.

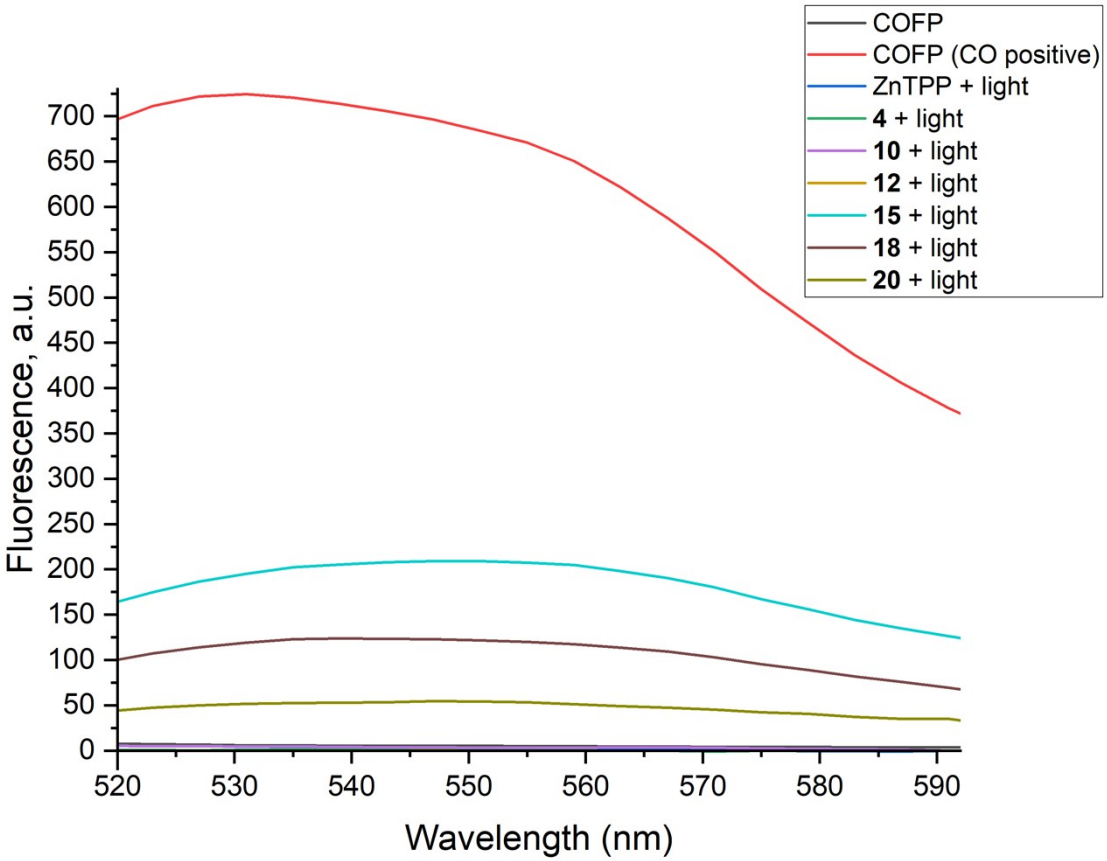

Figure S73. Detection of CO release by fluorescence probe COFP (λ_{Exc} = 470 nm).

Solutions of COFP (100 µM) and tested photoCORM (20 µM each) were incubated for 15 min at room temperature in the dark followed by measurements of background fluorescence. Then solutions were illuminated with a 530 nm laser for 2 min, and COFP fluorescence was re-measured. The solution of COFP (no photoCORM) exposed to the CO gas source was used as a positive control (red curve). No CO release was observed in the dark (not shown).

References

1. L. Yue, Y. Tang, H. Huang, W. Song, W. Lin, *Sens. Actuator B-Chem*, 2021, **344**, 130245.

2. B. Das, S. Lohar, A. Patra, E. Ahmmed, S. K. Mandal, J. N. Bhakta, K. Dhara, P. Chattopadhyay, *New J. Chem.*, 2018, **42**, 13497–13502.